RHEOLOGICAL CHARACTERIZATION OF CROSSLINKED WAXY MAIZE STARCH SOLUTIONS UNDER LOW ACID ASEPTIC PROCESSING CONDITIONS USING TUBE VISCOMETRY TECHNIQUES

By

Robert Vernon Dail

A THESIS

Submitted to
Michigan State University
in partial fulfillment of the requirements
for the degree of

MASTER OF SCIENCE

in

Agricultural Engineering

Department of Agricultural Engineering

1989

ABSTRACT

RHEOLOGICAL CHARACTERIZATION OF CROSSLINKED WAXY MAIZE STARCH SOLUTIONS UNDER LOW ACID ASEPTIC PROCESSING CONDITIONS USING TUBE VISCOMETRY TECHNIQUES

by

Robert Vernon Dail

A rheological characterization of 1.82 and 2.72% (g dry starch/100g water) waxy maize starch solutions was performed at 121.1, 132.2, and 143.3°C using tube viscometry techniques. The data were fit with the power law model, and dilatant behavior was observed in 22 out of 23 experiments. The flow behavior index was observed to increase with concentration and decrease with temperature. Dilatancy and changes in the flow behavior index were explained in terms of the rigidity and volume fraction of the swollen granules combined with small shear stresses in the fluid due to the high temperatures and low shear rates. A parameter correlation analysis showed the rheological parameters to be nearly correlated with the flow behavior index being the dominant parameter. This made the observed

behavior of the consistency coefficient difficult to interpret. The effect of dilatant flow behavior on residence time and heat transfer rates are discussed in regards to aseptic processing of both particulate and nonparticulate foods. A reexamination of whether aseptic processing is appropriate for foods with large particles is encouraged.

ACKNOWLEDGEMENTS

I would like to sincerely thank my major professor, Dr. James F. Steffe, for his support (both financial and moral) and interest in this project. I hope that we will be able to continue both a friendship and a working relationship long into the future.

I would also like to express thanks to the guidance committee, Drs. Robert Ofoli, Ajit Srivastava, and Elaine Scott, for their time and help.

Great appreciation goes to Dr. John Gerrish and Gary Connor for their help in resolving the instrumentation problems, which were considerable. The modification of the frequency board on the mass flow meter by Gary saved literally months of time.

I also express appreciation to Dr. Dennis Gilliland (Department of Statistics) and Dr. James V. Beck (Department of Mechanical Engineering) for their help with the statistical analysis and parameter estimation problems, respectively.

Thanks also to Messrs Kueck, Gyde, and Mata all now or formerly with the Dial Corporation for their support and encouragement.

Thanks to the many friends (including Brian, Marc,

Jill, Scott, Elaine, and Larry) who made the whole process enjoyable.

The starch in this study was donated by National Starch and Chemical Corporation, and partial funding was provided by the Center for Aseptic Processing and Packaging Studies at North Carolina State University. The Dial Corporation donated the recorder/controller and lent us the air operated flow control valve used in this study.

Finally, I reserve the most special thanks for the love and support of Betsy.

TABLE OF CONTENTS

LIST OF TABLES

LIST OF FIGURES

NOMENCLATURE

C = concentration (g/ml)

D = diameter (m)

E = activation energy (Kcal/mole)

K = consistency coefficient (Pa s^n)

L = length (m)

L_e = entrance length (m)

m_m = meter indicated mass flow rate (lbm/min)

m_t = true mass flow rate (lbm/min)

n = flow behavior index (dimensionless)

ΔP = pressure drop (Pa)

Q = volumetric flow rate (m^3/s)

R = tube radius (m) or gas constant (Cal/mole) in Chapter Three

r = radius of fluid core (m)

r^2 = coefficient of determination

Re = generalized Reynolds number (dimensionless)

Re_N = Newtonian Reynolds number (dimensionless)

t = arbitrary quantity

T = temperature (°C)

T_{in} = fluid temperature going into the tube viscometer (°C)

T_{out} = fluid temperature leaving the tube viscometer (°C)

u = local fluid velocity (m/s)

u_w = fluid velocity at wall (m/s)

U_{ave} = average fluid velocity (m/s), Chapter Six

U_{max} = maximum local fluid velocity (m/s)

U_s = effective slip velocity (m/s)

v = average fluid velocity (m/s), Chapter Three

V = pressure transducer voltage output (mV)

α = level of significance

β = slip coefficient (m/(Pa s))

$\dot{\gamma}$ = shear rate (s^{-1})

π = circumference of circle divided by its diameter

σ = shear stress (Pa)

σ_0 = yield stress (Pa)

σ_w = wall shear stress (Pa)

ρ = density (kg/m^3)

Ψ = arbitrary quantity

ϕ = arbitrary parameter

ϕ_1 = arbitrary parameter

ϕ_2 = arbitrary parameter

CHAPTER ONE

INTRODUCTION

1.1. Overview

In aseptic processing, also called high temperature short time (HTST) continuous processing, liquid food is rapidly heated to a temperature where undesirable microorganisms are destroyed at a rate much greater than the desirable chemical constitutents (vitamins, flavor and aroma components). The product is held at this temperature until commercial sterility is achieved, then rapidly cooled. Heating and cooling are achieved using some form of heat exchanger, and the product is held at the elevated sterilizing temperature for a relatively short period of time depending on the product and target microorganism involved. After cooling, the product is filled into a sterile container in a sterile environment (hence the term aseptic).

Currently, there is renewed interest in the food industry in aseptic processing of liquid foodstuffs. There are a number of reasons for this interest. First, the U.S. Food and Drug Administration (FDA) approved a petition by Brik Pak to use hydrogen peroxide as a sterilizing agent on

polyethylene food contact surfaces (FDA, 1981). Since that time, the FDA has approved the use of hydrogen peroxide as a sterilant of food contact surfaces for many other compounds (FDA, 1984a; FDA, 1985). Therefore, many of the packaging machines used in aseptic systems utilize plastic containers which are lightweight and/or microwavable. Some of the new packages provide the consumer the convenience of eating directly out of the container. Microwavable containers are important, from a marketing perspective, given the number of single households and the current and projected sales of microwave ovens in the United States. The lightweight containers also reduce shipping costs. Secondly, due to the difference in destruction kinetics between desirable chemical constituents and undesirable microorganisms, the potential exists for a large improvement in product quality. Finally, many foods which are heat labile, such as wine containing sauces, can be commercially produced by aseptic processing but cannot be produced by conventional retorting methods. This enables food companies to get into new product areas.

Some aseptically processed products enjoying commercial success in the United States are fruit juice drinks, tomato based sauces, applesauce, puddings, fruits, dairy products including cheese sauces, yogurt, milk, and smooth soups. The fruit, juice drinks, tomato based products, applesauce and yogurt have a pH of 4.6 or below (high acid or acidified foods). The microorganisms

destroyed in the processing of these products are very heat labile; consequently, the thermal treatment these products receive is relatively mild. Milk, smooth soups, puddings and cheese sauces have a pH greater than 4.6 (low acid foods). The microorganism of concern in products with a pH greater than 4.6 is Clostridium botulinum which causes the fatal food poisoning known as botulism. This organism forms spores which have a high thermal resistance requiring a thermal treatment that is more severe than that given acid or acidified foods.

Figure 1.1 shows a typical system for aseptically processing viscous liquid foods. The heat exchangers are scraped surface type which are superior for viscous liquid foods because they greatly reduce fouling. The product is held at the elevated sterilizing temperature by allowing it to flow through an insulated tube which is often called a hold tube. For products that contain suspended particulate matter, there is an energy transfer as heat from the liquid to the particles as the mixture flows through the hold tube. Therefore, the liquid phase cools as the particles are heated. For products that contain particulate matter, the particles must be sterilized by the time the mixture leaves the hold tube (USDA, 1984; Dignan, 1988).

None of the commercially successful low acid liquid foods mentioned above contain discrete particulate matter. Liquid foods, with particulate matter, pose a special problem when it comes to developing thermal treatments.

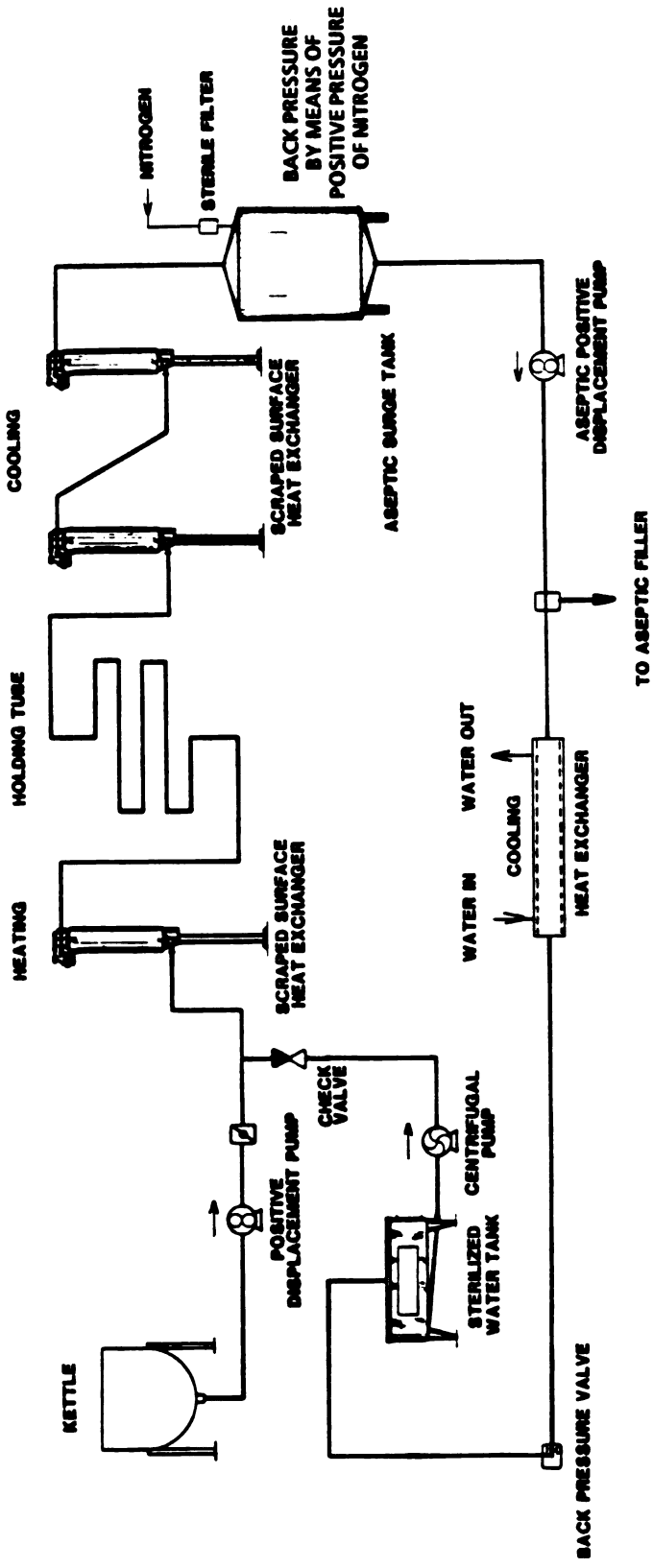

FIGURE 1.1. A TYPICAL SYSTEM FOR PROCESSING VISCOUS LIQUID FOODS

When particulate containing foods are thermally processed by conventional retorting methods, the heat penetration rate into the can and the particle are determined by impaling the particle with a thermocouple, mounted in the center of the can, and monitoring the temperature during the process. An empirical temperature history is obtained which serves as a basis for calculating the required thermal process. In aseptic processing systems, the particles are being transported through the system by the liquid phase of the food. Therefore, the internal temperature of the particles cannot be measured by thermocouples, but must be mathematically estimated based on the temperature of the surrounding fluid.

Recently, a British firm (Cross and Blackwell) introduced an aseptically processed low acid product containing discrete particulate matter (meat and vegetable pieces) into the European market. This product has not been introduced in the United States. Also, two U.S. firms have attempted to file low acid particulate processes with the U.S. Food and Drug Administration which have not been accepted for filing (Larkin, 1988). For a process to be accepted for filing with FDA, or for a process to be approved by USDA, a firm must satisfactorily show that the product does not present a public health hazard. For product sterilization, this includes data from inoculated pack studies. The FDA also requests that viscosity data be submitted if it is deemed critical to the delivery of the

thermal process, asking that the product be characterized as Newtonian, pseudoplastic or dilatant (FDA, 1984b). The United States Department of Agriculture, Food Safety and Inspection Service, also states that flow properties of the formulated product may be included in the assessment of commercial sterility (USDA,1984). The FDA states that viscosity data may be taken from handbooks or technical literature, or it can be obtained by direct measurement (FDA, 1984b).

A widely used thickener for low acid foods is crosslinked waxy maize starch. The extra crosslinking in these starches inhibits swelling of the starch granules at lower temperatures (Fennema, 1976; Hosney, 1986). Thus, liquid foods thickened with this material are better able to withstand the thermal abuse undergone by low acid foods. To date, no rheological data exists for crosslinked waxy maize starch in the low acid aseptic processing temperature range (121-143°C). Lack of this data is inhibiting progress in bringing aseptically processed low acid particulate foods to market in the United States, whether foreign or domestic. First, processors of low acid particulate foods are unable to provide rheological information to the U.S. regulatory agencies. Second, engineering design of required thermal processes is not possible without it. The data are required to determine velocity profiles in hold tubes, residence times and residence time distributions of suspended food particles, heat exchanger design, and to

obtain heat transfer rates into particles being transported by the fluid.

Producers of aseptically processed low acid nonparticulate foods that are starch thickened and that cannot provide rheological data to the regulatory agencies have been required to design hold tube length on the assumption that the flow behavior index is infinitely large (because starch thickened foods are suspected to be non-Newtonian), or establish the process with large inoculated pack studies (Stefanovic, 1988). Assuming the flow behavior index to be infinitely large results in the maximum fluid velocity in the hold tube being three times the bulk average velocity. This represents a worst case situation which results in overprocessing the product. Consequently, most producers of low acid nonparticulate starch thickened foods have established the thermal processes solely by inoculated pack studies (Stefanovic, 1988). The disadvantage in doing this is that any change in the system, such as hold tube diameter or speed of the mutator blades in the heat exchanger, etc., requires reestablishment of the thermal process by inoculated pack. This is quite labor intensive and time consuming. It is easily seen that a large benefit in process design flexibility can also be gained by producers of low acid, nonparticulate starch thickened foods by a rheological characterization of crosslinked waxy maize starch solutions.

In summary, rheological characterization of crosslinked waxy maize starch solutions will aid in moving aseptic low acid particulate thermal processes through the approval or acceptance process at the U.S. regulatory agencies, enable engineering design of aseptic equipment and thermal processes, and provide greater process design flexibility for low acid nonparticulate foods already on the market.

1.2. Objectives

The general objective of this research was to complete a rheological characterization of two crosslinked waxy maize starch solutions (1.82 and 2.72%, g dry starch/100g water) at three temperatures in the low acid aseptic processing temperature range (121, 132 and 143°C) using tube viscometry techniques. Specific objectives included building and instrumenting a tube viscometer that would prevent boiling of a test fluid heated above its boiling point and investigation of temperature, concentration, and their possible interaction effects on the rheological parameters.

CHAPTER TWO

LITERATURE REVIEW

2.1. Introduction

It was mentioned in the introduction that modified waxy maize starches are widely used as a thickener for low acid foods that are either conventionally retorted or aseptically (HTST) processed. The mechanism by which starches thicken the water in which they are suspended has been well understood for years, and a description of this mechanism can be found in textbooks on food or starch chemistry (Hoseney, 1986; Whistler, et al., 1984; Fennema, 1976). In the following three sections, starch, starch gelatinization, and starch modification will be briefly reviewed prior to reviewing the literature on starch rheology.

2.1.1. Starch

Starch is the primary means by which plants store energy. Most plant starches are composed of two polymer fractions: amylose and amylopectin. These polymers are polysaccharides composed of the monosaccharide glucose (Lehninger, 1973). Amylose is a linear molecule in which

the glucose residues are linked α-1,4 and has a molecular weight of approximately 250,000. Most of the linkages in amylopectin, a branched molecule, are also α-1,4; however, 4-6% of the linkages are α-1,6. The α-1,6 linkages cause the molecule to be branched instead of linear, and the molecules are very large with molecular weights as large as 100 million. Most plant starches are approximately 30% amylose with the remainder being amylopectin. However, the waxy starches are approximately 100% amylopectin, and there are hybrid plants that produce starches that are approximately 70% amylose (Hoseney, 1986).

Plants store starch in granular form. The granules range in size from 2-150μm (Zobel, 1984). Waxy maize starch granules are approximately 15μm in diameter (Lineback, 1984). The granules possess a high degree of order as evidenced by the display of birefringence when viewed with polarized light. X-ray diffraction also shows the granules to be semi-crystalline which is thought to be due to the amylopectin. Approximately 30% of a granule is crystalline with the rest being amorphous (Hoseney, 1986).

2.1.2. Starch Gelatinization

When starch granules are heated in the presence of water, they undergo morphological and chemical change. When the energy in the water becomes great enough to disrupt the hydrogen bonds between the starch molecules, the granule will swell and imbibe water causing an increase in

viscosity. This phenomena is called gelatinization and is accompanied by a loss of birefringence (Hoseney, 1986; Fennema, 1976) and a change in X-ray diffraction (Katz, 1928). The temperature at which gelatinization occurs depends on the plant source of the starch and whether or not the starch has been modified. For corn and waxy maize (a corn hybrid) starches which have not been modified (native starch), gelatinization starts to occur at approximately 62°C. Gelatinization is 50% complete at 67°C and 100% complete at 72°C (Lineback, 1984). Heating beyond this temperature range results in a continued increase in viscosity and is termed pasting.

As a part of the gelatinization and pasting process, starch granules solubilize. In starches that contain amylose, the amylose fraction is the first to solubilize. This starts to happen early in the gelatinization process, and the solubilized amylose leaches out of the granule into the intergranular space. Christianson et al. (1982) showed that, for native corn starch, about 10% of the starch granule is solubilized at 70°C. Doublier (1987) states that most of the amylose in cereal starches (e.g. corn or wheat) does not solubilize until 80-90°C because internal lipids form insoluble complexes with amylose below 90°C. The solubilization of amylose leaves the granule composed primarily of amylopectin. However, the solubilization process is continuous, and the amylopectin can be made to solubilize with increasing temperature. Solubilization of

the amylopectin destroys the integrity of the granule with a subsequent loss of viscosity. The solubilization of amylopectin happens slowly (Zobel, 1984), and, even for native starches, complete loss of granular structure may not occur until a temperature of approximately 120°C (Hoseney, 1986). The increase in viscosity which occurs during pasting is thought to be due to hydrogen bonding of the solubilized amylose to two or more starch granules (Christianson, et al., 1982).

2.1.3. Starch Modification

There are four primary types of starch modification: acid, crosslinking, oxidation, and substitution. The starch that will be used in this study is a crosslinked starch. Therefore, crosslinking will be reviewed here.

Crosslinking is the forming of covalent bonds between two starch molecules to form a larger molecule (Hoseney, 1986). Crosslinking is performed primarily in two ways. First, a diester can be formed between the two molecules. This is usually done with phosphorous oxychloride ($POCl_3$). The second method is to form an ether bond between the molecules which is typically done using epichlorhhydrin (Hoseney, 1986). Other compounds used to a lesser extent to form covalent bonds between the molecules include acrolein, sodium trimetaphosphate, succinic anhydride, and adipic anhydride (Fennema, 1976).

Crosslinking increases the gelatinization temperature

(Fennema, 1976) and causes starches to swell less, give a lower viscosity upon pasting, be less soluble, and not as subject to shear-thinning (Hoseney, 1986).

2.2. Starch Rheology

Table 2.1 presents a summary of information from the pertinent works on starch rheology. Presented are the investigators, type of starch, type of viscometer, shear rate range, temperatures at which the rheological tests were conducted, length of time the starch was cooked, temperature at which the starch was cooked, and starch rheology. It can be seen that there are no rheological tests above 100°C. In fact, the only rheological testing on a liquid food that would normally boil at 100°C was that done by Bertsch and Cerf (1983) on milk and cream using a capillary rheometer. Despite there being no rheological testing on starch above 100°C, a review of the works listed in Table 2.1 is still deemed beneficial, because the explanation of flow phenomena at the lower temperatures may still be applicable at higher temperatures.

Evans and Haisman (1979) performed a rheological characterization of corn, modified corn, potato, and tapioca starches. The modified corn starch was an acetylated waxy maize distarch adipate. Two types of rheometers were used: a Weissenberg Rheogoniometer (cone and plate) covering a shear rate range of 0.0007-56 s^{-1}, and a Haake Rotovisco (concentric cylinder) covering a

Table 2.1. A summary of information from the pertinent works on starch rheology.

Investigators	Starch	Viscometer	Shear Rate	Test Temp.	Cook Time	Cook Temp.	Rheology
Christianson & Bagley, 1983	Corn, 5-26%	Concentric Cylinder	3-500 s^{-1}	60 & 23C	15, 30,45, 60 &75 min.	65, 67, 70, 75 & 80C	Dilatant for short cook time, pseudoplastic for long cook time,dilatant for intermediate cook time at low shear rates
Bagley & Christianson, 1982	Wheat, 7-25%	Concentric Cylinder	1-1000s^{-1}	60 & 23C	15, 30, 45, 60, & 75 min.	60, 65, 70, & 75C	Same as above.
Christianson, et al., 1982	Corn, 5-26%	Concentric Cylinder	3-500s^{-1}	60 & 23C	15, 30, & 75 min.	65-85C	Same as above.
Evans & Haisman, 1979	Corn, potato, & tapioca, up to 10%	Concentric Cylinder; Cone & Plate	0.0007-1142s^{-1}	60C	various, depending on starch	90C	All pseudoplastic. Flow behavior index increased w/concentration.
Wong & Lelievre, 1982	Wheat, 3.1-6.1%	Cone & Plate	0.4-4000s^{-1}	30C	5-60 min.	85-95C	All pseudoplastic.
Doublier, 1981	Wheat, 0.3-8%	Concentric Cylinder	1-700s^{-1}	25-70C	30 min.	96C	Newtonian for 0.3-1.5% at low shear rate; otherwise pseudoplastic. Consistency coefficient decreased w/temp.

Table 2.1. Continued.

Investigators	Starch	Viscometer	Shear Rate	Test Temp.	Cook Time	Cook Temp.	Rheology
Colas, 1986	Crosslinked waxy maize, 3.3%	Concentric Cylinder	0-330s^{-1}	25C	6.5 min.	95C	All pseudoplastic. Flow behavior index decreased w/ conc. and the consistency coefficient decreased w/temp.
Doublier, 1987	Wheat, corn, faba bean, & smooth pea, 5-10%	Concentric Cylinder	0-660s^{-1}	60C	Various; cooked on viscoamylo-graphs.	96C	All pseudoplastic. Consistency coeffi-cient increased w/conc.

shear rate range of 7-1142s^{-1}. The starches were cooked at 90°C until maximum viscosity was achieved. Rheological tests were conducted at 60°C on concentrations up to 10%. The results showed that all solutions acted as shear-thinning, power-law fluids. They also found that the flow behavior index was a strong function of concentration with the flow behavior index increasing as the concentration was increased. Upon centrifuging, the starch pastes would separate into a clear supernatant and a semi-solid. They concluded from this that starch solutions were, in reality, particulate. The supernatant was found to have a low viscosity despite having a high solids content, and consequently, they suggest that (apart from intermolecular bonding that would cause bridging between granules by amylose) the supernatant contributes little to the rheology. Apparent viscosity was observed to increase with concentration with little effect on viscosity occurring until a critical concentration was achieved.

To explain the observed rheological phenomena, the authors determined particle interaction by examining sedimentation rates and determined the volume that the swollen starch granules occupy by dye exclusion methods. The extent to which sedimentation rates are dependent on concentration is indicative of strength of particle interaction and the degree of aggregation of the particles. The volume of the swollen granules was deemed important because abrupt changes in rheological properties

had been observed for other systems (polymer microgels and polyacrylonitrile graft co-polymer solutions) at particular concentrations where the particles became close-packed. Results of the sedimentation test showed strong particle interaction. The close-packing point of corn and modified corn starch were determined to be 2.7 and 2.8%, respectively. Significant increases in apparent viscosity and the appearance of a yield stress were seen to occur at 3.3% for corn starch and 2.7% for modified corn starch. The authors concluded that the main factors effecting the rheology of gelatinized starch suspensions is intergranular interactions (e.g. hydrogen bonding), the volume fraction occupied by swollen granules, and the compressibility and deformability of the starch granules, since the pastes were still observed to be fluid even at concentrations greater than the close-packing point.

The work reviewed above was performed on a fully pasted starch i.e., the starch was cooked until a maximum viscosity was achieved. Three works from the U.S. Department of Agriculture's Agricultural Research Service examined the effects of cooking time at cook temperatures throughout gelatinization and into the pasting range.

In the first of these works, Bagley and Christianson (1982) characterized 7-25% (db) concentrations of native wheat starch cooked for 15, 30, 45, 60, and 75 minutes at 60, 65, 70 and 75°C. Rheological tests were performed on a Haake Rotovisco (concentric cylinder) viscometer at 60 and

23°C
sus
coo
int
at
she
plo
val
Als
ino
of
obs
fo
co
vi
16
vi
co

as
(d
pa
ac
th
We
Co
re

23°C covering a shear rate range of 1-1000 s^{-1}. Starch suspensions were found to be shear-thickening for short cook times, shear-thinning for long cook times, and for intermediate cook times, were found to be shear-thickening at low shear rates ($0<\dot{\gamma}<100\ s^{-1}$) and shear-thinning at high shear rates ($\dot{\gamma} \geq 100\ s^{-1}$). These results were presented in plots of apparent viscosity versus shear rate; actual values of the rheological parameters were not presented. Also, apparent viscosity was observed to increase with increasing concentration which agrees with the observations of Evans and Haisman (1979). Apparent viscosity was observed to increase with cook time, and the authors also found rapid increases in viscosity above certain concentrations, depending on temperature. At 60°C, the viscosity increased very rapidly with concentration above 16%. As the cooking temperature was raised, the rapid viscosity increases occurred at progressively lower concentrations.

Explanation of the observed rheological phenomena was as follows; the authors first noted that shear-thickening (dilatancy) occurs in closely packed assemblages of solid particles for which system volume must increase to accommodate flow under shear. From this they concluded that the starch granules were rigid at the short cook times and were deformable at the long cook times. At the intermediate cook times, the granules were still fairly rigid and required greater stress to cause them to deform and for the

solution to appear shear-thinning. Greater shear stress occurred at the rheological test conducted at the lower temperature (23°C). Consequently, a solution that appeared to be dilatant at 60°C might appear to be shear-thinning at 23°C. In summary, if the particles are not swollen enough to be readily deformed, or if the shear stress levels are too low to force the particles to deform, then dilatancy will be observed. Also, the extent of swelling and plasticization of the granules depends on cook time.

As with the work of Evans and Haisman (1979), the observation that rapid increases in viscosity occur at certain threshold concentrations was explained in terms of the amount of granule swelling. However, because the cook times and temperatures were such that maximum viscosity was not achieved, a slightly different approach was used. Instead of directly determining the volume fraction of the swollen granules, the amount that the granules would swell if excess water was present was first determined (in a separate experiment) for each of the cook time/cook temperature combinations. For excess water to be present, the solutions had to be dilute (2-4%). The swollen gel from these experiments was weighed, and a variable, Q, was constructed which was grams of swollen gel/grams of dry starch used to make the gel. Then, instead of plotting apparent viscosity versus concentration, c, apparent viscosity was plotted against cQ. Since the concentration, c, has the units of grams of dry starch/grams starch

suspension, cQ has the units of grams of swollen gel/grams of starch suspension. Hence, when cQ<1, excess solvent exists between the particles, and when cQ>1, all of the solvent has been absorbed by the particles. In this way, the authors were able to unify their data.

When cQ is less than one it is the volume fraction. Because swollen starch granules are both deformable and compressible, cQ can be greater than one, and the authors state that for values of cQ>1, the system is a "dough." The rapid increase in viscosity observed for certain threshold concentrations, depending on temperature, were found to occur at a cQ value of approximately 0.7. The authors reported difficulty in plotting the apparent viscosity versus cQ for those cases where dilatancy occurred. They stated that the method should theoretically be usable for the shorter cook times (where dilatancy occurred), but the data were quite scattered.

Lastly, it should be noted that at the cook temperatures used in the Bagley and Christianson (1982) work, little of the amylose was solubilized. Consequently, the rheological phenomena observed were free of the effects solubilized amylose.

In a second work, Christianson et al. (1982) performed a rheological characterization of native corn starch in conjunction with scanning electron microscopy of the starch granules to examine the morphological changes caused by cooking temperatures and times along with the effect of

shearing stresses applied to them. The emphasis was on presentation of the scanning electron micrographs, and the rheological findings were presented as examples of the type of flow that exist as a function of the starch morphology. Consequently, the experimental conditions for the rheological testing were not completely clear. However, the experimental conditions appear to be as follows; concentrations of native corn starch suspensions of 5-26% (db) were cooked for 15, 30, and 75 minutes at temperatures between and including 65-85°C. Rheological tests were performed on a Haake Rotovisco (concentric cylinder) viscometer at 60 and 23°C covering a shear rate range of 3-500 s^{-1}.

Christianson et al. (1982) observed dilatancy for short cook times and shear-thinning behavior for long cook times. Either dilatancy or Newtonian behavior was observed for intermediate cook times at low shear rates. For the intermediate cook times, the dilatant or Newtonian behavior changed to shear-thinning behavior at shear rates above, approximately, 100 s^{-1}. The same explanations for the observed rheological phenomena were given for this work as were given for the Bagley and Christianson (1982) work; dilatancy occurs when the starch granules are rigid and closely packed, which occurs at short cook times. The rigidity of granules cooked for short times and at lower temperatures was supported by scanning electron micrographs, as was the plasticization and deformability of

granules cooked for long cook times or at higher temperatures.

Two additional rheological observations were noteworthy: 1.) The shear stress developed in the fluid is concentration dependent. The rheological effect of this is that a starch suspension which appears Newtonian or dilatant at a particular cook time and temperature at a particular concentration can appear shear-thinning at the same cook time and temperature but a higher concentration. The additional shear stress developed at the higher concentration causes the the starch granules to deform where they were too rigid to deform at the lower concentration. 2.) Cooking time has no effect on the extent of swelling. The viscosities are different at different cook times despite the amount of swelling being the same. The difference in viscosity is attributed to the degree of solubilization of amylose.

The final work in rheological characterization of native corn starch by Christianson and Bagley (1983) considered 5-26% (db) concentrations of corn starch cooked at 65, 67, 70, 75, and 80°C for 15, 30, 45, and 75 minutes. Rheological tests were conducted on a Haake Rotovisco (concentric cylinder) viscometer at 60 and 23°C covering a shear rate range of 3-500 s^{-1}. Results were the same as the previous two works where dilatancy appears for short cook times and intermediate cook times at low shear rates ($\dot{\gamma}$<150 s^{-1}). Newtonian behavior was observed for 25% (water

limited) solution at 60°C over the shear rate range of 3-30 s^{-1}. The apparent viscosity increased with concentration and the increase became very rapid when a threshold concentration was achieved. This was again explained in terms of the variable cQ. Apparent viscosity also was observed to decrease with temperature and increase with cooking time. Rheological data were presented in plots of apparent viscosity versus shear rate, concentration, or cQ. Actual values of the rheological parameters (n and K) were not presented.

A notable observation made by the authors was that when the amount of swelling of the corn starch granules was equal to that of the wheat starch granules from the earlier work (Bagley and Christianson, 1982), the apparent viscosities were the same. Since the cook temperatures used were in the range where little solubilization of amylose takes place, the conclusion was that viscosity and other rheological behavior is due solely to the volume occupied by the starch granules. Consequently, as with wheat starch pastes, corn starch pastes increase in viscosity very rapidly for values of cQ greater than 0.7.

It should finally be noted that, for the three works involving Bagley and Christianson above, the authors acknowledge that, in the rheological tests conducted at 60°C, the starch may have continued to paste contributing to the dilatancy observed. However, they discounted the effect on the results because the same behavior was seen to

occur for the same material at 23°C.

Doublier (1981) performed a rheological characterization of wheat starch pastes where concentrations ranged from 0.3-8%. Rheological tests were conducted on two different viscometers; a Rheomat 30 (concentric cylinder) was used for concentrations greater than 2.5%. Test temperatures were 25-70°C and covered a shear rate range of 1-700 s^{-1}. A Low Shear 30 (concentric cylinder) was used for concentrations less than 2.5% and covered a shear rate range of 10-128 s^{-1}. All tests on this viscometer were done at 25°C. The starch was heated to 96°C and held for thirty minutes. It was then cooled to the temperature at which the test was being conducted. Part of the objective of this work was to examine the influence of heating rate and mixing speeds on rheological properties.

For concentrations less 1.5% at 25°C, the author observed Newtonian behavior for shear rates less than 10 s^{-1}; otherwise, shear-thinning behavior was observed. The majority of the tests for concentrations of 2.5-8% were done at 70°C and the consistency coefficient was observed to increase with concentration. The author derived the following expression for the consistency coefficient as a function of concentration:

$$K=8.74*10^{-7}C^{3.88} \quad .....(2.1)$$

where C is concentration in grams/milliliter. Other tests

conducted for concentrations of 2.5-8% at temperatures other than 70°C enabled a determination of temperature effects on the consistency coefficient using an Arrhenius relationship:

$$K=K_0\exp[E/(RT)] \quad \ldots\ldots\ldots\ldots(2.2)$$

where $K_0=1.51*10^{-4}$ Pa, R=1.984 Cal/mole, and E=5.13 kcal/mole.

From the rheological tests at a shear rate of 1 s^{-1}, the author was able to show that macromolecular entanglements (in this case, granule bridging by amylose) starts to occur at 0.5% which is also seen for certain types of polymers. At 1.5%, the rheology of the solution is transformed from one governed by macromolecular entanglements to that of a suspension governed by the volume fraction of the swollen granules. For higher shear rates and concentrations, the rheology was said to be primarily determined by the volume fraction of swollen granules.

From the portion of the work where the effects of mixing and heating rates were examined, it was shown that rapid heating yields a higher consistency coefficient and that the amount of swelling was dependent on the heating rate. Greater swelling was seen to occur with rapid heating.

Wong and Lelievre (1982) examined the behavior of

wheat starch pastes under steady shear conditions using concentrations of, approximately, 3.1-6.1%. The suspensions were cooked from 5-60 minutes at 85-95°C. Rheological tests were conducted at 30°C on a Ferranti-Shirley cone and plate viscometer covering a shear rate range of 0.4 - 4000 s^{-1}. Part of the objective was to examine the effect of wheat variety on rheology.

All of the suspensions were found to be shear-thinning for shear rates greater than 10 s^{-1}. For shear rates less than 10 s^{-1}, a yield stress was seen to exist in all varieties except at the lowest concentrations. The close packing percentages were given for two of the varieties and were found to be 2.82% for Raven and 3.92% for Kamaru. Large increases in viscosity occurred when the concentration was approximately 0.7 of the close packing concentration. This agrees with the work of Bagley and Christianson (1982) and Christianson and Bagley (1983). Apparent viscosity was observed to increase with increasing concentration. The final conclusion was that the rheology of the wheat starch pastes are primarily governed by the volume the swollen particles would occupy if close-packed (with excess solvent present) and the size distribution of the particles.

Colas (1986) performed the only rheological characterization of the type of starch used in this study: crosslinked waxy maize. Three waxy maize starches with different degrees of crosslinking were used in addition to

a native waxy maize which served as a control. The concentration used for all experiments was 3.3% (g dry starch/100g water), and the suspensions were heated to 95°C in 6.5 minutes. A Rheomat 30 (concentric cylinder) viscometer was used covering a shear rate range of 0-330 s^{-1}. All tests were performed on pastes at 25°C.

All pastes were found to be shear-thinning. The greater the degree of crosslinking, the less viscous the paste. This was explained by virtue of the fact that the greater the degree of crosslinking, the less the granules are able to swell. The consistency coefficient decreased with increased crosslinking while the flow behavior index was observed to increase. The increase in the flow behavior index as was attributed to the ability of the granules to resist deformation as crosslinking is increased. Lastly, the tendency toward a yield stress decreased with increased crosslinking, because the granules are less able to swell and imbibe water.

Starch pastes at other concentrations were made to obtain other information. The consistency coefficient was observed to increase with increasing concentration which confirmed the observations made by Doublier (1981, 1987). The flow behavior index decreased with increasing concentration which contradicts the observation of Evans and Haisman (1979). The author also determined the concentration at which the starches would imbibe all of the available water (the close-packing concentration). It was

1.76% for native waxy maize and increased with the degree of crosslinking (2.60, 3.44, and 4.22%). The close-packing concentration for the native waxy maize is notably less than those seen by Christianson and Bagley (1982) for native corn starch. This may be due to lack of amylose in the starch granules or the difference in cook temperatures (the close-packing percentage decreases as the cook temperature increases). During the determination of the close-packing concentration, the author saw that very little starch had solubilized after being cooked at 90°C, particularly for the crosslinked starches. In fact, there was so little solubilization that the author states that the pastes can be treated as dispersions of swollen granules with no influence from solubilized starch.

The final work on starch rheology to be reviewed is that by Doublier (1987) where the rheology of two cereal starches (wheat and maize) was compared to the rheology of two legume starches (faba bean and smooth pea). The effect of heating rate was also examined. The starches were cooked on two different viscoamylographs to 96°C. Concentrations of 5-10% were cooked on a Brabender viscoamylograph which heated the suspensions at a rate of 1.5°C/minute. A 9% concentration of the starches was heated on an Ottawa Starch Viscometer which heated the suspensions at a rate of approximately 6°C/minute. Rheological tests were done on a Rheomat 30 (concentric cylinder) viscometer at 60°C covering a shear rate range of 0-660 s^{-1}.

The legume starches were found to solubilize at lower temperatures than the cereal starches but yielded pastes of comparable consistency. For all of the starches, the heating rate was seen to greatly affect the amount of solubilization and the degree of swelling; the slower the heating rate, the less viscous the paste. The rheology of the pastes could be explained in terms of the solubilization and the degree of swelling; the rapid heating rate increased the consistency coefficient. Legume starches were more affected in this regard than were the cereal starches. In other words, the rheology of the legume starches is more sensitive to pasting conditions than cereal starches. All of the starches considered were shear-thinning, and the consistency coefficient was observed to increase with concentration which is consistent with all previous observations. The author finally sought to explain the rheology in terms of the amount of starch solubilized and the volume fraction and deformability of the swollen granules.

It should lastly be noted that Hoseney (1986) states that shear-thinning is due to solubilized molecules orienting themselves in the direction of flow when a stress is applied to the fluid, and that the more soluble the starch, the more shear-thinning it is. This statement does not necessarily contradict the findings of Bagley and Christianson (1982) and Christianson and Bagley (1983), because their experiments were done on pastes where little

of the amylose was solubilized. However, the statement by Hoseney (1986) is incomplete because it does not account for the deformability of the starch granules. If orientation of the macromolecules in the continuous phase in the direction of flow enhances shear-thinning, one might speculate that starches containing amylose are more prone to exhibit slip, because molecular alignment would first occur in the boundary layer where the shear stress is highest. Also, waxy starches (which contain no amylose) might exhibit Newtonian or dilatant behavior until the temperature is high enough to solubilize amylopectin and soften the granule.

2.3. Summary

Several observations, distilled from the works reviewed above, are summarized here.

1.) Gelatinized starch "solutions" are two phase and are comprised of a continuous phase containing solubilized macromolecules and dispersed phase comprised of swollen granules. The amount of dissolved macromolecules depends on the type of starch (waxy, legume or cereal, etc.) and the temperature at which it is cooked. The degree to which the granules are swollen depends on the cook temperature, the rate of heating, and whether the starch is crosslinked.

2.) Apart from the effects of the solubilized macromolecules, the rheology of starch suspensions depends on the volume fraction of the swollen granules and how

deformable they are. When the granules are deformable, shear-thinning behavior is usually observed for all concentrations. When the volume fraction reaches 0.7 there is a rapid increase in viscosity with further increases in concentration. If the granules are not deformable, and the concentration is such that the granules are near close packing, dilatancy will be observed. Increasing the shear stress by reducing the temperature of the suspension, or by increasing the concentration, may induce Newtonian or shear thinning behavior in a suspension that was previously dilatant.

3.) The consistency coefficient was always observed to increase with starch concentration.

4.) The flow behavior index is a function of concentration.

5.) In the one study where it was examined, the consistency coefficient was observed to decrease with temperature and was modeled with an Arrhenius relationship.

CHAPTER THREE

ANALYTICAL METHODS IN TUBE VISCOMETRY

3.1. Introduction

The theory associated with tube viscometry has been well established for many years. In this chapter, the pertinent equations and their assumptions are presented for completeness and to serve as a reference for the rest of the text.

3.2. Shear Stress and Shear Rate Calculations.

An expression for the shear stress acting on a fluid flowing through a tube can be obtained by performing a force balance on an arbitrary core of fluid, which yields:

$$\sigma=(\Delta Pr)/(2L) \quad \ldots\ldots\ldots\ldots\ldots (3.1)$$

This expression can also be obtained by performing a shell momentum balance (Bird et al., 1960). At the wall of the tube, i.e. at r=R, the shear stress is a maximum and is denoted σ_w. Therefore, the wall shear stress can be obtained by measuring the pressure drop, ΔP, over a length of tube, L, with a known radius, R. There are no

assumptions associated with this equation.

The expression for the volumetric flow rate in a tube is:

$$Q=((\pi R^3)/\sigma_w^3)\int_0^{\sigma_w}\sigma^2 f(\sigma)\,d\sigma \quad .....(3.2)$$

for any time-independent fluid. For viscometric flow in a pipe, $f(\sigma)$ is the fluid velocity gradient i.e., the shear rate and is a unique function which relates the shear rate to the shear stress (Whorlow, 1980). Rabinowitsch (1929) and Mooney (1931) manipulated this equation to obtain the shear rate explicitly:

$$du/dr=\dot{\gamma}=(3Q)/(\pi R^3) + \sigma_w\left[\frac{d(Q/\pi R^3)}{d\sigma_w}\right] \quad .....(3.3)$$

This is the classic Rabinowitsch-Mooney equation (Bird et al., 1960; Whorlow, 1980). Several assumptions have to be met in the application of Equation 3.3: laminar flow, homogeneous and isotropic material, isothermal, steady state conditions, incompressible fluid, and no slip (the velocity of the fluid at the wall is zero). Slip is discussed in the following section.

The derivative in Equation 3.3 is evaluated at values of wall shear stress that correspond to the volumetric flow rate, Q. Equation 3.3 is general, meaning that no particular fluid model was assumed in the derivation. Also,

Equation 3.3 is is most easily evaluated for fluids where plots of $Q/(\pi R^3)$ versus σ_w are nearly linear, which is common for fluids with Newtonian, Bingham, and power law behavior (Whorlow, 1980).

Plots of shear stress versus shear rate are called rheograms, and there are many models available to describe the rheological properties exhibited in these plots. The Herschel-Bulkley model is very useful, because the Newtonian, Bingham, and power law models are all special cases of it. The Herschel-Bulkley model is:

$$\sigma = K(\dot{\gamma})^n + \sigma_0 \quad \ldots\ldots\ldots\ldots (3.4)$$

When n equals one the fluid is Bingham, when σ_0 equals zero the fluid is power law, and when n equals one and σ_0 equals zero, the fluid is Newtonian.

3.3. Evaluation of Slip (Wall Effects).

Slip is the phenomenon where the velocity of a fluid flowing under an applied stress appears not to be zero at the stationary wall containing the fluid. At a molecular level, slip never occurs, because the smoothest wall is sufficiently rough to prevent it. However, for suspensions and two phase systems, the portion of the fluid system having a viscosity less than the bulk viscosity may form a layer at the wall which acts as a lubricant for the main body of material causing slip. An example of a two phase

system is paper pulp where a thin layer of water forms at the wall. A second type of two phase system is frozen orange juice concentrate where liquid orange juice forms a layer at the wall. Figure 3.1 is a diagram of velocity profiles with and without slip. If slip is present, the flow rate is larger than it would be if slip was not present causing errors in shear rate calculations.

To account for slip, the following modification to the expression for the volumetric flow rate in a tube is made (Whorlow, 1980):

$$Q=((\pi R^3)/\sigma_w^3)) \int_0^{\sigma_w} \sigma^2 f(\sigma) d\sigma + \pi R^2 U_s \quad ...(3.5)$$

where U_s is the slip velocity (m/s) and is a function only of the wall shear stress. If a slip coefficient is defined as $\beta=U_s/\sigma_w$, then the modified expression for the volumetric flow rate can be written as:

$$Q/(\pi R^3 \sigma_w)=\beta/R + (1/\sigma_w^4) \int_0^{\sigma_w} \sigma^2 f(\sigma) d\sigma \quad ...(3.6)$$

The slip coefficient, β, can be evaluated from tube viscometer measurements from tubes of the same length but different radii. Skelland (1967) and Darby (1976) have summarized the procedure which has become the standard for the determination of the slip coefficient. What is finally obtained is the slip coefficient as a function of the wall

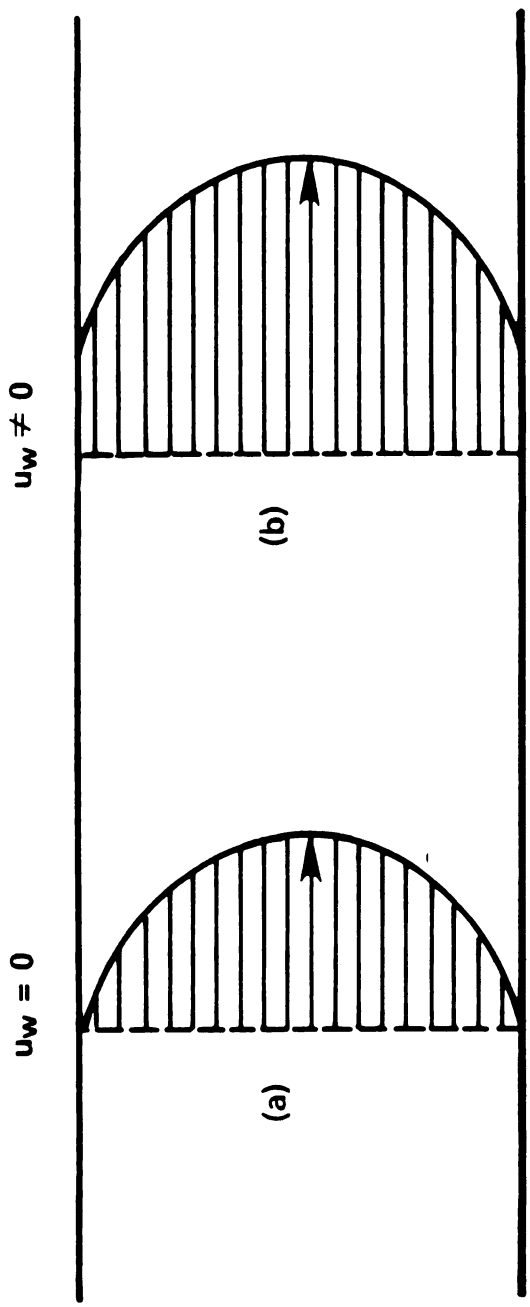

FIGURE 3.1. VELOCITY PROFILE OF A POWER LAW FLUID IN A PIPE: WITHOUT SLIP (a) - WITH SLIP (b).

shear stress which is used to correct volumetric flow rates as follows:

$$Q_{\text{no slip}} = Q_{\text{measured}} - \beta\sigma_w\pi R^2 \quad \text{.....(3.7)}$$

where the wall shear stress is that corresponding to the measured volumetric flow rate. The corrected volumetric flow rate values are then used in the Rabinowitsch-Mooney equation (Equation 3.3) to obtain shear rate values. It should be noted that the wall shear stress values should be corrected for excess pressure loss due to end effects, if they are a problem. End effects are discussed in the following section.

3.4. End Effects

End effects are mechanical energy losses associated with flow transitions at the entrance and exit of the tube viscometer. At the end of the tube, part of the work done by the driving pressure is converted to the kinetic energy of the emerging stream (Whorlow, 1980). At the entrance of the tube, a certain length is required before the boundary layer, which starts developing at the entrance of the tube, converges on the center line and fully developed flow ensues. The length required for fully developed flow is called the entrance length. Static pressure drop along the entrance length is greater than that along an equal length of tube in the fully developed region

(Skelland, 1967). Consequently, placement of a pressure tap in the entrance length, or too close to the end of the tube, can result in erroneous pressure drop readings. In turn, this makes the calculated values of wall shear stress in error.

Whorlow (1980) presents a method for correcting for the kinetic energy loss at the end of the tube. However, it is stated that, in practice, the correction is important only for low viscosity liquids at high flow rates. The criteria given is to compare ρv^2 to the total pressure drop. If small compared to the pressure drop, the correction can be neglected. The kinetic energy correction is more important for capillary (extrusion) viscometers where the force required to push a fluid through a capillary open to the atmosphere is recorded. For large tube viscometers where a pressure tap can be placed upstream from the end of the tube, the kinetic energy correction is not needed, because the streamlines are still parallel to the tube wall.

The correction for entrance length effects is a more difficult problem. Theoretically, for a non-Newtonian power law fluid, the entrance length can be calculated if the rheological parameters are known. Skelland (1967) presents a review of the methods available to do this. These methods, however, are of little use in the characterization of an unknown fluid. Skelland (1967) also reviews an empirical method, developed by Bagley (1957), that

compensates for entrance length effects. In this method, pressure drop measurements are collected for various ratios of length over diameter for constant values of volumetric flow rate. The pressure drop is plotted against the length over diameter ratio yielding a fictitious length which is added to the "L" in Equation 3.1. The effect is to yield values of wall shear stress unaffected by entrance length. Alternatively, from the same plots, a correction to the pressure drop term can be obtained which achieves the same outcome. The correction is subtracted from the pressure drop term in Equation 3.1.

Some experimental work has been completed examining entrance length effects. Yoo (1974) observed that for Newtonian and inelastic non-Newtonian fluids, pressure drop readings were unaffected beyond forty diameters from the entrance. For viscoelastic fluids, he observed that eighty diameters were required. Tung (1978) was able to confirm the observations of Yoo (1974) while observing that an entrance length of one-hundred diameters was required for certain solutions of Separan. Therefore, placement of the leading pressure tap greater than one-hundred diameters downstream from the entrance should eliminate entrance length effects on pressure drop readings.

Finally, the analytical relationship for determining the entrance length for Newtonian fluids is given as a reference (Potter and Foss, 1982):

$$L_e = 0.0575D\ Re_N \quad \text{.....(3.8)}$$

where L_e is the entrance length, D is the diameter, and Re_N is the Newtonian Reynolds number.

3.5. Laminar Flow Criteria

The most general expressions for laminar flow criteria in non-Newtonian fluids are those developed by Hanks and Ricks (1974) for Herschel-Bulkley fluids. The Herschel-Bulkley model is general, and Bingham, Newtonian, and power-law fluids can all be considered a special case of it, as mentioned previously. Steffe and Morgan (1986) summarized the work of Hanks and Ricks (1974) in a paper on pipeline design and pump selection for non-Newtonian fluid foods. The critical Reynolds number for pipe flow of a power-law fluid is:

$$\text{Critical Re} = \frac{6464\ n\ (2+n)^{(2+n)/(1+n)}}{(1+3n)^2} \quad \text{.....(3.9)}$$

The generalized Reynolds number for a Herschel-Bulkley fluid and all of its special cases is:

$$Re = \frac{D^n (v^{2-n}) \rho}{8^{n-1} K} \left[\frac{4n}{1+3n}\right] \quad \text{.....(3.10)}$$

To determine the critical Reynolds number for fluids with a yield stress, calculation of the generalized

Hedstrom number is also required. This is covered by Steffe and Morgan (1986) and will not be presented here. The equations presented above will be used to determine if the laminar flow criterion, required by the Rabinowitsch-Mooney equation (Equation 3.2), is met.

CHAPTER FOUR

MATERIALS AND METHODS

4.1. Description of the Tube Viscometer System.

To perform a rheological characterization of crosslinked waxy maize starch solutions under low acid aseptic processing conditions, a viscometer system that allowed heating of the starch solution to 143°C, while simultaneously preventing boiling of the fluid, was required. This was achieved with a tube viscometer system.

Figure 4.1 is a pictorial diagram of the tube viscometer system built for this purpose. Parts are listed in Table 4.1, with the part numbers corresponding to the label numbers in Figure 4.1. The system consisted of two Cherry Burrell Model UAS 50 vats (Cherry Burrell, Cedar Rapids, IA), a Waukesau Model 10 positive displacement pump (Abex Corp., Waukesau, WI), an air filled shock tube with a dial pressure gauge mounted on top, a Micro Motion Model DL100 mass flow meter (Micro Motion, Denver, CO), a concentric tube heat exchanger, and several tube viscometers of different diameters. The lines leading from the pressure taps in the tube viscometer to the pressure transducer are 0.95 centimeter in diameter, stainless steel

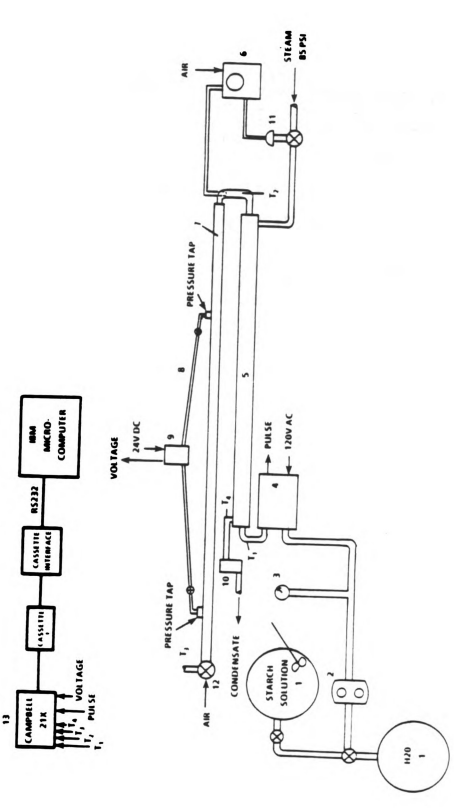

FIGURE 4.1. DIAGRAM OF TUBE VISCOMETER SYSTEM.

Table 4.1. Parts list for the tube viscometer system (part numbers correspond to Figure 1.1).

1. Cherry Burrell UAS 50 vats
2. Waukesha Model 10 positive displacement pump
3. Air filled shock tube with dial pressure guage
4. Micro Motion Model DL 100 mass flow meter
5. Concentric tube heat exchanger
6. Taylor Model D 121R Fullscope recorder/controller
7. Tube viscometer
8. Stainless steel braid flexible hydraulic lines with bleeder petcocks
9. Taylor Model 405 T capacitive diaphram differential pressure transducer
10. Steam trap
11. Masoneilen "Little Scotty" air to open flow regulator
12. Cherry Burrell air to close flow control valve
13. Data acquisition system

braid, flexible hose fitted with petcocks located approximately 0.3 meters from the pressure taps to facilitate cleaning. The length between pressure taps on all of the tube viscometers is 4.59 meters. The diameter of the tube viscometer used for these experiments was 1.27 centimeters. The length from the entrance of the tube viscometer to the first pressure tap is 105 diameters. Consequently, end effects were assumed to have no effect on pressure readings.

Flow in the system was controlled by an air operated (air to close) flow control valve (Cherry Burrell, Cedar Rapids, IA) located at the end of the tube viscometer operating in conjunction with the pump. The valve and the pump work against each other to create the pressure in the system necessary to prevent boiling of fluid heated above the atmospheric boiling point and prevent gas bubbles from forming at the heat exchanger wall, while controlling the flow rate.

Pressure drop in the tube viscometer was measured by a Taylor Model 405T capacitive diaphram type differential pressure transducer (Taylor Instruments, Rochester, NY). This type of pressure transducer was chosen because early tests showed that the inherent error associated with two individual strain gage type transducers was larger than the smallest pressure drop being measured. This test is described in Section 4.5.1. Capacitive diaphram type transducers are capable of higher resolution than either

strain gage or variable reluctance type transducers.

Fluid temperature was controlled by a Taylor Model D 121 Fullscope recorder/controller (Taylor Instruments, Rochester, NY) operating a Masoneilen "Little Scotty" flow regulator (Dresser Industries, Canton, MA). The regulator operates air to open and regulates the high pressure steam supplied to the heat exchanger. The recorder/controller measured the temperature of the fluid leaving the heat exchanger while controlling the steam (via the flow regulator) going to the heat exchanger. To achieve this, the sensitivity of the recorder/controller was set at the lowest possible setting.

The data acquisition system used was a Campbell 21X Micrologger (Campbell Scientific, Inc., Logan, UT). After each run, the accumulated data was recorded on a cassette tape which was downloaded to a floppy disk using a Campbell Model C20 cassette interface with a microcomputer.

The shock tube was installed to dampen pump pulsation in addition to eliminating a resonance problem encountered at certain combinations of system pressure and pump frequency, which was affecting output from the pressure transducer.

One of the vats was supplied with an agitator paddle controlled by a two speed motor. This same vat was also supplied with steam to allow cooking of the starch in the vat, if desired.

Finally, the tube viscometer system was insulated with

a fiberglass based insulation, approximately one inch in thickness, from the entrance of the heat exchanger to the end of the tube viscometer. Insulation of the tube viscometer was done primarily to minimize temperature loss effects on viscosity.

4.2. Modification and Calibration of the Mass Flow Meter.

The Micromotion (Micromotion, Denver, CO) mass flow meter consists of a sensor and a remote electronics unit. The sensor is a tube wound into a square spiral which is encased in a stainless steel box. A magnetic coil, located on the spiral wound tube, forces the tube and the fluid inside it to vibrate. When fluid flows through the spiral tubing, a torque is created which causes the legs of the spiral wound tube to change position relative to each other. The amount of twist is proportional to the mass flow rate. As the tube vibrates and twists, magnetic position detectors define the time that the legs of the coil pass their midpoints. Since the legs are twisting in opposite directions, a phase shift is created that is converted to a voltage. This voltage is then amplified and sent to a voltage to frequency converter. Amplification is user selectable through gain switch settings, and the maximum amplification results in a three volt output. Optimum performance is obtained from the meter when there is a three volt output at the maximum flow rate of the span. When the mass flow meter was received, the gain switch

settings were set so that a three volt output was obtained for a mass flow rate of 136.3 kg/min. Since the experiments to be conducted herein occur at low shear rate values, the span of the meter was changed to the lowest range possible for this meter: 0 to 18.1 kg/min. In other words, the gain switch settings were changed so that a three volt output was obtained for a flow rate of 18.1 kg/min. Using the smallest span provided maximum sensitivity and resolution. The gain switch settings for both flow rates are presented in Table 4.2. A more detailed explanation of changing the meter span can be obtained from the instruction manual that accompanies the meter.

The zero to three volt output of the meter is converted to a zero to 10,000 Hz frequency at the voltage to frequency converter. This frequency can be scaled before final output to a data acquisition system which is part of the act of calibration. Scaling is done using rotary switches on the frequency board in the remote electronics unit. When the meter was received, the frequency range switches were set so the meter output was 600 pulses per pound per minute. The switches were changed so that the output of the meter was 100 pulses per pound per minute. This was done so that a digital flow indicator attached to the meter could be used. The digital flow indicator provided knowledge of the mass flow rate without having to read the data acquisition system. Also, using 100 pulses per pound per minute makes calculation of the mass flow

Table 4.2. Gain switch settings for the mass flow meter

Switch #	1	2	3	4	5	6	7	8
Old Setting	on	off	off	on	on	off	off	off
New Setting	on	on	off	off	off	off	on	off

Table 4.3. Frequency switch settings for the mass flow meter.

Switch #	1	2	3	4
old setting	5	9	4	2
new setting	7	9	2	2

Table 4.4. Final five readings from point calibration of the mass flow meter (lbs/min).

reading #	meter indicated rate	true rate
1	39.08	39.06
2	38.31	38.58
3	38.31	38.52
4	38.33	38.54
5	38.42	38.68

rate simple. The flow indicator only indicates flow rate in lbm/min, i.e., non-metric.

Suggested initial values for the frequency range switches were obtained from technical support personnel at Micromotion. Final switch settings were then obtained by comparing the mass flow rate indicated by the mass flow meter to the true mass flow rate determined by weighing water accumulated in a bucket. If necessary, the switch settings were changed and the procedure was repeated. This is the first part of the calibration process. The total mass flow rate, as determined by the mass flow meter, was obtained by using a pulse totalizer and totalizing the pulses over the time the water was being accumulated in the bucket. The last five readings for the final switch settings are presented in Table 4.4. Frequency range switch settings for both 600 and 100 pulses per pound per minute are presented in Table 4.3. Note that this part of the calibration process is essentially a point calibration performed at the upper end of the span. This was done because the meter is most accurate at the upper end of the span.

The second and final part of the calibration process was the creation of a calibration curve. To obtain this, the mass flow rate indicated by the meter was compared to the true mass flowrate at various points throughout the span. Initial readings were at the top of the span, were gradually decreased to the bottom of the span, then were

increased to the top of the span again. This process yields a relationship where the true mass flow rate can be obtained from the mass flow rate indicated by the meter at any point in the span. Hysteresis effects are also incorporated into this curve. Thirty-two readings were taken in all. The raw data are presented in Table 4.5. The calibration curve is presented in Figure 4.2. Again, the calibration was done in English units because the digital flow indicator on the meter only indicates in units of lbm/min. The equation for the calibration curve, rearranged to solve for the true mass flow rate, is

$$m_t = (m_m+0.410)/1.005 \quad \ldots\ldots\ldots\ldots\ldots \quad (4.1)$$

where:

m_t = true mass flow rate (lbm/min)

m_m = meter indicated mass flow rate (lbm/min)

Equation 4.1 was used to calculate true mass flow rates for all experiments; the data, however, were converted to SI units prior to doing shear stress calculations.

Using the equation for the calibration curve (Equation 4.1 rearranged to solve for m_m) to calculate predicted values from the meter indicated values given in Table 4.5 enables calculation of the total sum squared error and the mean squared error for the calibration curve: total sum squared error is 0.4247 and the mean squared error is

Table 4.5. Raw data points used to create the calibration curve for the mass flow meter (lbs/min).

reading #	meter indicated rate	true rate
1	38.37	38.94
2	38.05	38.00
3	36.14	36.20
4	33.59	33.96
5	30.19	30.54
6	29.91	28.24
7	25.24	25.44
8	22.39	22.60
9	19.82	20.06
10	17.34	17.70
11	14.47	14.72
12	11.77	12.02
13	8.99	9.35
14	6.35	6.73
15	3.06	3.47
16	0.98	1.37
17	0.33	0.74
18	2.19	2.60
19	3.82	4.24
20	6.51	6.89
21	9.25	9.62
22	11.74	12.15
23	14.65	14.99
24	17.22	17.49
25	19.91	20.34
26	22.71	23.06
27	25.35	25.68
28	28.20	28.38
29	30.92	31.18
30	33.49	33.80
31	35.94	36.34
32	39.18	39.14

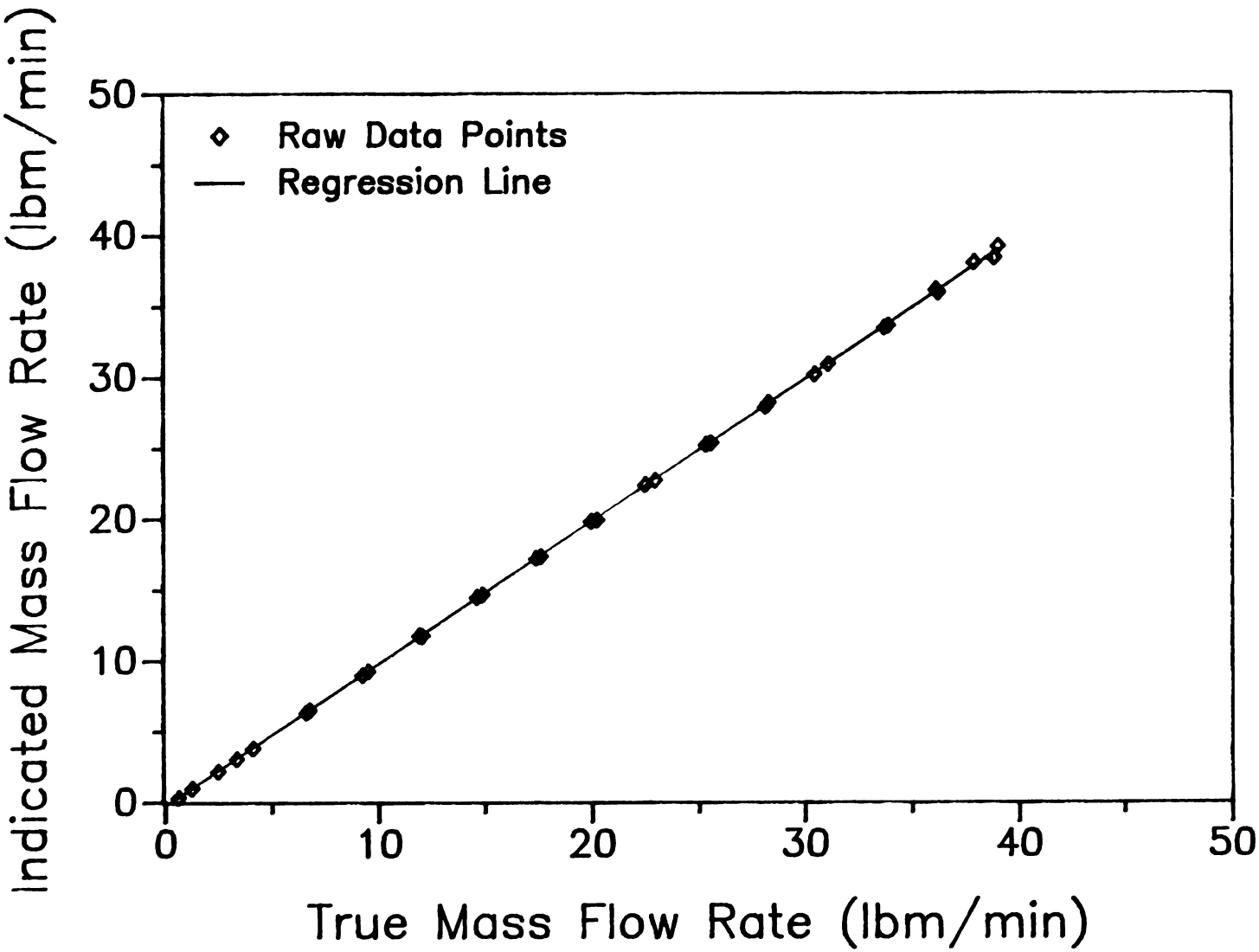

Figure 4.2 – Mass Flow Meter Calibration Curve

0.0142. The square root of the mean squared error is the standard deviation of the calibration curve which is 0.119 lbm/min. The standard deviation of the true mass flow rate, m_t, is approximately the standard deviation of the calibration curve divided by the slope (Doebelin, 1983) which is equal to 0.119 lbm/min.

Equation 4.1 was used to obtain predicted mass flow rates from the meter indicated values in Table 4.5. The predicted values are compared to the true mass flow rate in Table 4.6. It can be seen that Equation 4.1 does an excellent job of compensating for meter error, particularly at the lower flow rates where the meter error becomes large when viewed as a percentage of total flow.

Finally, modification of the frequency board in the remote electronics unit was required. The mass flow meter, as received from Micromotion, came with the standard output setup on the frequency board. This output is a fifteen volt square-wave which is suitable for operating electro/mechanical counters. To operate the digital flow indicator, and the pulse counter in the data acquisition system, the optional isolated output was required. Rather then send the meter back to Micromotion for modification, the modification was performed at Michigan State University. Figure 4.3 shows electrical diagrams of the output portion of the frequency board. Figure 4.3a is the optional isolated output as it would be received from Micromotion, and Figure 4.3b is the the modified board.

Table 4.6. Mass flow meter calibration curve performance; meter indicated, predicted, and the true mass flow rate.

meter indicated rate	predicted rate	true rate
38.37	38.59	38.94
38.05	38.27	38.00
36.14	36.37	36.20
33.59	33.83	33.96
30.19	30.45	30.54
27.91	28.18	28.24
25.24	25.52	25.44
22.39	22.69	22.60
19.82	20.13	20.06
17.34	17.66	17.70
14.47	14.81	14.72
11.77	12.12	12.02
8.99	9.35	9.35
6.35	6.73	6.73
3.06	3.45	3.47
0.98	1.38	1.37
0.33	0.74	0.74
2.19	2.59	2.60
3.82	4.21	4.24
6.51	6.89	6.89
9.25	9.61	9.62
11.74	12.09	12.15
14.65	14.99	14.99
17.22	17.54	17.49
19.91	20.22	20.34
22.71	23.00	23.06
25.35	25.63	25.68
28.20	28.47	28.38
30.92	31.17	31.18
33.49	33.73	33.80
35.94	36.17	36.34
39.18	39.39	39.14

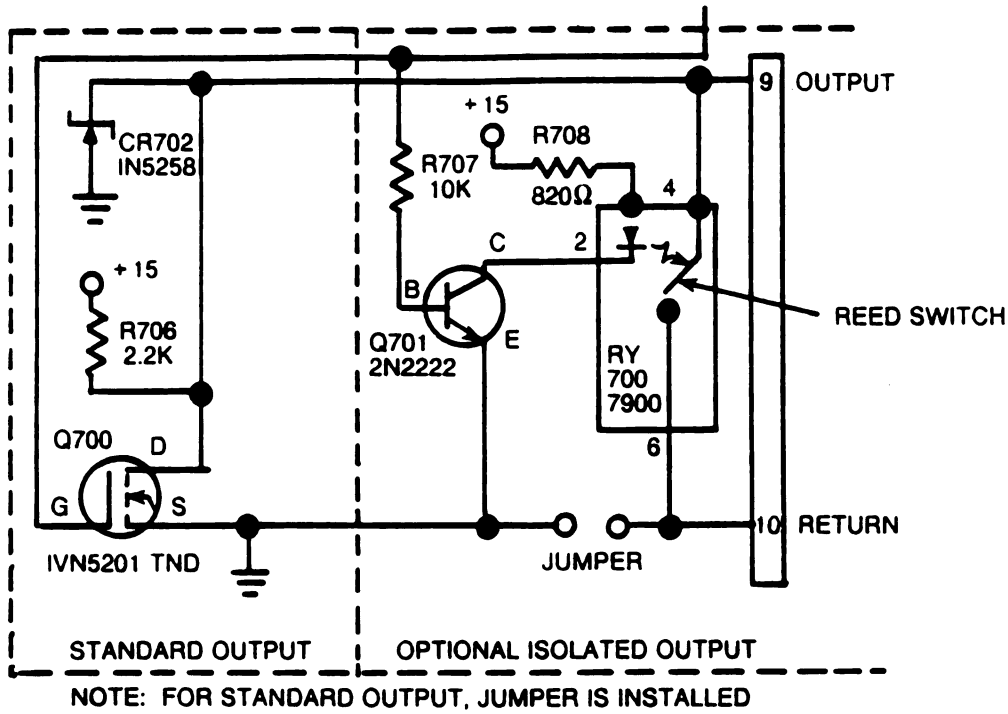

FIGURE 4.3a. STANDARD ISOLATED OUTPUT AS RECEIVED FROM MICROMOTION.

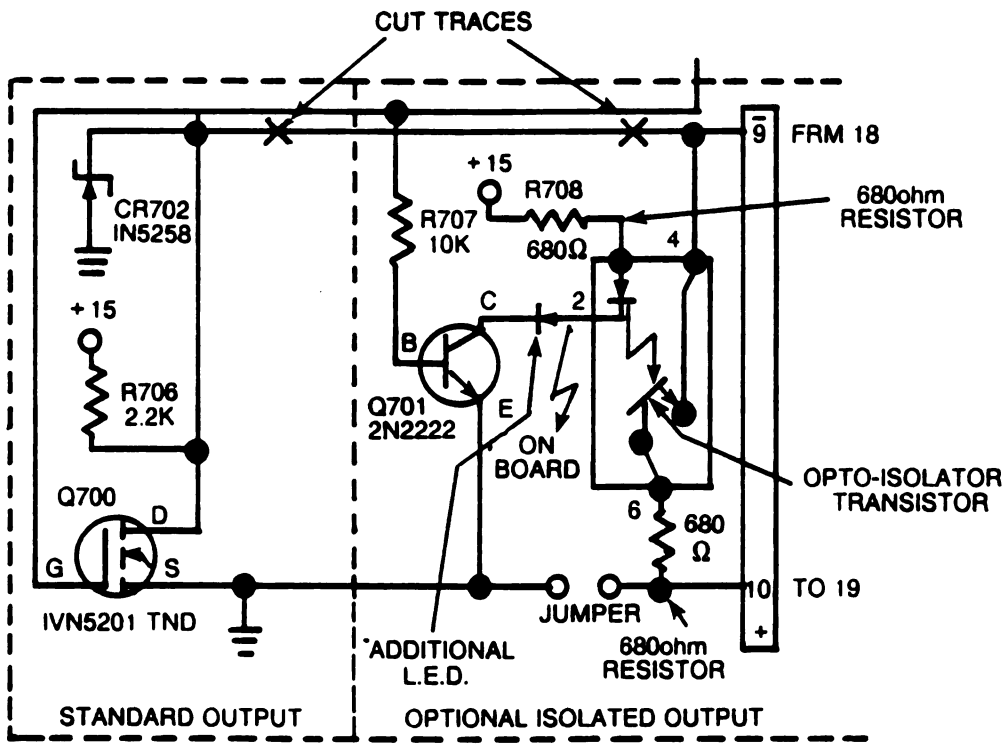

FIGURE 4.3b. MODIFIED BOARD

Isolation was achieved by cutting traces in two places (Figure 4.3b). In place of the Reed switch in Figure 4.3a, an opto-isolated transistor was installed (Figure 4.3b). Two 680 Ohm resistors were installed as circuit protection as well as an extra light emitting diode for diagnostic purposes (Figure 4.3b). The modification had the effect of interchanging terminals 18 and 19 on the terminal board. Note again that the modification described here is not necessary if the optional isolated output is ordered with the meter.

4.3. Pressure Transducer Calibration

The differential pressure transducer selected is one of the 400T series supplied by Taylor Instruments (Rochester, NY). The particular model chosen was the 405T where the selection of the particular model is based on the span requirement. Model 405T spans 0-6 to 0-38 kPa. A particular preset span from within this range is selected by the customer, and is set by the supplier, prior to shipment. The span requested for the transducer used in these experiments was 0-13.8 kPa. This was based on a preliminary test conducted to determine the maximum pressure drop expected (the preliminary test is described in Section 4.5.1).

The calibration of the transducer is the act of creating a calibration curve. To accomplish this, the transducer was fitted with a barbed hose fitting attached

to the high side port so that a clear tygon hose could be run straight up from the transducer. Small increments of water were then added to the hose creating a head over the high side port. The low side port was left open to the atmosphere. The height of the water in the hose was measured after each water addition and converted to a pressure. Output from the transducer for each water height was recorded to develop a relationship between transducer output and pressure. Increments of water were added until the head was roughly equal to the maximum span, after which water was drained in increments until the head was near zero. The calibration curve consequently includes hysteresis effects. The pressure transducer is a two wire transmitter with a 4-20 milliamp output. A 250 Ohm resistor was placed across the two wires to convert the 4-20 milliamp output to the 1000-5000 millivolts required by the data acquisition system. The raw data (Table 4.7) were used to create the calibration curve (Figure 4.4). The pressure transducer calibration curve rearranged to solve for the pressure drop is

$$\Delta P = (V - 1001.4)/0.2975 \quad \text{..... (4.2)}$$

where:

ΔP = pressure drop (Pa)

V = transducer voltage output (mV)

Equation 4.2 was used to determine pressure drop from

Table 4.7. The raw data points used to create the pressure transducer calibration curve.

reading #	pressure (Pa)	millivolts
1	0	1001
2	603.3	1176
3	1163.1	1347
4	2158.9	1644
5	2687.0	1804
6	3309.0	1984
7	4226.5	2260
8	4926.2	2467
9	6030.3	2798
10	7149.9	3132
11	7880.7	3348
12	8829.3	3633
13	9980.0	3973
14	11814.9	4516
15	12390.2	4689
16	12918.9	4840
17	13540.9	5026
18	13261.0	4943
19	13043.3	4879
20	12576.8	4739
21	11892.6	4540
22	11146.2	4319
23	10602.0	4155
24	9948.9	3964
25	9342.4	3782
26	8736.0	3600
27	8114.0	3416
28	7227.6	3153
29	6465.7	2927
30	5797.0	2730
31	4957.3	2476
32	4179.8	2245
33	3371.2	2009
34	2858.1	1853
35	2189.4	1652
36	1567.4	1464
37	1054.3	1309
38	572.2	1168

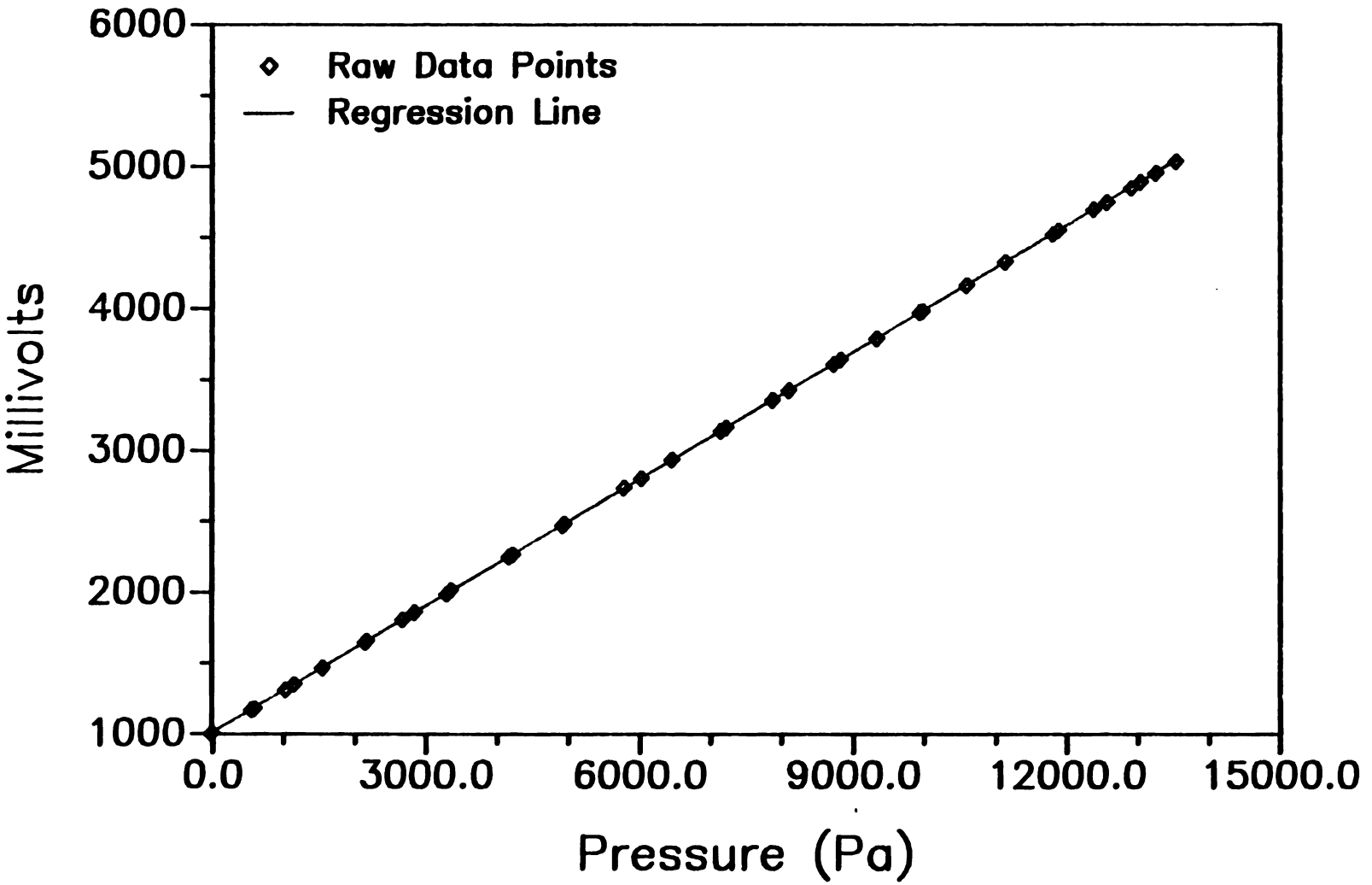

Figure 4.4 – Pressure Transducer Calibration Curve

the pressure transducer output for all experiments. As with the calibration curve for the mass flow meter, the sum squared error and the mean squared error were calculated and were 292.753 and 8.132, respectively. The square root of the mean squared error is the standard deviation of the calibration curve which is 2.852 millivolts. The standard deviation of the pressure drop is approximately the standard deviation of the calibration curve divided by the slope (Doebelin, 1983) which is equal to 9.59 Pa.

4.4. Description of Starch, Starch Preparation and a Typical Experimental Run

The starch used in all experiments was National 465 supplied by National Starch and Chemical Corporation of Bridgewater, NJ (lot# DH4763). National 465 is a crosslinked waxy maize (corn) starch. The manufacturer recommends the product for low acid foods that are either conventionally retorted or aseptically processed. Three samples dried in a moisture oven for twenty-four hours at 100°C had an average moisture content of 9.24%. Two starch concentrations were used in the experiments: 2 and 3% on a wet basis (1.815 and 2.723% on a dry basis). The percentages are based on g starch/100g water, and are typical for the liquid portion of foods such as chili and beef stew.

To prepare the starch, the vat equipped with the motor and agitator paddle was filled with 156.2 kg of tap water

at room temperature. The appropriate amount of starch (3.12 kg for 1.82% or 4.69 kg for 2.72%) was added to the vat in the following way; a small portion of the water was removed from the vat in a bucket. A starch slurry was created by slowly dispersing the starch into the bucket of water using a wisk to prevent clumping. The slurry was immediately added to the vat while the agitator paddle was running. This prevented settling of the starch while it was being pumped into the system. Tap water was used because of the large amount of starch solution required for each experiment and because this is standard industry practice for food production. A sample of tap water was taken to measure pH for each experiment. Note that the starch was not partially gelatinized prior to sending it into the system. A preliminary test conducted to determine the time required to achieve a stable viscosity of starch gelatinized in the vat showed that the starch continually increases in viscosity when maintained at 80°C. This test is described in detail in Section 4.5.4.

In a typical experimental run, the system was first brought up to operating conditions by pumping room temperature water through it at a rate of 16 kg/min for thirty minutes. This allows proper warm-up time for the mass flow meter, and the high flow rate insures evacuation of all air bubbles from the system (the mass flow meter is extremely sensitive to air bubbles within the sensor tube). After thirty minutes, the pump was turned down to the

lowest setting, and the three way valve between the two vats was turned so that starch solution was pumped into the system instead of water. The flow rate was then increased to 16 kg/min for four minutes to insure displacement of all water from the system. After this, the system was pressurized while simultaneously bringing the flow rate to the appropriate level for the first measurement. This was achieved by turning up the pump speed while closing the air operated flow control valve at the end of the system (Figure 4.1).

The system was operated at a pressure between 552 and 690 kPa which was read from the dial pressure gauge on top of the shock tube. This pressure was required to prevent boiling at the wall of the heat exchanger. After achieving the flow rate appropriate for the first measurement, steam was supplied to the heat exchanger by requesting a particular fluid temperature on the recorder/controller. When the correct temperature was achieved, a measurement was taken. The data acquisition system was programmed to take measurements every two seconds and average them every minute. This average value was stored in the memory of the data acquisition system for later retrieval. Data was recorded continuously after the data acquisition system was turned on. Therefore, it was necessary to syncronize the clock in the data acquisition system with a wrist watch to retrieve the correct data. Each measurement consisted of a one minute data collection period. The temperatures of the

starch solution going into, and coming out of, the heat exchanger were recorded along with the mass flow rate, the pressure drop in the tube viscometer, and the temperature of the starch solution at the end of the tube viscometer.

The flow rate was then decreased to a level appropriate for the next measurement. This was achieved by further closing the air operated valve at the end of the system, not by altering pump speed (changing pump speed causes gross changes in the flow rate). Controlling the flow rate in this way has the effect of slightly increasing the system pressure and further increasing slip at the pump. When the desired flow rate was attained, the correct fluid temperature was attained by adjusting the synchronizer wheel on the recorder/controller (Figure 4.5). This was necessary because, for the recorder/controller to control steam flow to the jacket of the heat exchanger while measuring fluid temperature, the sensitivity had to be set at the lowest value (Figure 4.5). This prevented the recorder/controller from making fine adjustments to the fluid temperature. The synchronizer wheel controls the air output from the recorder/controller to the steam regulator. By manually adjusting the synchronizer wheel, the fluid temperature could be controlled to better than ±1.2°C. A measurement was taken when the temperature of the fluid leaving the heat exchanger and entering the tube viscometer was within 1°C of the desired temperature, and the temperature at the end of the tube viscometer had

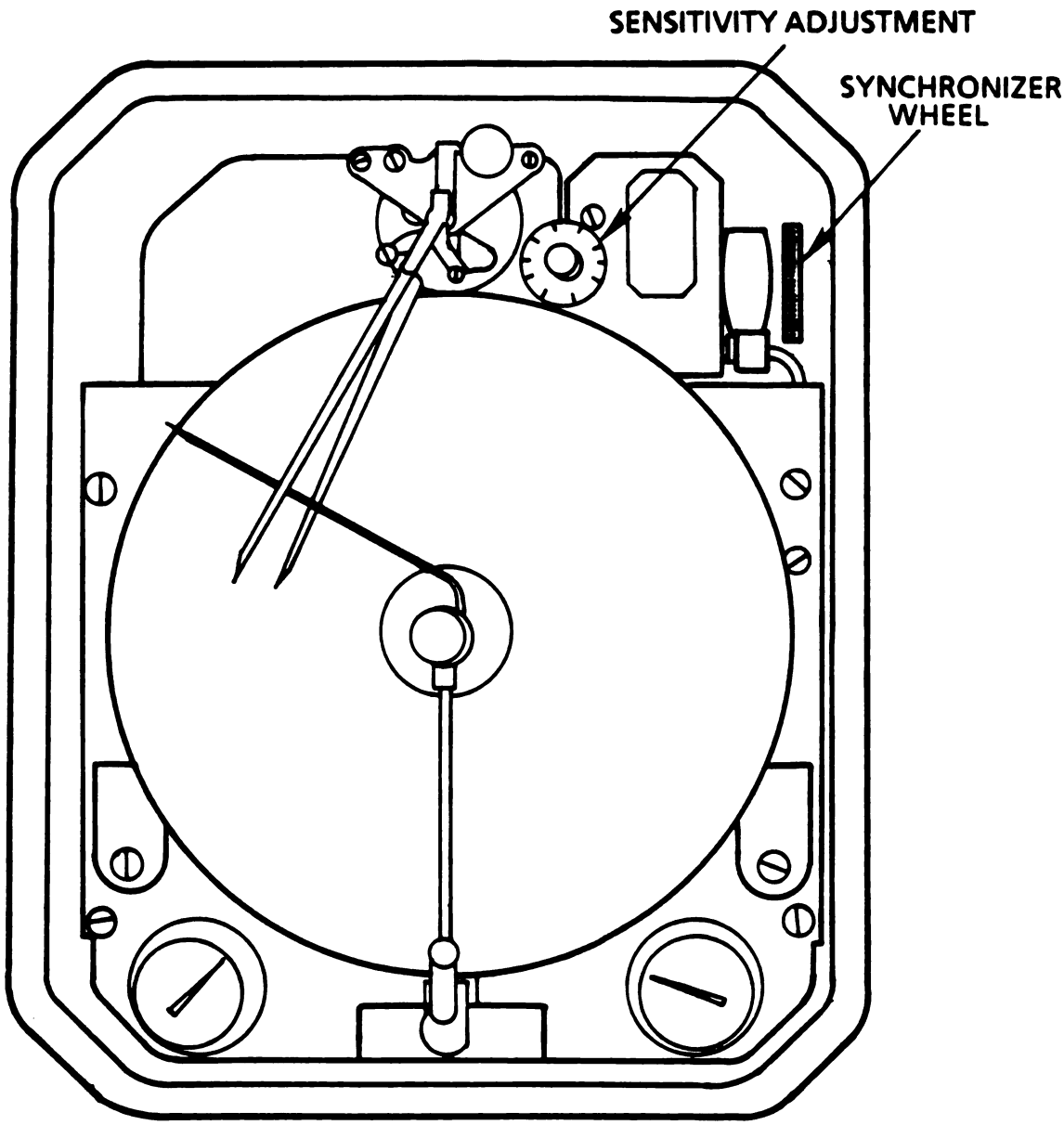

FIGURE 4.5 PICTORIAL DIAGRAM OF RECORDER / CONTROLLER SHOWING LOCATION OF SYNCHRONIZER WHEEL AND SENSITIVITY ADJUSTMENT.

stabilized. If the temperature of the fluid entering the tube viscometer ever drifted farther than 1.2°C from the target temperature, that data point was rejected. This process was repeated until a minimum of six measurements (six different flow rates) were taken. After exiting the tube viscometer, the starch solution flash cools within the body of the air operated valve at the end of the system and is discarded.

After the last measurement was taken, the steam to the heat exchanger was shut off by turning the temperature request indicator on the recorder/controller to the lowest setting. When the temperature of the fluid exiting the tube viscometer was below 100°C, the system was depressurized and the three way valve between the two vats was turned so that water was pumped into the system instead of starch solution. The flow rate was increased to 16 kg/min and allowed to run at this level for approximately twenty minutes to aid in cleaning starch solution from the system. During this time, the petcocks in the lines leading to the pressure transducer were opened to flush any starch solution accumulated in the pressure taps.

Finally, the data was downloaded from the data acquisition system to a cassette, then taken to another area where the data was transferred onto a floppy disk using the Campbell cassette interface and a micro-computer. The data, stored as an ASCII file, was printed out using the DOS print command so that a hard copy was obtained.

4.5. Preliminary Tests

Several preliminary tests were conducted to aid in the design of both the experiments and the tube viscometer system itself. The following is a description of those tests.

4.5.1. The Test for Maximum Pressure Drop

In the first tests on the tube viscometer system, two model 808 Sensotec flush diaphram strain gauge type pressure transducers (Sensotec, Columbus, OH) were used - one at each pressure tap on the tube viscometer. The diaphrams, to which the strain gages were bonded, were in direct contact with the hot starch solution. Results of these tests often showed "negative pressure drop," i.e., the pressure at the second (downstream) tap was higher than at the first tap - a physical impossibility. Inspection of the transducer specifications and subsequent calculations showed that the possible error in the transducers due to temperature effects, combined with inherent error, could produce error larger than the expected pressure drop for room temperature water at selected low flow rates. Discussions with personnel at the National Bureau of Standards led to the purchase of a capacitive diaphram type differential pressure transducer. As mentioned previously, capacitive diaphram transducers are capable of higher resolution than either strain gage or variable reluctance type transducers. Also, the use of a

differential transducer reduces, by half, the effect of inherent transducer error. Note too that the diaphrams of this transducer are not in direct contact with the hot starch solution.

The supplier of the capacitive diaphram transducer required specification of the span requirement prior to shipment. To make this specification, knowledge of the maximum pressure drop that would be seen in any of the experiments was required. Since the fluid properties were not available, the maximum pressure drop could not be calculated. Also, it was felt that the strain gage type transducers were too inaccurate to make the specification. It was important to accurately specify the span because the accuracy specification of the pressure transducer is given as a percent of span, i.e., requesting a span for the transducer that was larger than necessary would increase the possibility of inaccurate readings.

A manometer was used to determine the maximum pressure drop. Since a manometer was not commercially available that could withstand the operating pressure of the system, one was built. Redline gauge glass, supplied by Dow Corning and purchased at a local plumbing and fitting supply house, was used to build the manometer. This glass tubing is normally used as sight glass on boilers and is rated to withstand high temperatures and pressures. Two tubes approximately one meter long were purchased. Fittings were supplied with each tube that attach to the ends of the tube via

compression clamps. The fittings, attached to the bottom of the tubes, were joined together to form the bottom of the U tube. Fittings at the top of the tubes were turned outward and fitted with bushings to receive the flexible lines from the tube viscometer. The manometer was filled halfway with methylene chloride, a nonpolar fluid with a density slightly greater than water (1312 kg/m^3). Using a fluid with a density just greater than water provided maximum sensitivity. The rest of the manometer and the lines leading to the tube viscometer were filled with water.

The maximum pressure drop was determined using the highest starch concentration, the lowest temperature, and the highest flow rate that would be used in any of the experiments. This test showed a maximum expected pressure drop of approximately 9 kPa (692 mm of methylene chloride). Consequently, the pressure transducer with a span of 0 - 13.8 kPa was ordered, since the next lower preset span available was less than 9 kPa.

4.5.2. The Test for Time-dependency

Time-dependency for the starch solutions in this tube viscometer system would be the occurrence of thixotropy, rheopexy, or rheodestruction in the solution during the time it was moving between the pressure taps in the tube viscometer. One way of checking for this would be to recirculate the starch solution through the tube viscometer, while maintaining it at high temperature and

pressure, for a long period of time. A change in the rheological properties during this period would be evidence of time-dependency. However, since the starch solution is flash cooled at the end of the system, there is no real way to check for time-dependency under the actual test conditions. The best that could be done was to check for time-dependency in the flash cooled solution at the end of the system. If time-dependency did exist in this sample, one would expect it to exist under the actual test conditions. This would be particularly true if the time-dependency were rheodestruction, because the starch granules could be expected to be more susceptible to destruction by mechanical forces at the elevated temperatures.

A 2.27% (g dry starch/100g water) starch solution was prepared according to the procedure given in Section 4.4, and a sample was collected at the end of the system after flash cooling from 121°C to 100°C. The sample was refrigerated to lower the temperature as rapidly as possible from 100°C. After refrigeration for twenty-four hours, the sample was removed from the refrigerator and allowed to come to room temperature. Time-dependency testing was done on a Haake Rotovisco using the M150 head with the MV1 sensor using a speed setting of 140 RPM. The torque required to turn the bob was recorded every ten seconds for ten minutes (58 values were collected after eliminating the first value and the first value after the

five minute mark). The torque values are presented in Table 4.8. Values were slightly erratic, but it can be seen that there is no trend either up or down in the readings. Therefore, it was concluded that time-dependency did not exist in this sample.

4.5.3. The Test for Slip (wall effects)

The phenomenon of slip was described in Chapter Three. It was stated there that slip can be a problem for suspensions, two phase fluids, and certain polymers where alignment of linear molecules occur in the direction of flow at large flow rates. The starch solution used in these experiments might be considered two phase, and a suspension, when the starch granules have not imbibed any water and are ungelatinized. After gelatinization, the starch granules become deformable (at least to some degree) which make starch solutions different from, say, orange juice or wood pulp where the solid phase is not deformable. Therefore, slip was not expected to be present. However, because there is no previous experimentation under low acid aseptic processing conditions, it was decided to check for the presence of slip. To do this, a test was run through a larger diameter (0.0212 m) tube viscometer with a 1.82% starch solution at 121°C. The shear stress and shear rate values are presented in Table 4.9. These values were calculated by a computer program developed at Michigan State University. This data was used after the execution of

Table 4.8. Torque readings from the time dependency test (N m)

reading #	torque (*10^3)	reading #	torque (*10^3)
1	2.08	30	3.35
2	3.03	31	2.41
3	2.60	32	2.08
4	2.17	33	2.83
5	2.16	34	2.77
6	1.96	35	1.89
7	1.95	36	2.15
8	2.03	37	2.82
9	1.96	38	1.98
10	2.76	39	2.37
11	2.25	40	2.09
12	2.55	41	2.37
13	1.75	42	2.30
14	2.77	43	2.59
15	2.27	44	2.33
16	1.86	45	1.87
17	1.82	46	2.07
18	2.01	47	2.57
19	2.73	48	1.89
20	2.27	49	1.97
21	2.07	50	2.00
22	2.13	51	2.26
23	1.80	52	2.50
24	1.99	53	2.53
25	2.26	54	2.00
26	2.03	55	1.92
27	2.14	56	2.63
28	2.20	57	2.75
29	1.84	58	2.51

Table 4.9. Shear stress and shear rate values from 0.0212 m diameter tube viscometer.

measurement #	shear stress (Pa)	shear rate (1/s)
1	0.158	52.14
2	0.146	51.28
3	0.134	49.72
4	0.138	49.34
5	0.119	46.48
6	0.123	46.00
7	0.088	39.91
8	0.080	38.89
9	0.064	33.04
10	0.061	31.41
11	0.057	26.25
12	0.045	25.05
13	0.018	11.16
14	0.018	10.99

the experimental design to check for slip. The result of the analysis will be presented in Chapter Five.

4.5.4. Starch Gelatinization Test

Many low acid foods are cooked prior to canning or aseptic processing. The cooking temperatures are typically in the 80-100°C range which is high enough to completely gelatinize, and start pasting, a crosslinked starch (the amount of pasting depends on the degree of crosslinking). To imitate this in the experiments conducted here would require heating the starch solution in the vat prior to pumping it into the system.

For experimental purposes, it would be desirable to know if a stable viscosity is achieved and, if so, the time required for this to occur. To determine this, a simple test was conducted where water was heated in the vat to 80°C. A 1.82% (db) starch solution was created by adding a starch slurry according to the method described previously. When the contents of the vat again reached 80°C, a sample of starch solution was collected in a 400 ml Pyrex beaker after which, a sample was collected every five minutes. Fourteen samples were collected in all. A window reading from a Brookfield RVTD viscometer using spindle #1 was taken immediately after collecting each sample. The window readings were converted to torques and are presented, along with the time and the temperature, in Table 4.10. It can be seen that a stable viscosity is not achieved within an hour

Table 4.10. Brookfield readings from the starch gelatinization test.

time (min)	temperature (°C)	torque*10^7 (N m)
0	84	1.22
5	83	1.21
10	79	1.29
15	81	1.41
20	80	1.55
25	83	1.68
30	80	1.90
35	83	2.08
40	83	2.45
45	84	2.80
50	84	3.23
55	84	3.85
60	79	4.34
65	82	5.34

and

vi

st

of

ex

th

pa

Co

un

ex

4.

lo

wi

Th

ir

m

O

s

p

a

c

h

d

and five minutes.

The time required to execute an experiment in the tube viscometer system is variable, because the time required to stabilize fluid temperature after changing the flow rate is often unpredictable. It is unacceptable, from an experimental point of view, to conduct experiments where the starch solution has undergone different degrees of pasting prior to being pumped into the system. Consequently, it was decided to leave the starch solution ungelatinized insuring the same starting material for each experiment.

4.6. Calculation of flow rates required to obtain desired shear rates

The shear rate range germane to aseptic processing of low acid foods can be obtained by performing calculations with current flow rates and pipe sizes used in industry. The smallest pilot scale systems have hold tubes 0.0508 m in diameter and run at flow rates of, approximately, 0.0076 m^3/min. Production size systems have hold tubes 0.0635-0.0889 m in diameter, and flow rates are governed by filler speeds. To fill five-hundred containers with 227 grams of product per minute would require a flow rate of approximately 0.114 m^3/min. Since there is no information on the rheological properties of liquid foods under aseptic processing conditions, the shear rates can only be approximated by assuming them to be Newtonian fluids. Shear

rates in Newtonian fluids are calculated by

$$\dot{\gamma} = (4Q)/(\pi R^3) \quad \text{.....(4.3)}$$

where:

$\dot{\gamma}$ = shear rate (1/s)

Q = volumetric flow rate (m^3/s)

R = tube radius (m)

Using the Newtonian shear approximation for the conditions described above shows an approximate shear rate of 10 reciprocal seconds for the pilot scale system and 75 reciprocal seconds for the production system with the 0.0635 meter diameter hold tube.

The tube viscometer to be used in the execution of the experimental design had a diameter of 0.0127 m. If Equation 4.3 is rearranged to solve for the volumetric flow rate, Q, and the radius of the tube viscometer is substituted in the equation, the flow rates required to cover a shear rate range of 10 - 75 reciprocal seconds can be calculated directly. Performing these calculations shows flow rates of $2.01*10^{-6}$ and $1.51*10^{-5}$ m^3/s are required to obtain shear rates of 10 and 75 reciprocal seconds in the tube viscometer, respectively.

4.7. Experimental Design

Two starch concentrations (1.72 and 2.72% db) at three temperature levels (121.1, 132.2, and 143.3°C) for a

combination of six treatment levels, were examined. A two factor (concentration and temperature), randomized, complete block design was chosen to accomplish this. There are several advantages to using this design. First, a multifactor experiment allows for the examination of interaction effects that cannot be obtained with single factor experiments. Consequently, more information can be obtained with fewer experiments. Second, the complete block aspect allows for stopping experimentation and examining the variability of the data to determine if further experimentation needs to be done. Also, the statistical analysis of complete block designs is relatively simple (analysis of variance). Randomization insures the distribution of systematic effects so that when treatments are compared, differences are attributed to treatment effects and not to experimental biases caused by the experimenter or other factors (Neter, et al., 1985).

The experimental design is presented in Figure 4.6. Each block contains all six treatments. Consequently, each block is a replication. Blocking was done over time to eliminate experimental biases occurring over time. For example, if the experimenter becomes more proficient at running the equipment so that more accurate results are obtained from the later experiments, the effects are randomly distributed. Four blocks are presented in Figure 4.6 for a total of twenty-four experiments.

Time ----------→

Block One	Block Two	Block Three	Block Four
T1C2	T2C2	T1C2	T2C1
T3C2	T3C1	T2C2	T1C1
T2C2	T1C2	T3C2	T3C2
T2C1	T1C1	T2C1	T1C2
T3C1	T3C2	T1C1	T2C2
T1C1	T2C1	T3C1	T3C1

Where T1 = 121.1°C
T2 = 132.2°C
T3 = 143.3°C
and C1 = 1.82% Starch
C2 = 2.72% Starch

Figure 4.6. Experimental Design

CHAPTER FIVE

RESULTS

5.1. Determination of the Rheological Parameters from the Tube Viscometer Data.

The experimental design was executed over a fourteen day period. The raw data output from the data acquisition system is presented in Appendix B. These data include the temperatures going into and coming out of the heat exchanger, the pressure transducer output, and the mass flow meter output (meter indicated mass flow rates).

Equation 4.1 was used to convert the meter indicated mass flow rates to predicted true mass flow rates, and these values were then converted to volumetric flow rates by dividing by the density of water at the temperature of the experiment. The water density values were obtained from tables (Reynolds and Perkins, 1977). The millivolt output from the pressure transducer was converted to pressure drops with Equation 4.2. The pressure drops and volumetric flow rates are presented in Appendix C along with calculated values of shear stress, shear rate, the critical Reynolds number, and the generalized Reynolds number for

the maximum flow rate of the experiment. The pH of the tap water used to make the starch solution is also given. Average pH of the tap water for all of the experiments was 7.73±0.70 (95% confidence limits).

Shear stress and shear rate values were calculated by the computer program "Tubev" developed at Michigan State University. The program calculates shear stress by substituting the pressure drop values in Equation 3.1. Shear rate values are then calculated using the shear stress values along with the volumetric flow rates in the Rabinowitsch-Mooney equation (Eq. 3.3). The program evaluates the derivative term in the Rabinowitsch-Mooney equation by fitting $(Q/\pi R^3)$ versus σ_w with a polynomial equation and evaluating the derivative of the polynomial. The program values were checked against hand calculated values and found to be accurate. The program also performs a regression analysis to calculate values of the consistency coefficient (K) and the flow behavior index (n) for the two parameter power law model. This model was chosen because of its simplicity and, as will be seen later, it fit the data well. The values of consistency coefficient and flow behavior index for each experiment are presented in Table 5.1.

The theoretical basis for laminar-turbulent transition of Herschel-Bulkley and power law fluids in pipes is well established (Hanks and Ricks, 1974). The equations were programmed by Garcia and Steffe (1987). This program was

used to calculate the critical Reynolds number and the generalized Reynolds number for the highest flow rate which are presented in Appendix C. The laminar flow assumption was not violated in any of the experiments.

5.2. Analysis of Variance

The values of the consistency coefficient and flow behavior index (Table 5.1) were each treated as a single response for a particular experiment. Tables 5.2 and 5.3 are analysis of variance tables examining block and treatment effects for the flow behavior index and consistency coefficient, respectively. In both cases, block effects are not significant. For the flow behavior index, the probability of the F ratio (F^*) being greater than F for block effects is approximately 47%. For the consistency coefficient, the probability of the F ratio being greater than F for block effects is approximately 28%. Since block effects are not significant, the data from all four blocks for a particular treatment level (temperature/concentration combination) can be pooled, and the consistency coefficients and flow behavior indices can be averaged.

Tables 5.2 and 5.3 also show that treatment effects are significant for the flow behavior index at α=0.1 (nearly 0.05) and for the consistency coefficient at α=0.05. The conclusion drawn from this is that changes in treatment levels (temperature and/or concentration levels) are the primary cause for changes in the responses (K and n

Table 5.1. Values of the consistency coefficient, K (Pa s^n), and flow behavior index, n, from each individual block experiment.

experiment	block 1	block 2	block 3	block 4
T1C1	K=6.33E-4 n=1.286	K=3.49E-4 n=1.409	K=1.17E-4 n=1.612	K=6.37E-4 n=1.271
T2C1	K=7.27E-4 n=1.244	K=5.28E-4 n=1.304	K=3.62E-4 n=1.384	K=2.43E-4 n=1.461
T3C1	K=4.57E-3 n=0.828	K=1.69E-3 n=1.068	K=1.58E-3 n=1.033	K=2.37E-4 n=1.443
T1C2	K=2.38E-4 n=1.483	K=4.34E-5 n=1.861	K=6.21E-4 n=1.294	K=1.39E-4 n=1.592
T2C2	K=9.00E-5 n=1.666	K=1.83E-5 n=2.076	K=4.67E-4 n=1.333	K=2.77E-4 n=1.460
T3C2	failed	K=1.17E-3 n=1.114	K=3.98E-4 n=1.363	K=2.57E-4 n=1.466

where: T1=121.1°C
T2=132.2°C
T3=143.3°C
and C1=1.82% starch
C2=2.72% starch

Table 5.2. Analysis of variance table for the flow behavior index examining block and treatment effects.

source	sum of squares	degrees of freedom	mean square	F^*	prob (>F)
main	0.8618	8	0.1077	2.112	0.106
block	0.1351	3	0.0450	0.883	0.474
treatment	0.7445	5	0.1489	2.919	0.052
residual	0.7142	14	0.0510		

Table 5.3. Analysis of variance table for the consistency coefficient examining block and treatment effects.

source	sum of squares	degrees of freedom	mean square	F^*	prob (>F)
main	1178.03	8	147.25	2.422	0.070
block	258.97	3	86.324	1.420	0.279
treatment	921.44	5	184.29	3.031	0.046
residual	851.25	14	60.80		

values). In other words, the primary cause of changes in response are not due to unwanted experimental or systematic effects.

Tables 5.4 and 5.5 are analysis of variance tables examining treatment effects without block effects (since they are not significant). These tables show that treatment effects are significant at α=0.05 for both the flow behavior index and the consistency coefficient when block effects are not included.

Table 5.6 is an analysis of variance table examining the effects of temperature and concentration, along with possible interaction effects, on the flow behavior index. This table shows that the flow behavior index is significantly affected (at α=0.05) by changes in both the temperature and the concentration. Interaction effects are not significant (the probability of the F ratio being greater than F is eighty-six percent) which means that effects due to temperature or concentration change on the flow behavior index are additive. Therefore, the effect of temperature on the flow behavior index can be examined independently of concentration effects and vice versa. The table also shows that the flow behavior index is slightly more affected by changes in concentration than changes in temperature.

The last analysis of variance table repeats the analysis performed in Table 5.6 using the consistency coefficient. These results are presented in Table 5.7 and

Table 5.4. Analysis of variance table for the flow behavior index examining treatment effects with block effects removed.

source	sum of squares	degrees of freedom	mean square	F^*	prob (>F)
main	0.7226	5	0.1453	2.909	0.045
treatment	0.7226	5	0.1453	2.909	0.045
residual	0.8494	17	0.0500		

Table 5.5. Analysis of variance table for the consistency coefficient examining treatment effects with block effects removed.

source	sum of squares	degrees of freedom	mean square	F^*	prob (>F)
main	919.06	5	183.81	2.815	0.050
treatment	919.06	5	183.81	2.815	0.050
residual	1110.2	17	63.307		

Table 5.6. Analysis of variance table examining temperature, concentration, and their interaction effects on the flow behavior index.

source	sum of squares	degrees of freedom	mean square	F*	prob (>F)
main	0.7116	3	0.2372	4.748	0.014
temperature	0.3802	2	0.1901	3.805	0.043
concentrate	0.2851	1	0.2851	5.707	0.029
interaction	0.0150	2	0.0075	0.150	0.861
residual	0.8494	17	0.0500		

Table 5.7. Analysis of variance table examining temperature, concentration, and their interaction effects on the consistency coefficient.

source	sum of squares	degrees of freedom	mean square	F*	prob (>F)
main	746.18	3	248.72	3.808	0.030
temperature	514.99	2	257.50	3.943	0.039
concentrate	187.11	1	187.11	2.865	0.109
interaction	172.87	2	86.437	1.324	0.292
residual	1110.2	17	65.307		

shows that the consistency coefficient is significantly affected by changes in temperature (α=0.05). Effects caused by changes in concentration are nearly significant at α=0.1. It is concluded from these results that the consistency coefficient is a strong function of temperature and a weak function of concentration. Temperature/concentration interaction effects on the consistency coefficient are not significant since the probability of the F ratio being greater than F is approximately 29%. Therefore, the effects caused by temperature and concentration on the consistency coefficient are additive.

Average values (treatment means) of the flow behavior index and the consistency coefficient are presented in Table 5.8 for each treatment level (temperature/concentration combination). An examination of Table 5.8, together with Figures 5.1-5.4, reveal the following:

1. Generally, the flow behavior index decreases as temperature increases. However, for a given concentration, there is little change in the flow behavior index until the temperature is increased to 143.3°C from 132.2°C (Figure 5.1).
2. The consistency coefficient generally increases as temperature increases. However, as with the

Table 5.8. Average values (treatment means) of consistency coefficient (K) and flow behavior index (n) for each experiment.

experiment	n_{ave}	K_{ave} (*10^4)
121.1°C, 1.82% starch	1.395	4.34
132.2°C, 1.82% starch	1.348	4.65
143.3°C, 1.82% starch	1.093	20.2
121.1°C, 2.72% starch	1.558	2.60
132.2°C, 2.72% starch	1.634	2.13
143.3°C, 2.72% starch	1.314	6.08

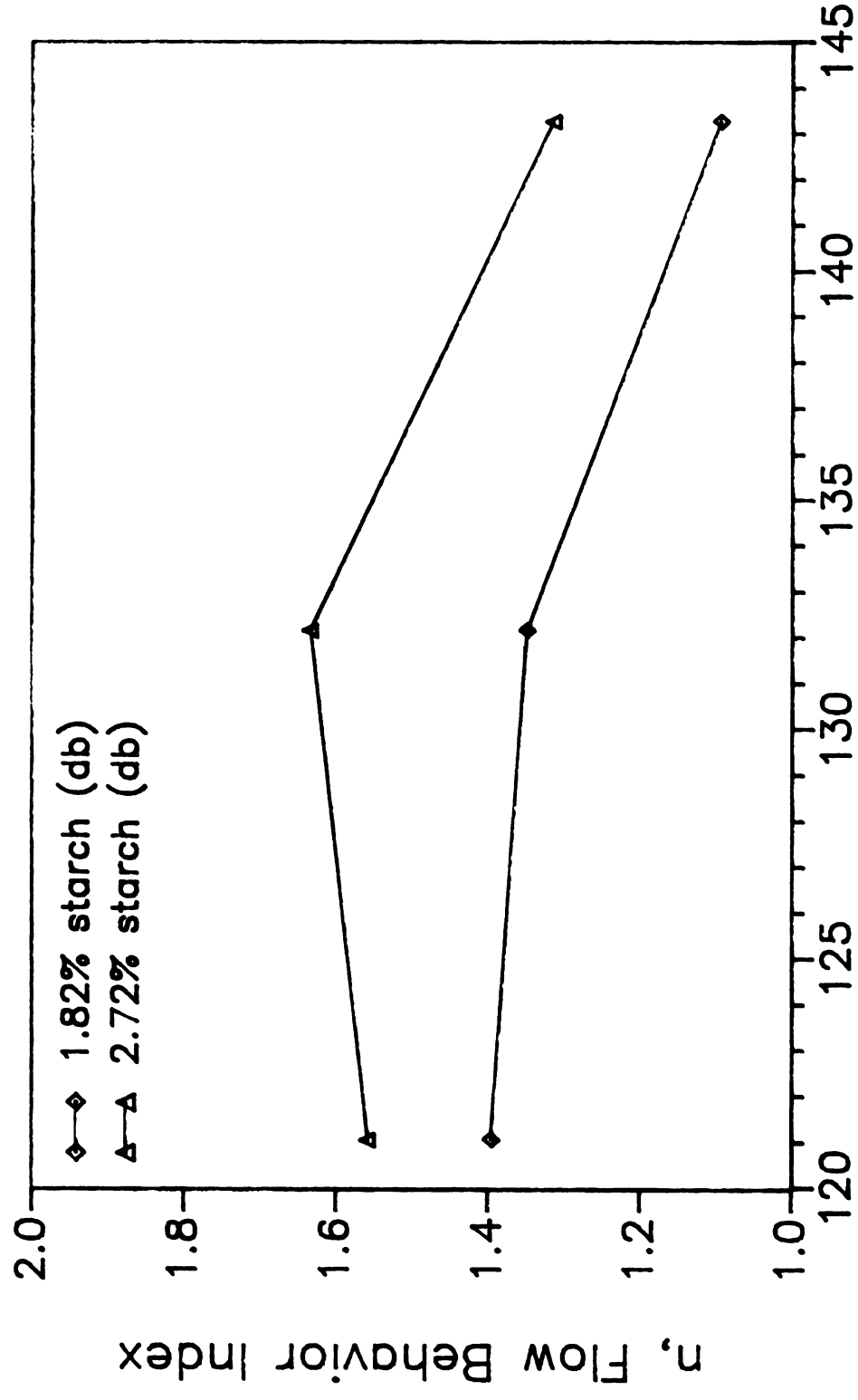

Figure 5.1 – Average Flow Behavior Index Values vs. Temperature

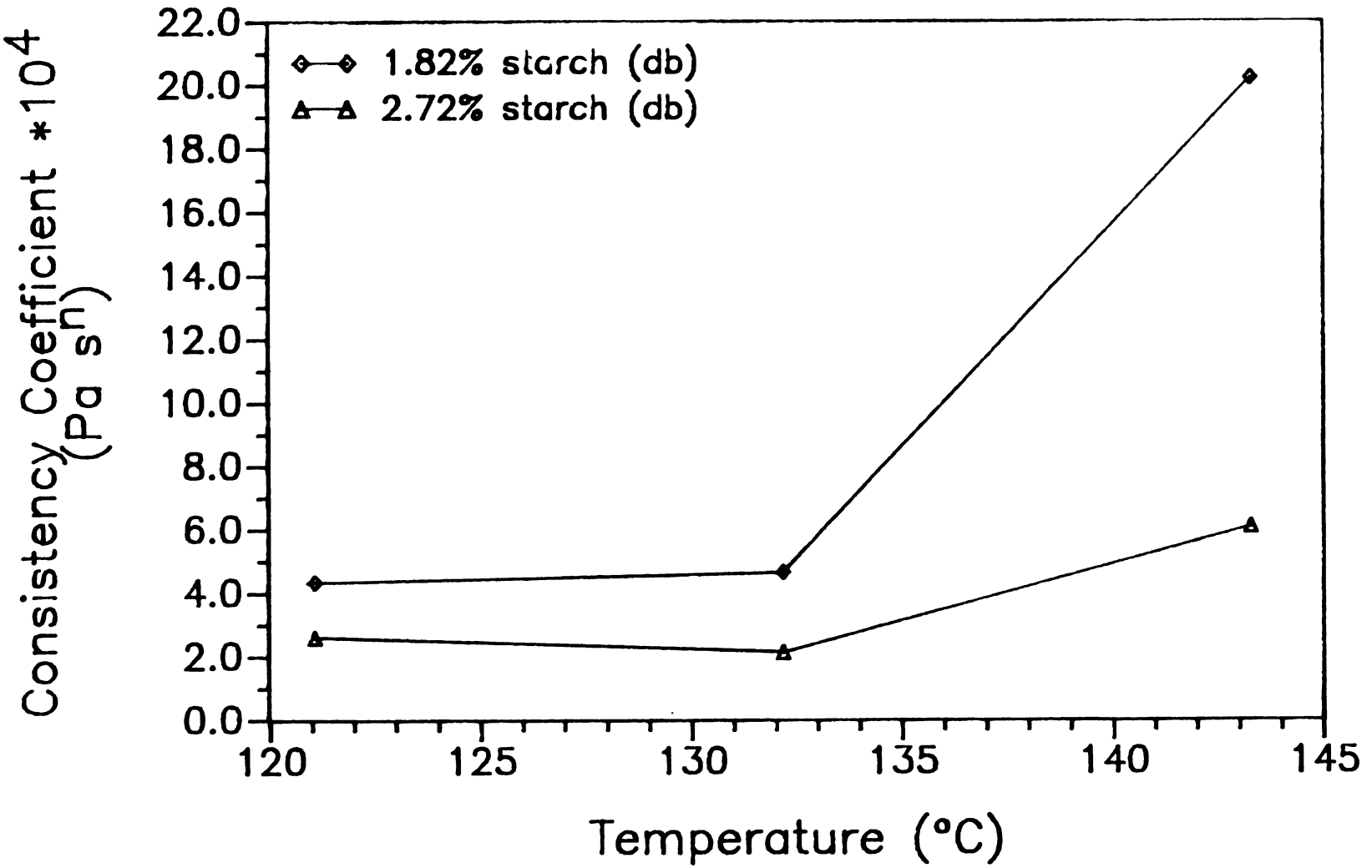

Figure 5.2 – Average Consistency Coefficient Values vs. Temperature

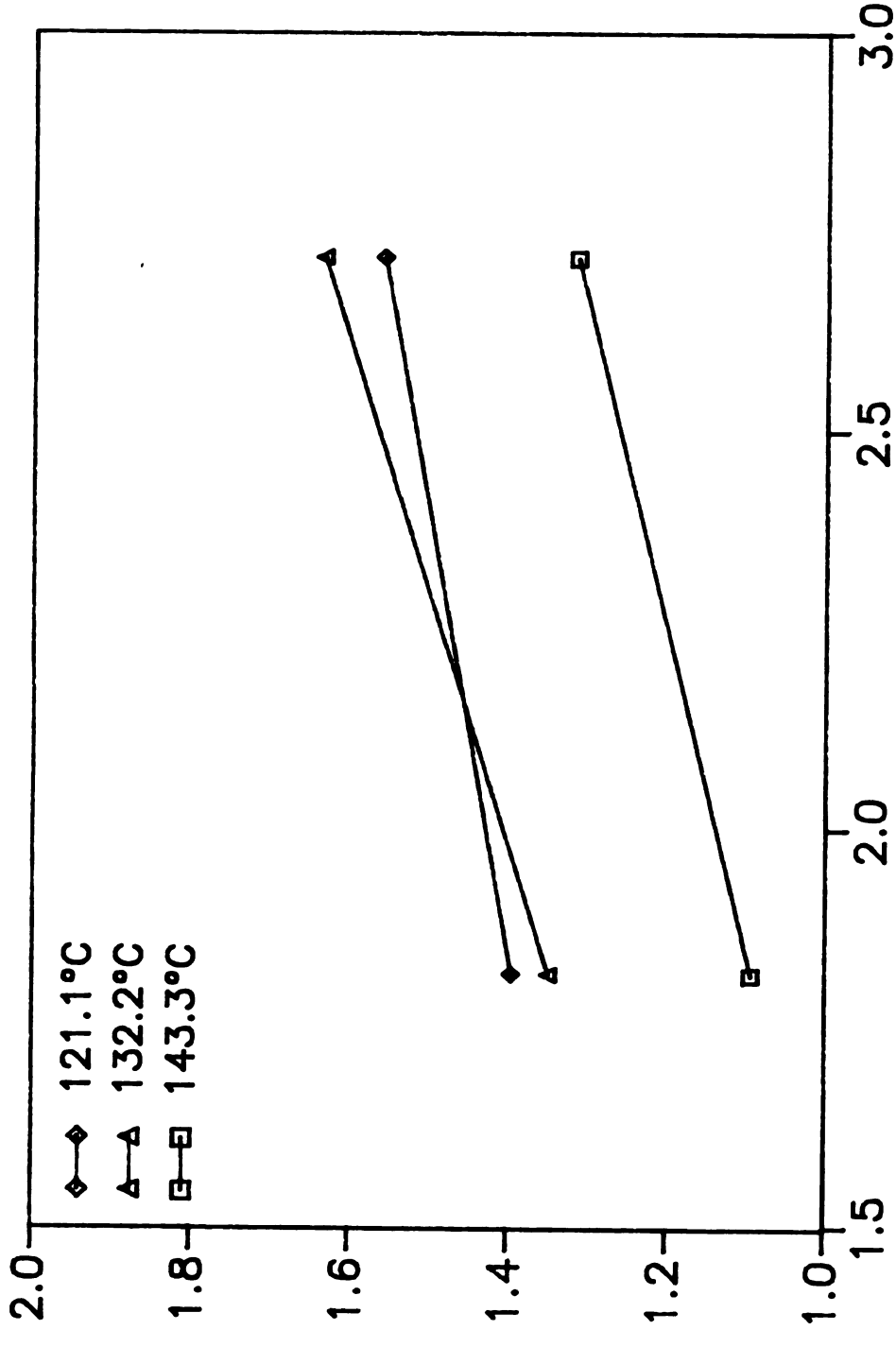

Figure 5.3 – Average Flow Behavior Index Values vs. Concentration

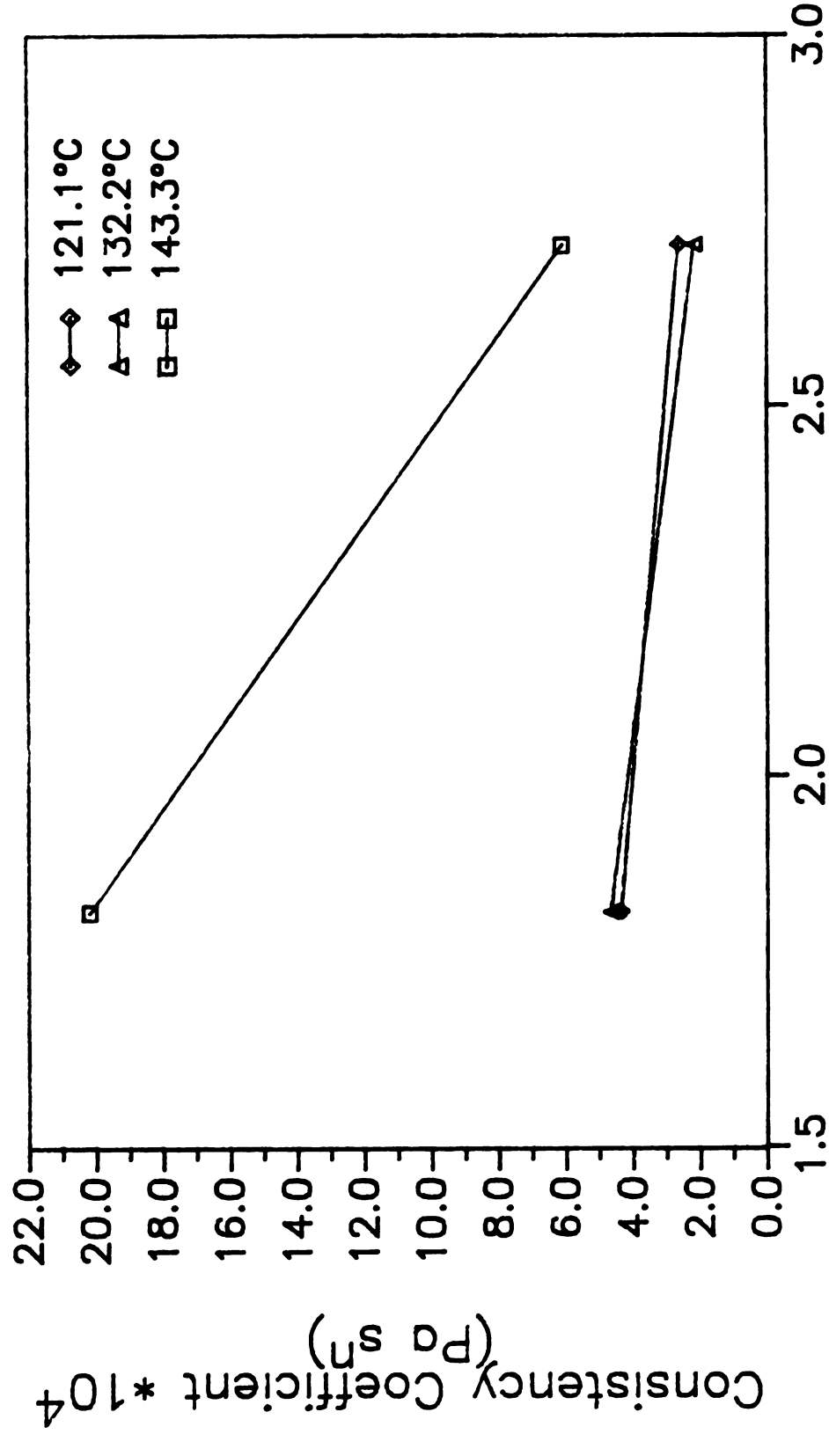

Figure 5.4 – Average Consistency Coefficient Values vs. Concentration

flow behavior index, there is little change until the temperature is increased to 143.3°C from 132.2°C (Figure 5.2).

3. The flow behavior index increases with concentration (Figure 5.3).
4. The consistency coefficient decreases with concentration (Figure 5.4).

Figures 5.1 to 5.4 are a statistical tool often used in conjunction with analysis of variance (Neter et al., 1985), and other information can be obtained from them. For instance, the degree to which the lines are parallel in the figures is an indication of the degree of interaction (Neter, et al., 1985). The high degree of parallelism in Figures 5.1 and 5.3 indicates almost no interaction which is confirmed in Table 5.6 ($P[F \geq F^*] \approx 0.86$). In Figures 5.2 and 5.4, there is a divergence going from 132.2 to 143.3°C indicating some interaction effects. However, Table 5.7 revealed this to be insignificant ($P[F \geq F^*] \approx 0.29$). Figures 5.3 and 5.4 present the same information as Figures 5.1 and 5.2 except it is viewed in a different way. Figures 5.3 and 5.4 allow observation of concentration effects on the parameters for a given temperature whereas, in Figures 5.1 and 5.2, the effect of temperature on the parameters is observed for a given concentration. Concentration effects can still be seen in Figures 5.1 and 5.2; if there were no concentration effects, the lines would superimpose.

It is most easily seen in Figures 5.3 and 5.4 that the responses at 121.1 and 132.2°C are essentially the same.

5.3. Rheograms

As mentioned previously, the insignificance of block effects allowed pooling of data and/or averaging of responses (K and n values). All of the analysis performed thus far has been with the average values of consistency coefficient and flow behavior index for each treatment level, i.e., treatment means. Another way of viewing the results is to pool the data from the four blocks and perform nonlinear regression to obtain the rheological parameters. There are several benefits in doing this. First, a comparison can be made between the parameters obtained from the pooled data and the treatment means. Second, it allows visual observation of the variation within a treatment level when plotted in a rheogram.

Nonlinear regression was performed, and rheograms were created, with a commercially available statistical/plotting package called "Plotit" (Eisensmith, 1987). The pooled data parameters are presented in Table 5.9 along with the nonlinear coefficients of determination. A comparison with the treatment means presented in Table 5.8 shows that, with the exception of the consistency coefficient at 143.3°C and 1.82% starch, the values are nearly the same and follow the same trends. This is the expected result. The rheograms for the six experiments where the data have been pooled are

Table 5.9. Flow behavior indices, consistency coefficients, and nonlinear coefficients of determination for the six experiments (temperature/concentration combinations) where block data has been pooled.

experiment	n	$K*10^4$ (Pa s^n)	r^2
121.1°C, 1.82% starch	1.444	2.87	0.973
132.2°C, 1.82% starch	1.389	3.49	0.978
143.3°C, 1.82% starch	1.111	12.01	0.871
121.1°C, 2.72% starch	1.477	1.71	0.955
132.2°C, 2.72% starch	1.556	1.69	0.911
143.3°C, 2.72% starch	1.222	7.38	0.988

Table 5.10. Nonlinear coefficients of determination for each of the individual block experiments.

experiment	block 1	block 2	block 3	block 4
T1C1	0.977	0.983	0.994	0.967
T2C1	0.981	0.958	0.983	0.996
T3C1	0.998	0.989	0.994	0.998
T1C2	0.988	0.957	0.968	0.986
T2C2	0.987	0.980	0.995	0.934
T3C2	failed	0.998	0.996	0.978

where: T1=121.1°C
T2=132.2°C
T3=143.3°C
and C1=1.82% starch
C2=2.72% starch

presented in Figures A7-A12 in Appendix A.

The rheograms in Figures A7-A12 can be presented in ways that allow examination of temperature or concentration effects. Figures A13 and A14 show temperature effect for 1.82 and 2.72% starch, respectively. Note that rheograms allow observation of the combined effect of the flow behavior index and the consistency coefficient, since both are required to define a rheogram. For example, it was shown earlier that the flow behavior index decreases with temperature whereas the consistency coefficient increases. Therefore, for a given concentration, the rheogram for 143.3°C would be expected to be slightly elevated and not as steep as observed in Figures A13 and A14.

Figures A15-A17 show concentration effects for 121.1, 132.2, and 143.3°C, respectively. As expected, the rheograms for 1.82% starch are slightly elevated and not as steep when compared to the 2.72% starch rheograms. However, the observational differences are not as great as one might expect, because the rheological parameters estimated from the pooled data are closer together in value than the treatment means.

Finally, the rheograms of the individual block experiments (replications), for all six temperature/concentration combinations are presented in Figures A1-A6. These were done to allow observation of variation between blocks, provide a check on the rheological parameters estimated by the computer program

"Tubev," and obtain nonlinear coefficients of determination for each of the twenty-three individual experiments. The rheological parameters estimated by Plotit exactly matched those estimated by "Tubev." The nonlinear coefficients of determination are presented in Table 5.10.

5.4. Evaluation of Slip

The standard evaluation for slip, as outlined in Chapter Three, could not be performed due to the inability of the heat exchanger to maintain fluid temperature at the higher flow rates required to cover the same shear rate range in the larger tube viscometer. Also, a smaller diameter tube viscometer could not be used, because the minimum pump speed provided a flow rate that yielded shear rate values that were too large. Consequently, the best that could be done was a qualitative evaluation.

The rheogram for the test conducted in the larger tube viscometer is presented in Figure 5.5 along with the rheogram from the pooled data at 121.1°C and 1.82% starch. If slip is not present, the rheograms from the two different diameter viscometers should superimpose when they cover the same shear rates. It can be seen from Figure 5.5 that the overlap in shear rates is approximately seven reciprocal seconds. The flow behavior index and consistency coefficient for the larger diameter viscometer are 1.365 and $6.25*10^{-4}$ Pa s^n, respectively. These values are not the same as those for the pooled data from the smaller

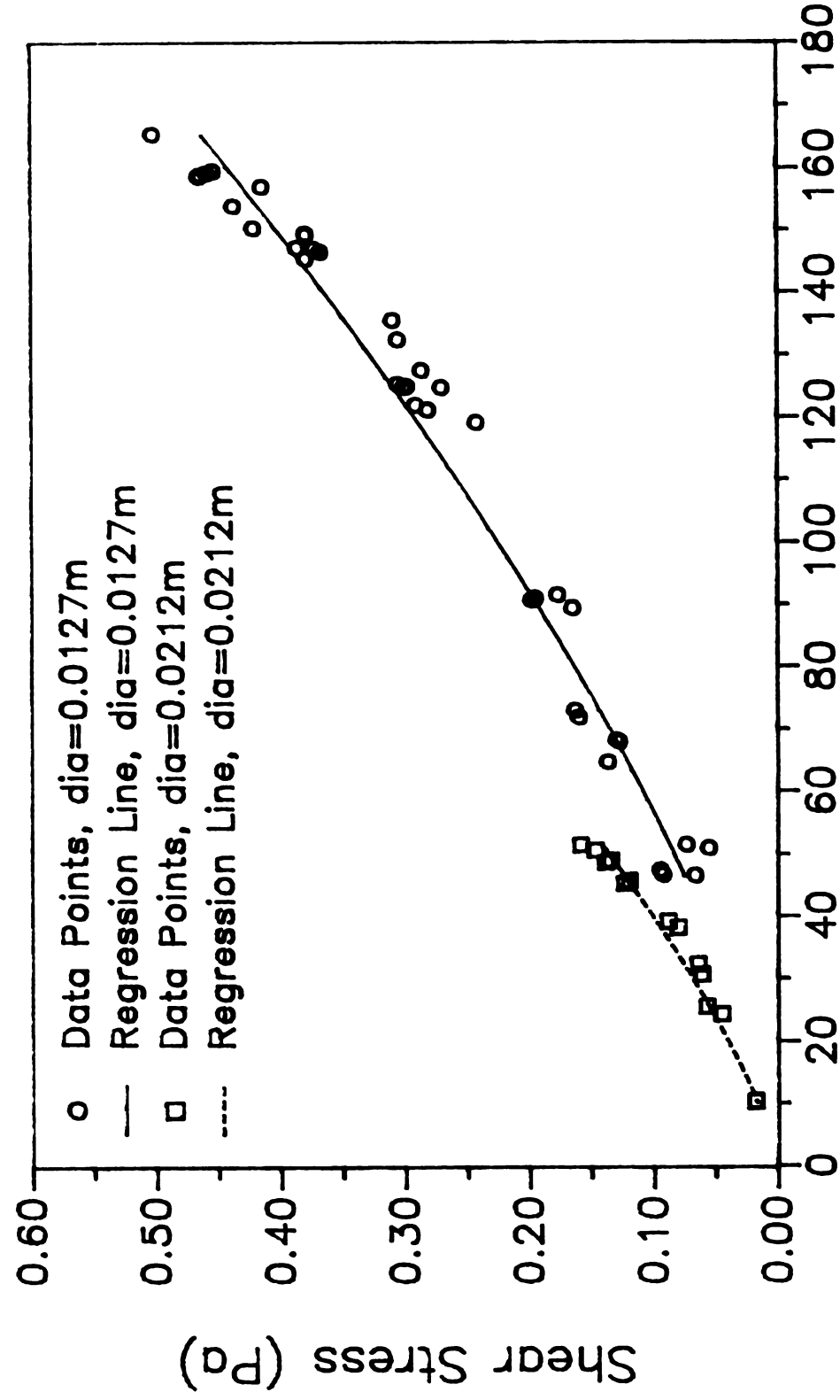

Figure 5.5—Rheograms of 1.82% starch at 121°C Through Viscometers of Different Diameters

viscometer (Table 5.9). However, the values from the larger tube viscometer do fall within the variation between the block experiments that, together, comprise the rheogram for the smaller diameter viscometer (Table 5.1). Since slip was not expected to occur in these fluids, and the rheogram for the larger diameter viscometer falls within the block variation, the conclusion is drawn that slip is negligible. However, if a larger heat exchanger can be obtained, future research should include a quantitative evaluation of slip.

5.5. Parameter Correlation Analysis

During the execution of the nonlinear regression analyses required to obtain the coefficients of determination (Tables 5.9 and 5.10), it was noticed that the parameter correlation matrix was yielding a value near one for the off diagonal elements. This indicates that the flow behavior index and consistency coefficient might be correlated. Evidence to support this can be seen in Table 5.8 and Figures 5.1-5.4: As the flow behavior index decreases with increasing temperature, the consistency coefficient increases (Figures 5.1 and 5.2). Also, as the flow behavior index increases with increasing concentration, the consistency coefficient decreases (Figures 5.3 and 5.4). If the parameters are correlated, then one of the parameters should be eliminated in favor of a simpler, one parameter model. In simpler terms, this

means that only one of the parameters (K or n) would be required to describe all changes in fluid behavior.

To determine if the parameters are correlated, sensitivity coefficients were determined and plotted against an independent variable (Beck and Arnold, 1977). The sensitivity coefficients constructed for this purpose were:

$$(K)\frac{\partial Q}{\partial K} \qquad\qquad (n)\frac{\partial Q}{\partial n}$$

An expression for the volumetric flow rate, Q, was obtained from an alternative version of the power law model:

$$\sigma = K[((3n+1)/(4n))*((4Q)/(\pi R^3))]^n \quad .....(5.1)$$

This version of the power law model was obtained by substituting an alternate form of the Rabinowitsch-Mooney equation for the velocity gradient. Equation 5.1 was then rearranged to solve the volumetric flow rate explicitly, and the derivatives were obtained from this expression.

Either the volumetric flow rate or the pressure drop could have been chosen to construct the sensitivity coefficients. Volumetric flow rate was chosen because it was thought to have larger error associated with it. Also, the derivatives of the volumetric flow rate with respect to the parameters could both be obtained analytically. Derivatives were calculated for values of pressure drop

between 50 and 700 pascals which is the approximate range seen in the experiments. This was done for two values of the flow behavior index (n=1 and n=1.5) while the value of the consistency coefficient was held constant at $5.0*10^{-5}$ Pa s^n. These values are within the range seen in the experiments. Calculated values of the sensitivity coefficients are presented in Tables 5.11 and 5.12. The third column of these tables is the ratio of the sensitivity coefficients. Plots of the sensitivity coefficients versus pressure drop are presented in Figures 5.6 and 5.7. The ordinates in Figures 5.6 and 5.7 have been multiplied by negative one for convenience.

If the sensitivity coefficients are found to be linearly dependent, then one would conclude that the parameters are correlated (Beck and Arnold, 1977). It can be seen in Tables 5.11 and 5.12 and Figures 5.6 and 5.7 that the sensitivity coefficients are not linearly dependent but are nearly so. Therefore, the conclusion is that both parameters are required to describe flow behavior, i.e., eliminating one by expressing it as a function of the other would result in a loss of information and a larger sum squared error.

The near correlation of the parameters makes it impossible to unambiguously estimate the parameters and causes problems in the interpretation of their behavior. The reason for this is that the behavior of each parameter is influenced by the other. One of the objectives of this

Table 5.11. Values of the sensitivity coefficients (m^3/s) and thier ratio for various values of pressure drop (Pa) when n=1 and $K=5.0*10^{-5}$ Pa s^n.

ΔP	$K(\partial Q/\partial K)*10^5$	$n(\partial Q/\partial n)*10^5$	ratio
50	-1.391	-5.564	3.987
100	-2.782	-13.02	4.681
150	-4.173	-21.21	5.083
200	-5.564	-29.90	5.374
250	-6.995	-38.91	5.595
300	-8.346	-48.23	5.779
400	-11.13	-67.51	6.066
500	-13.91	-87.49	6.290
600	-16.69	-108.0	6.472
700	-19.47	-129.0	6.626

Table 5.12. Values of the sensitivity coefficients (m^3/s) and thier ratio for various values of pressure drop (Pa) when n=1.5 and $K=5.0*10^{-5}$ Pa s^n.

ΔP	$K(\partial Q/\partial K)*10^6$	$n(\partial Q/\partial n)*10^6$	ratio
50	-2.465	-9.801	3.976
100	-3.912	-18.21	4.655
150	-5.126	-25.95	5.062
200	-6.210	-33.23	5.351
250	-7.260	-40.17	5.575
300	-8.138	-46.84	5.756
400	-9.858	-59.57	6.043
500	-11.44	-71.69	6.267
600	-12.92	-83.30	6.447
700	-14.32	-94.55	6.603

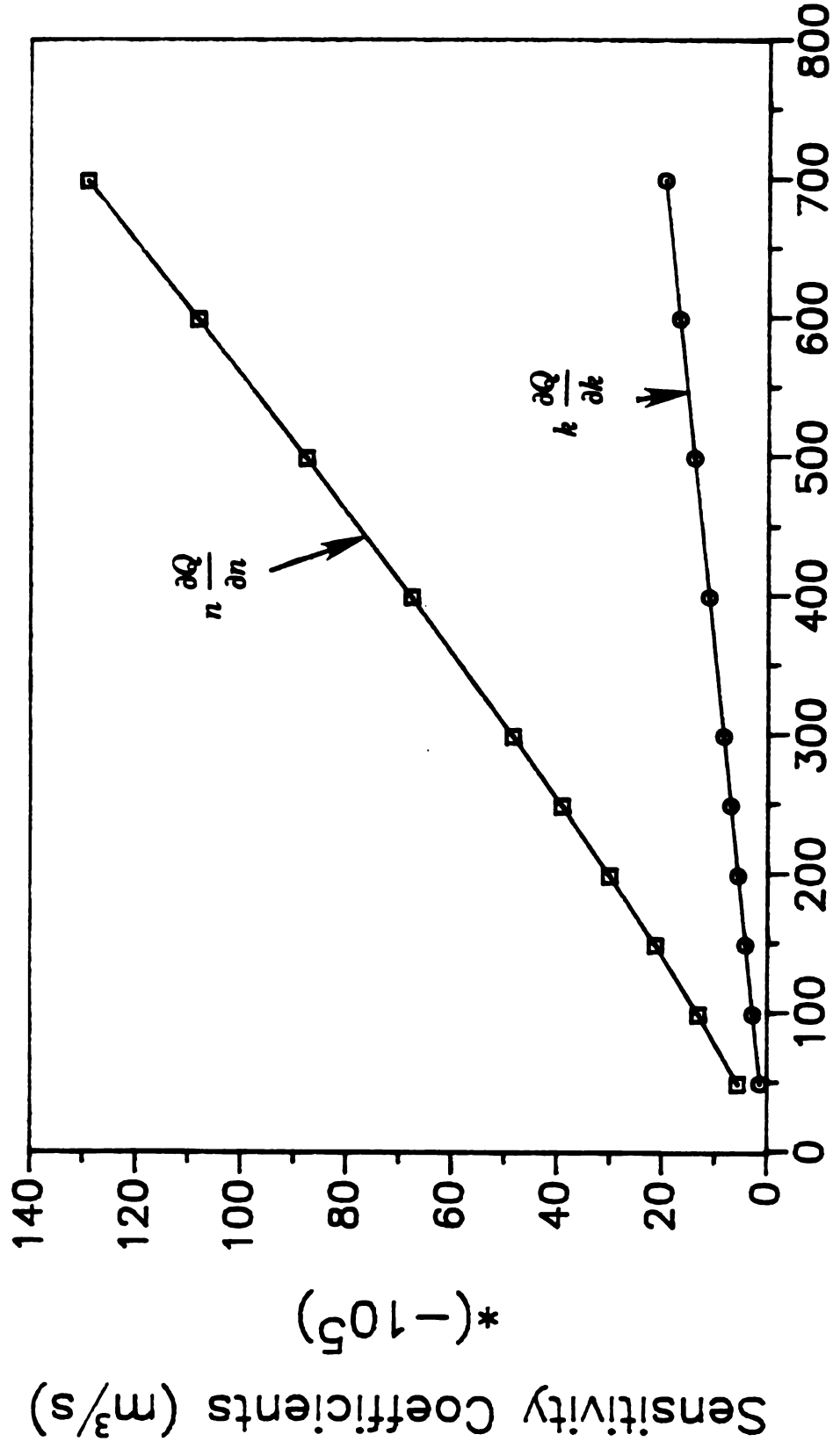

Figure 5.6—Sensitivity Coefficients Versus Pressure Drop for n=1.0

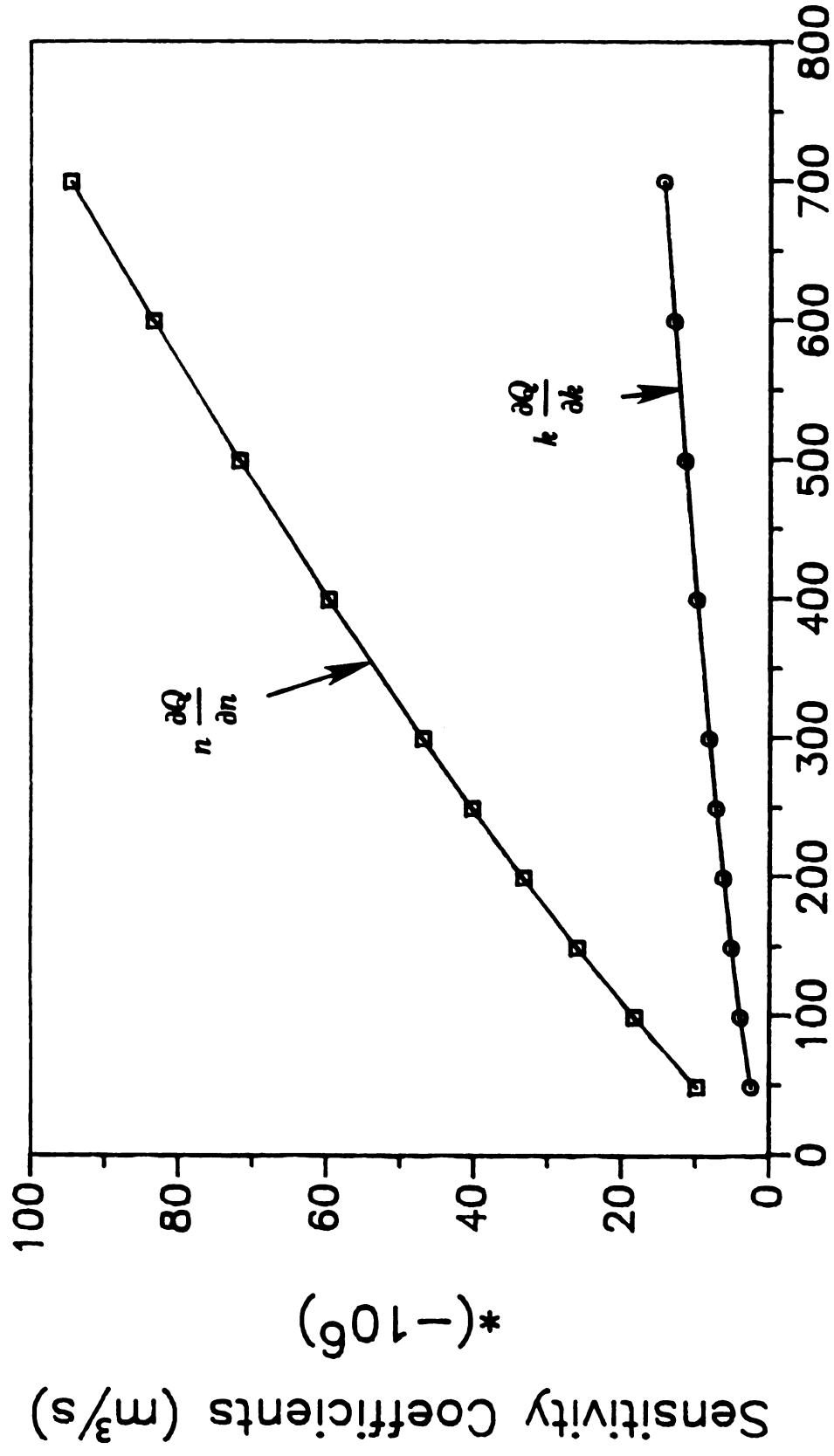

Figure 5.7—Sensitivity Coefficients Versus Pressure Drop for n=1.5

research was to examine the influence of temperature and concentration on the behavior of the rheological parameters, and it would seem that unambiguous estimates of the parameters would make the analysis of variance results, obtained earlier, meaningless. However, the fact that the parameters were shown to be significantly affected by changes in concentration and temperature suggests that one of the parameters is dominating the fluid behavior i.e., that one of the parameters is highly dependent on the other. An examination of Figures 5.6 and 5.7 reveals the flow behavior index to be the dominating parameter, because small perturbations in the flow behavior index cause larger changes in the volumetric flow rate than small perturbations in the consistency coefficient. Consequently, the behavior of the consistency coefficient is mostly determined by the behavior of the flow behavior index, and not by changes in concentration and temperature. Evidence of the near correlation of the parameters can be seen in Figure 5.8 where a plot of the consistency coefficient versus the flow behavior index is presented. An equation that fits this relationship well is

$$K = \exp[-4.534n-1.647] \quad \text{.....(5.2)}$$

Using the first three values of the flow behavior index from Table 5.9 in the Equation 5.1 yields values of $2.76*10^{-4}$, $3.55*10^{-4}$, and $12.50*10^{-4}$ Pa s^n for the

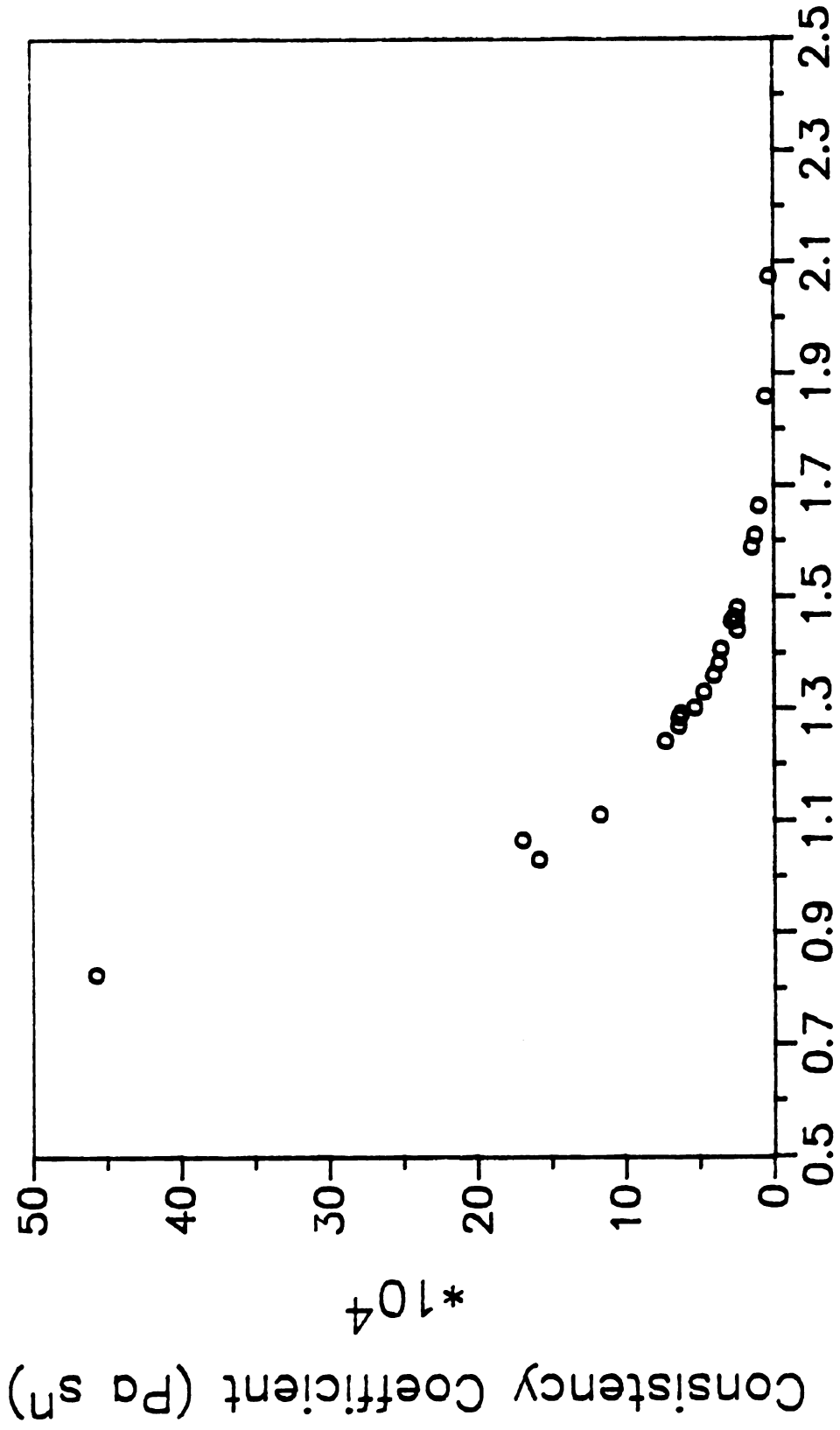

Figure 5.8—Consistency Coefficient Versus Flow Behavior Index

consistency coefficient, respectively. These values compare favorably to the estimated values in the table of $2.87*10^{-4}$, $3.49*10^{-4}$, and $12.01*10^{-4}$ Pa s^n, respectively. However, not all of the changes in the consistency coefficient can be predicted by the flow behavior index, because the parameters are not absolutely correlated, i.e., some of the variation is due to the changes in temperature and concentration. For this reason, it is inappropriate to incorporate Equation 5.1 into the power law model to create a new, one parameter model.

Another way of examining the degree to which the flow behavior index is dominating the fluid behavior is to fit the data with the following model:

$$\sigma = K_o \exp[-4.534n-1.647]\gamma^n \quad \ldots\ldots(5.3)$$

The exponential term is a "parameter" that is completely dependent on the flow behavior index. This term will also be recognized as the approximate representation for the consistency coefficient given above. Therefore, the parameter K_o will represent the amount of information in the consistency coefficient not attributable to the flow behavior index. An estimated value of one for K_o would indicate that the consistency coefficient is completely dependent on the flow behavior index, and a large value would indicate that the consistency coefficient is dominating the fluid behavior. The data in Table C4 of

Appendix C was arbitrarily chosen, and the parameters in Equation 5.1 were estimated using Gauss minimization (Beck and Arnold, 1977). The estimated value of K_o was 1.028 indicating that the consistency coefficient is highly dependent on the flow behavior index and that the fluid behavior is almost entirely described by the flow behavior index.

The final indicator of the dominance of the flow behavior index, and of the reliability of the estimates of this parameter, can be seen in the standard error of the estimates. The standard error of the estimated values of the flow behavior index were always less than 10% of the estimated value, whereas, the standard errors of the estimated values of the consistency coefficient could be 1000% of the estimated value. Part of the large standard errors associated with the consistency coefficient can be attributed to the lowest shear rates in these experiments being 40 s^{-1}, i.e., if lower shear rates could have been obtained, the standard errors would have been smaller. The main point is that the small standard errors of the estimates associated with the flow behavior index indicate that the estimates are reliable and that the analysis of variance on this parameter is meaningful.

The influence of the flow behavior index on the consistency coefficient makes the analysis of variance performed with the consistency coefficient meaningless. This is due to the consistency coefficient being influenced

by the flow behavior index in an inverse way, i.e., if the flow behavior index is significantly affected by changes in concentration or temperature, the consistency coefficient is likely to be significantly affected, but in an inverse way. Figures 5.1-5.4 together with Tables 5.6 and 5.7 reveal this to be the case. The fact that the consistency coefficient is only weakly affected by concentration, while the flow behavior index is strongly affected, is probably due to correlation not being absolute.

CHAPTER SIX

DISCUSSION

6.1. Near Correlation of the Parameters: Effect on the Prediction of Hold Tube Velocity Profiles and Implications for the Power Law Model

Near correlation of the parameters in this study might have been avoided if the sensitivity coefficients in Chapter Five were investigated beforehand. However, to do this requires knowledge of the parameter values which were not available. Near correlation may have also been avoided if a broader range of volumetric flow rate (and consequently, shear rate) had been used. This would have been difficult to achieve because of the laminar flow requirement of the Rabinowitsch-Mooney equation. Also, broadening the shear rate range beyond that seen in aseptic processing may have made the results useless.

The laminar flow restraint of the Rabinowitsch-Mooney equation (Eq. 3.3) raises the question as to whether it is possible to achieve a broad enough flow range to reduce the degree of correlation between the parameters. An inverse relationship between the flow behavior index and the consistency coefficient has also been seen in other studies

(Ford, 1984; Vercruysse, 1987; Salas-Valerio, 1988; Doublier, 1981) which raises a suspicion that some degree of correlation between the parameters existed in these studies. Note that these studies used different materials and/or different rheometers than used in the current work, and a broader shear rate range was covered. If it is true that it is not possible to reduce the degree of correlation between the parameters due to laminar flow constraints on flow rate, then serious questions can be raised about the appropriateness of the power law model for liquid foods, if physical significance is to be given to the parameters.

A method for dealing with nearly correlated parameters is to combine them into a new parameter which, in effect, creates a new model. This is different than eliminating a parameter, because both parameters define the value of the new parameter. Therefore, no information is lost. As an example, consider a model of the form:

$$\Psi = \phi_1 \phi_2 t \quad \text{.....(6.1)}$$

If ϕ_1 and ϕ_2 are nearly correlated, then a new parameter can be introduced such that $\phi = \phi_1 \phi_2$. This new parameter will yield the same value of Ψ for a given value of t, and no information is lost (Beck and Arnold, 1977).

A way of combining the parameters of this study is to define a new parameter:

$$\phi = K^{1/c_n}$$

where c is the median value of the ratio of the sensitivity coefficients (Beck, 1989). However, how this new parameter could be used to express the relationship between the stress and rate of deformation tensors is not clear.

A question that remains is whether the inability to unambiguously estimate the parameters due to the near correlation has any effect on predicting velocity profiles in hold tubes. It will be seen in the following section that the design of hold tube lengths is dependent only on the flow behavior index when the hold tube length is designed on the basis of the fastest moving fluid or food particle. Since the estimates of the flow behavior index have been shown to be reliable, the values obtained in this study can be used for engineering design of hold tube lengths based on the fastest moving fluid or food particle. The consistency coefficient has been shown to be primarily dependent on the flow behavior index; therefore, it has lost most of it physical significance. However, it is still useful in predicting the relationship between pressure drop and flow rate (witness the high values of the coefficient of determination in Table 5.10) and consequently, hold tube velocity profiles. The conclusion is that the values of consistency coefficient determined in this study have no physical significance by themselves, but they can be used

with the values of flow behavior index for engineering design purposes. This allows the hold tube to be treated as a laminar flow reactor, i.e., microbial lethality can be integrated across the hold tube, if that method of hold tube design is preferred.

6.2. Effect of Dilatancy on Hold Tube Velocity Profiles and its Implications for Aseptic Processing

Shear-thickening behavior results in the velocity differential between the fastest and slowest moving fluid stream to be greater than if the material was shear-thinning. Mathematically, for laminar flow of power law fluids in tubes:

$$U_{max}=[(3n+1)/(n+1)]U_{ave}$$

therefore

If n=infinity	$U_{max}=3.00U_{ave}$
If n=2	$U_{max}=2.33U_{ave}$
If n=1	$U_{max}=2.00U_{ave}$
If n=0.5	$U_{max}=1.67U_{ave}$
If n=0	$U_{max}=U_{ave}$

Figure 6.1 is a diagram of velocity profiles for the cases when n<0.5 (shear-thinning), n=1 (Newtonian), and n>1 (shear-thickening). Since the starch solutions in this study were shear-thickening, hold tubes must be designed so that the velocity of the fastest moving fluid stream is

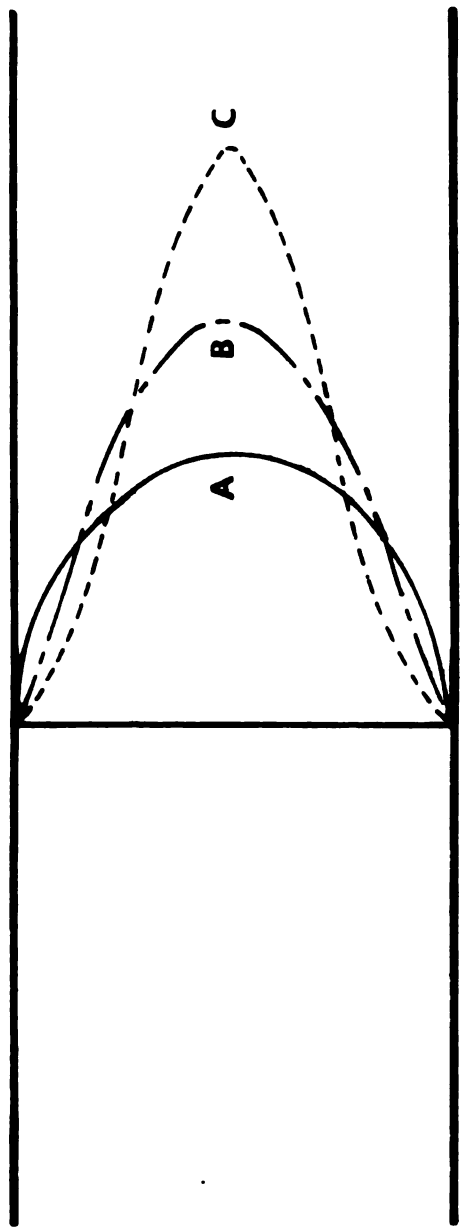

FIGURE 6.1 SUPERIMPOSED VELOCITY PROFILES OF A POWER LAW FLUID SHOWING A) SHEAR THINNING ($n < 1$), B) NEWTONIAN ($n = 1$), AND C) SHEAR THICKENING ($n > 1$).

greater than twice the bulk average velocity.

It was mentioned in the introduction that the microorganism of concern in the thermal processing of low acid foods is Clostridium botulinum. This requires that hold tubes be designed based on the worst case value of the flow behavior index for each temperature/concentration combination, i.e., the treatment mean flow behavior index values in Table 5.8 should not be used for hold tube design. Instead, the largest value of the flow behavior index for each temperature/concentration combination should be used (see Table 5.1). Table 6.1 presents the largest value of flow behavior index for each temperature/concentration combination along with the ratio of U_{max}/U_{ave}. It can be seen from this table that the largest value of flow behavior index from any of the experiments is 2.076 which results in a U_{max}/U_{ave} ratio of 2.35. Note that these results are only good for the conditions of these tests; producers of low acid foods should perform their own rheological characterization if processing conditions are different. Examples of different processing conditions that would affect the results here would be a change in pH, addition of salts, sugars, or hydrocolloids, and markedly different heat exchanger residence times.

For processors of low acid foods containing particulate matter, dilatant flow behavior has several implications. First, the fluid next to the particles will

Table 6.1. Maximum values of flow behavior index for each temperature/concentration combination and the associated V_{max}/V_{ave} ratios

experiment	n_{max}	V_{max}/V_{ave}
121.1°C, 2% starch	1.612	2.23
132.2°C, 2% starch	1.461	2.19
143.3°C, 2% starch	1.443	2.18
121.1°C, 3% starch	1.861	2.30
132.2°C, 3% starch	2.076	2.35
143.3°C, 3% starch	1.466	2.19

be more viscous than the bulk fluid due to the velocity gradient in the boundary layer of the particle. This will have the effect of decreasing heat transfer rates, because the more viscous fluid will act as an insulator. On the positive side, form drag on the particle should be increased which will aid in keeping the particle suspended and moving with the fluid. Dilatant behavior will also result in greater overprocessing of the fluid phase than if the starch solutions were shear-thinning, because the differential between the fastest moving particle and the slowest fluid stream is greater. Since heat is being transferred from the fluid to the particle, i.e., the fluid is acting as a heat transfer medium, it is dubious that producers of foods that contain large particles will gain much in the way of product quality. Given the other problems that exist in developing thermal processes for particulate containing foods, producers may want to reexamine whether aseptic processing is appropriate for foods containing large particles.

6.3. Response of the Flow Behavior Index to Changes in Concentration and Temperature and an Explanation for the Observation of Dilatancy

It was seen in Chapter Five that the flow behavior index increased with concentration and decreased with temperature. The fact that the flow behavior index increases with concentration is in agreement with the

results of Evans and Haisman (1979) but in disagreement with the results of Colas (1986). The observation of the flow behavior index increasing with concentration and decreasing with temperature can be explained with the same logic used by Bagley and Christianson (1982), Christianson et al. (1982), and Christianson and Bagley (1983) for starch pastes at lower temperatures; increasing the concentration causes the granules to become more closely packed and will increase the flow behavior index if the granules are still somewhat rigid. They observed rigidity in the starch granules for low cook temperatures where all of the granules have not gelatinized and/or short cook times.

In this system, the starch is cooked in the heat exchanger, and the cook time is the residence time in the heat exchanger. If the fluid is assumed Newtonian and an average density value is used, an estimate of the average residence time can be obtained. Doing this shows that the minimum residence time is approximately 0.284 minutes (17 seconds) and the maximum residence time is approximately 2.41 minutes (144 seconds). With such short cook times, it may be that little of the amylopectin is solubilized, and the granules are still rigid. Colas (1986) showed that the close-packing concentration for unmodified waxy maize was 1.76% and was 2.60% (g dry starch/100 g water) for the most lightly crosslinked waxy maize. Starch concentrations used in this study are within, or exceed, this range. In

light of this, if the granules in the solutions of this study were still rigid, it is reasonable to expect the flow behavior index to increase with concentration. This, combined with the fact that the high temperatures and low shear rates of this study caused the shear stresses in the fluid to be very small, also serves as a reasonable explanation for the observation of dilatancy.

Other factors may have also contributed to dilatancy. First, starch continued to cook (paste) during the residence time in the tube viscometer. If continued pasting affected the solutions at the slower flow rates causing the granules to be significantly less rigid than those at higher flow/shear rates, an apparent dilatancy would be caused. Whether this significantly affected the results is questionable, because the average residence time in the tube viscometer is approximately the same as that for the heat exchanger. Second, despite the hold tube being insulated, temperature losses were experienced. Losses depended on the temperature of the solution and on the flow rate. At 121.1°C, the loss was 2-2.5°C; for 132.2°C, 2-3°C; and for 143.3°C, the loss was 3.5-4°C. Changes in the viscosity of starch pastes upon cooling at these temperatures is mostly due to increased interaction between starch molecules and an increase in viscosity of the continuous phase (water). For water, the decrease in viscosity going from 147 to 127 °C is $1.7*10^{-5}$ Pa s (Incropera and Dewitt, 1985). Apparent viscosities of the

starch solutions in this study are all on the order of 10^{-3} Pa s. Therefore, the viscosity change in the continuous phase is negligible. The effect of increased interaction between starch molecules at these temperatures is unknown. However, it is difficult to imagine that it is significant at such high temperatures. It is acknowledged that both ongoing pasting and temperature losses may have contributed to an apparent dilatancy. Overall though, it is felt that the observation of dilatancy is best attributed to the mechanism described above. Finally, it should be noted that slip is not a reasonable explanation for the observation of dilatancy, because not accounting for slip causes a fluid to appear more shear thinning than it is in reality.

The observation that the flow behavior index decreased with increasing temperature might be expected, because increasing temperature would cause a more rapid disruption of the hydrogen bonds within the starch granules. In this case, granules would gelatinize quickly allowing more time for the solubilization of amylopectin and softening of the granule. Then, following the logic of Bagley and Christianson (1982), the granules would be more likely to deform under stress, decreasing the flow behavior index. Also, if significant amounts of solubilization have taken place, and shear stress causes the solubilized molecules to align in the direction of flow, then a decrease in the flow behavior index would be expected according to Hoseney (1986).

The temperature dependence of the flow behavior index (and consequently the consistency coefficient in this work) has several implications for aseptic processing. First, for processors of particulate foods where there is cooling of the liquid phase as the particles are being heated, the rheology of the suspending solution will be changing as the temperature of the solution changes. In turn, the velocity profile and residence time of the fastest moving particle will be changing. This effect becomes greater as the percentage of particles is increased. If the change in fluid temperature is known as a function of hold tube length, it is possible to recalculate the velocity profile along the length of the hold tube. An alternative approach, that is microbiologically conservative, would be to design the hold tube on the basis of constant rheological properties using the highest value of the flow behavior index, i.e., the value corresponding to the temperature at the end of the hold tube. This would result in some overprocessing. The flow behavior of the starch used in this study (National 465) is more sensitive to temperature change between 132 and 143°C. Hence, overprocessing caused by assuming constant rheological properties in the hold tube is minimal if hold tube temperature is between 121 and 132°C.

A second implication of the temperature dependence of the flow behavior index is that the differential between the fastest and slowest fluid stream is minimized for

higher temperatures, since the flow behavior index generally decreases with temperature (Table 6.1). This means that processors should obtain higher quality product from processing at the higher temperatures.

The concentration dependence of the flow behavior index (n increases with increasing concentration) indicates that higher quality product will be obtained with the lower starch concentration, since this will minimize the differential between the fastest and slowest fluid stream. For the material in this study, the highest quality product will be obtained for product formulated with the lower starch concentration which is processed at higher temperature. This is particularly true for nonparticulate foods or foods with small rapidly heating particles. In foods that contain large, slow heating particles (e.g., meat pieces) the quality gained by minimizing the differential between the fastest and slowest fluid streams by processing at higher temperatures will be lost to the extra time at the high temperature required to sterilize the particles.

6.4. Use of Rheological Data in Aseptic Processes

FDA (1984b) states, with regard to using rheological data in an actual process, that "consistency must be controlled during processing and records of the measurements must be kept." To do this will require some kind of on-line viscometer, i.e., the ability to measure

pressure drop of the fluid flowing through the hold tube. The design of such an instrument would be challenging, because it would need to be done in a way that would preclude the entry of bacteria into the system. Differential pressure transducers are not flow through, and it is undesirable to expose the diaphrams of the transducer to the temperature seen in aseptic processing of low acid foods. Therefore, some kind of sanitary pressure tap using a flexible diaphram might be appropriate. If such a pressure tap could be designed, producers of aseptic processing equipment could incorporate them directly in to the hold tubes during manufacturing.

Control of flow rate is a critical process parameter in aseptic processing, since it determines the residence time in the hold tube. To evaluate the rheology of non-Newtonian fluids requires varying the flow rate so that the derivative term in the Rabinowitsch-Mooney equation (Eq. 3.3) can be evaluated. Consequently, it is not possible to determine the rheology on-line; instead, it must be determined beforehand. The velocity profile in the hold tube can then be determined by simply measuring the pressure drop in the hold tube, and the volumetric flow rate.

CHAPTER SEVEN

SUMMARY AND CONCLUSIONS

A rheological characterization of two waxy maize starch solutions (1.82 and 2.72% db) was completed under the following conditions:

Temperature	Shear Rate Range
121.1°C	40 - 165 s^{-1}
132.2°C	40 - 135 s^{-1}
143.3°C	40 - 100 s^{-1}

The solutions were found to be shear thickening (dilatant) in 22 out of 23 experiments. The dilatancy was explained in terms of the rigidity and volume fraction of the swollen starch granules combined with exceedingly small shear stresses in the fluid due to the high temperatures and low shear rates. Due to the experimental conditions (the pressure and temperatures of the tests), the volume fraction occupied by the granules could not be verified. Instead, close-packing concentrations for crosslinked waxy maize starches were taken from the published literature. Contributions to dilatancy from ongoing pasting and

temperature loss were acknowledged but thought to be minor compared to the volume fraction effect.

Analysis of variance showed the flow behavior index to be significantly affected by changes in both temperature and concentration: increasing with concentration and decreasing with temperature. The analysis also showed the consistency coefficient to be significantly affected by changes in temperature but only marginally affected by changes in concentration. The consistency coefficient acted in a manner inverse to the flow behavior index.

The construction of sensitivity coefficients showed the two power law fluid parameters to be nearly correlated with the flow behavior index being the dominant parameter. This effectively made the observed behavior (and the analysis of variance) of the consistency coefficient difficult to interpret, because most (not all) of its behavior was determined by the flow behavior index. Because the correlation is not absolute, the sum of squares function has a unique minimum, and the estimated values of the parameters are unique. Therefore, the consistency coefficient could not be expressed as a function of the flow behavior index to reduce the relationship between the stress tensor and the rate of deformation tensor to a one parameter model.

The effect of dilatancy on power law fluid velocity profiles is to increase the differential between the fastest and slowest fluid stream. For low acid foods that

contain discrete particles, this will cause greater overprocessing of the fluid phase since the differential between the fastest moving particle and the slowest fluid stream is greater than if the carrier fluid was shear-thinning. A dilatant fluid will also act as an insulator because of shear-thickening in the boundary layer of the particle. Consequently, food producers are encouraged to reexamine whether aseptic processing is appropriate for foods containing large particles. For producers of nonparticulate foods, it was shown that (for the material considered in this study) the highest quality product will be obtained for foods with lower starch concentrations that are processed at higher temperatures due to depression of the flow behavior index.

CHAPTER EIGHT

SUGGESTIONS FOR FURTHER RESEARCH

1. If the explanation given for dilatancy is correct, then Newtonian or shear-thinning behavior should be induced if the concentration is increased due to the increased shear stress. Confirming this would validate the explanation given for dilatancy and substantiate the reasoning of Bagley and Christianson (1982), etc., for starch at these temperatures.

2. If a heat exchanger were placed in the system after the tube viscometer, it may be possible to cool the starch below the atmospheric boiling point so that the volume fraction of the starch granules can be determined. Knowing the volume fraction as a function of temperature and concentration would be useful in the interpretation of the rheological results. This system would also allow determination of the amount of solubilized amylopectin which may also be useful in interpreting rheological results.

3. Now that rheological parameters exist for National 465 starch under the conditions of this study, it is possible to verify the theoretical equations of Hanks and Ricks (1974) for laminar-turbulent transition by measuring pressure drop as a function of flow rate. This information would be very useful to producers of aseptically processed non-particulate foods in designing thermal processes based on turbulent flow regime. Large gains in product quality should be realized because holds tube lengths could be shortened by one-half to one-third.

4. The parameters in this study were nearly correlated and acted inversely to one another. The inverse behavior of the parameters has been observed in other studies using different rheometers and materials which raises the suspicion of near correlated or correlated parameters in these studies. The reason for this may be due to the limitation of the flow rate range caused by laminar flow requirements. This raises questions about the value of the power law model for liquid foods. An investigation into the value of a one parameter model that contains a fixed "consistency constant" might be useful.

5. A quantitative evaluation of slip should be performed.

APPENDICES

APPENDIX A
RHEOGRAMS

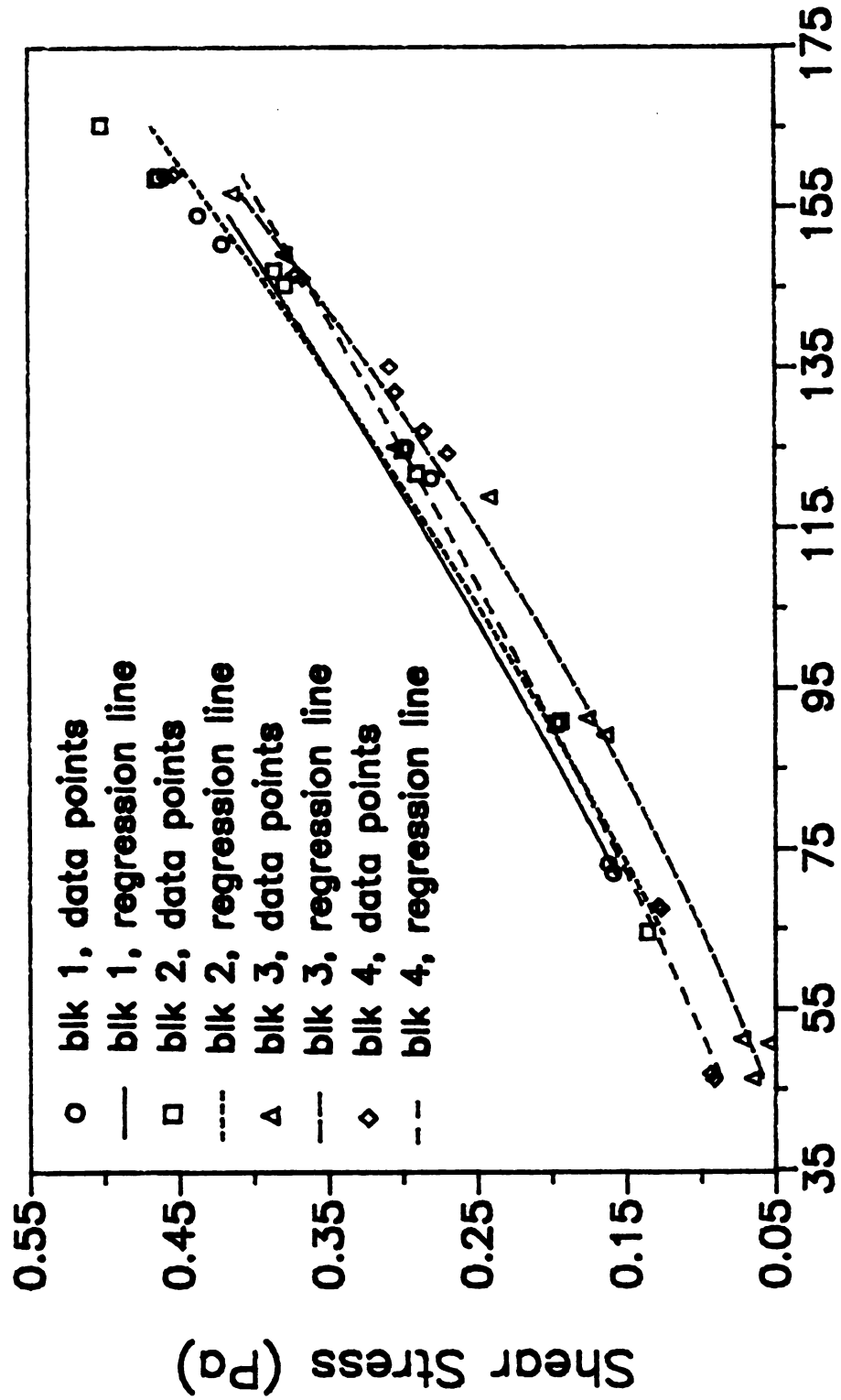

Figure A1 – All Experiments at 121.1°C, 1.82% Starch

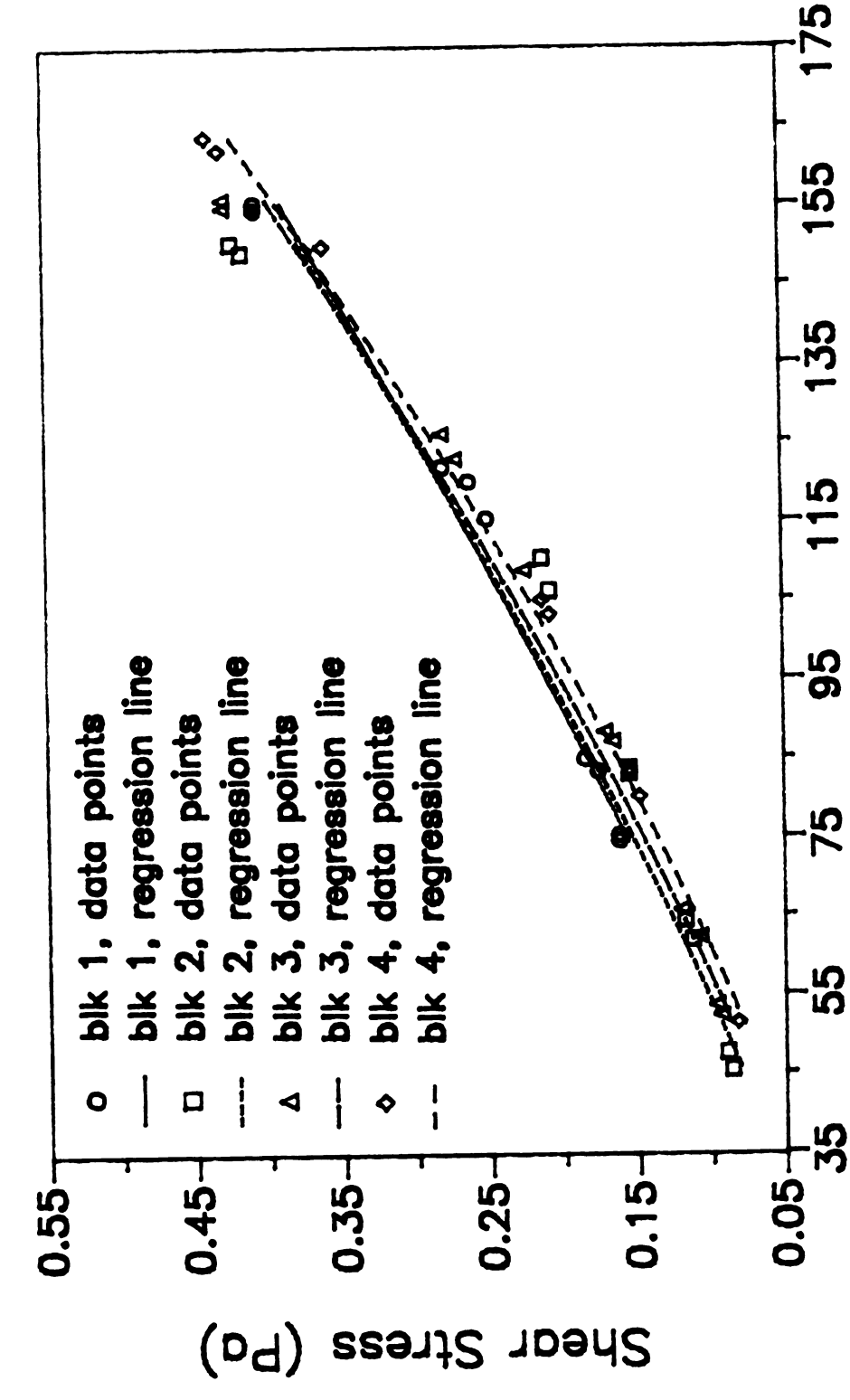

Figure A2 — All Experiments at 132.2°C, 1.82% Starch

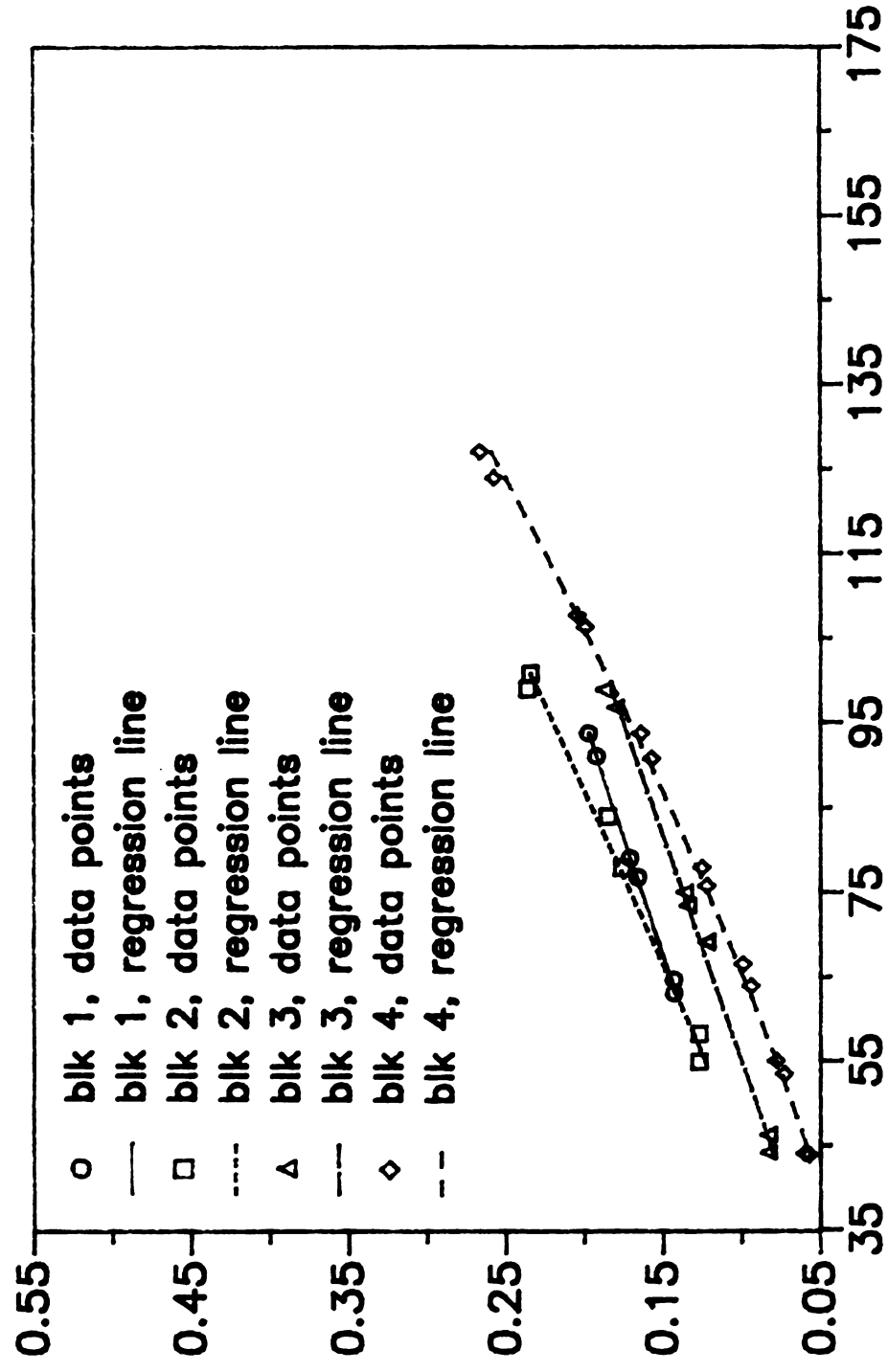

Figure A3 – All Experiments at 143.3°C, 1.82% Starch

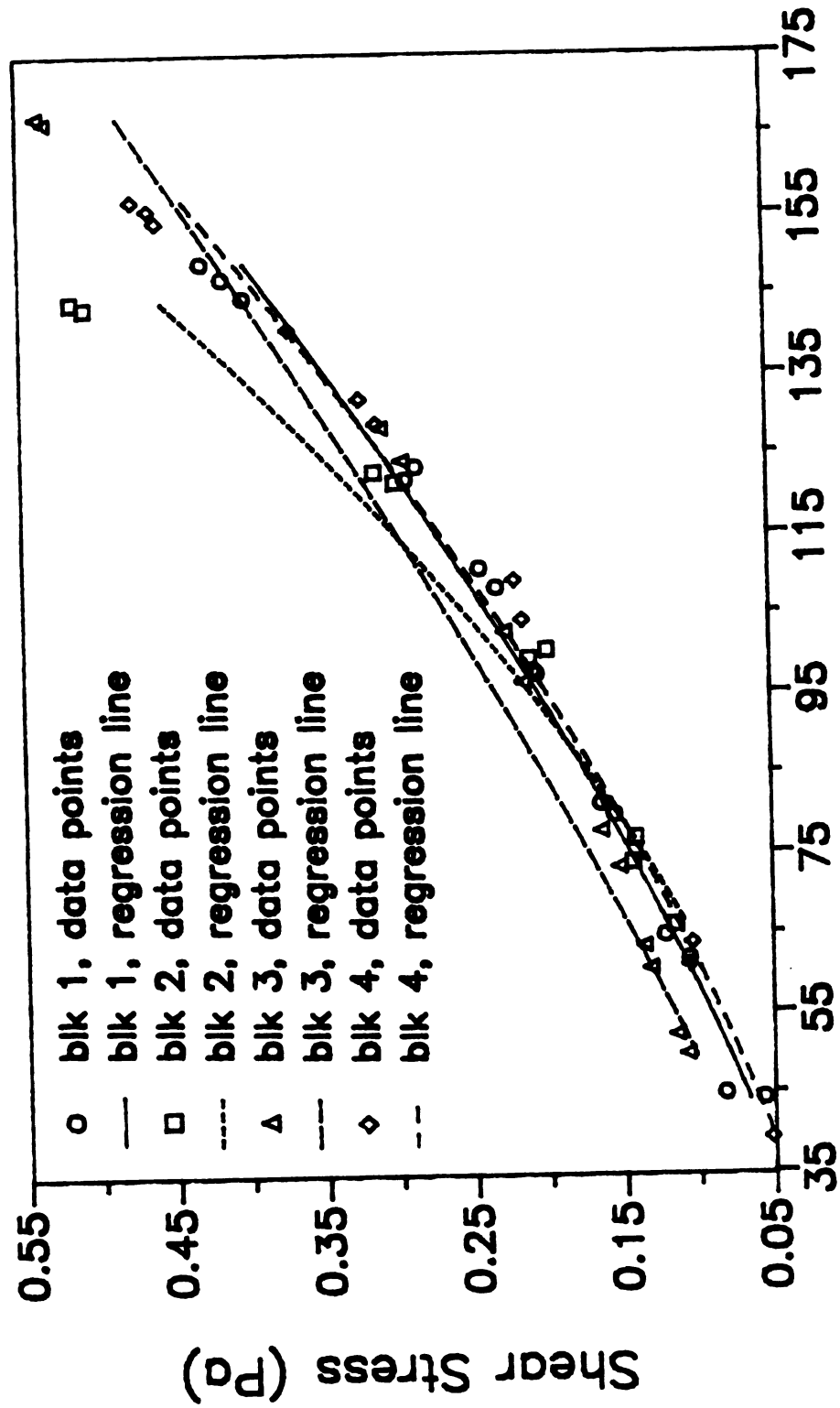

Figure A4 — All Experiments at 121.1°C, 2.72% Starch

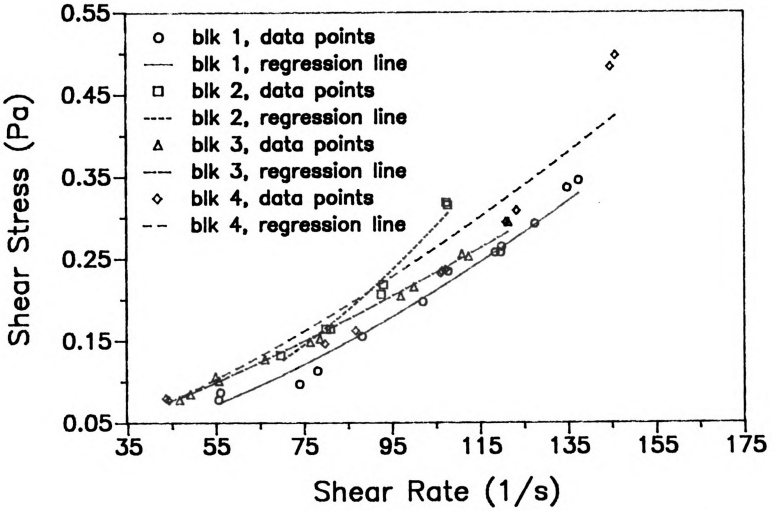

Figure A5 – All Experiments at 132.2°C, 2.72% Starch

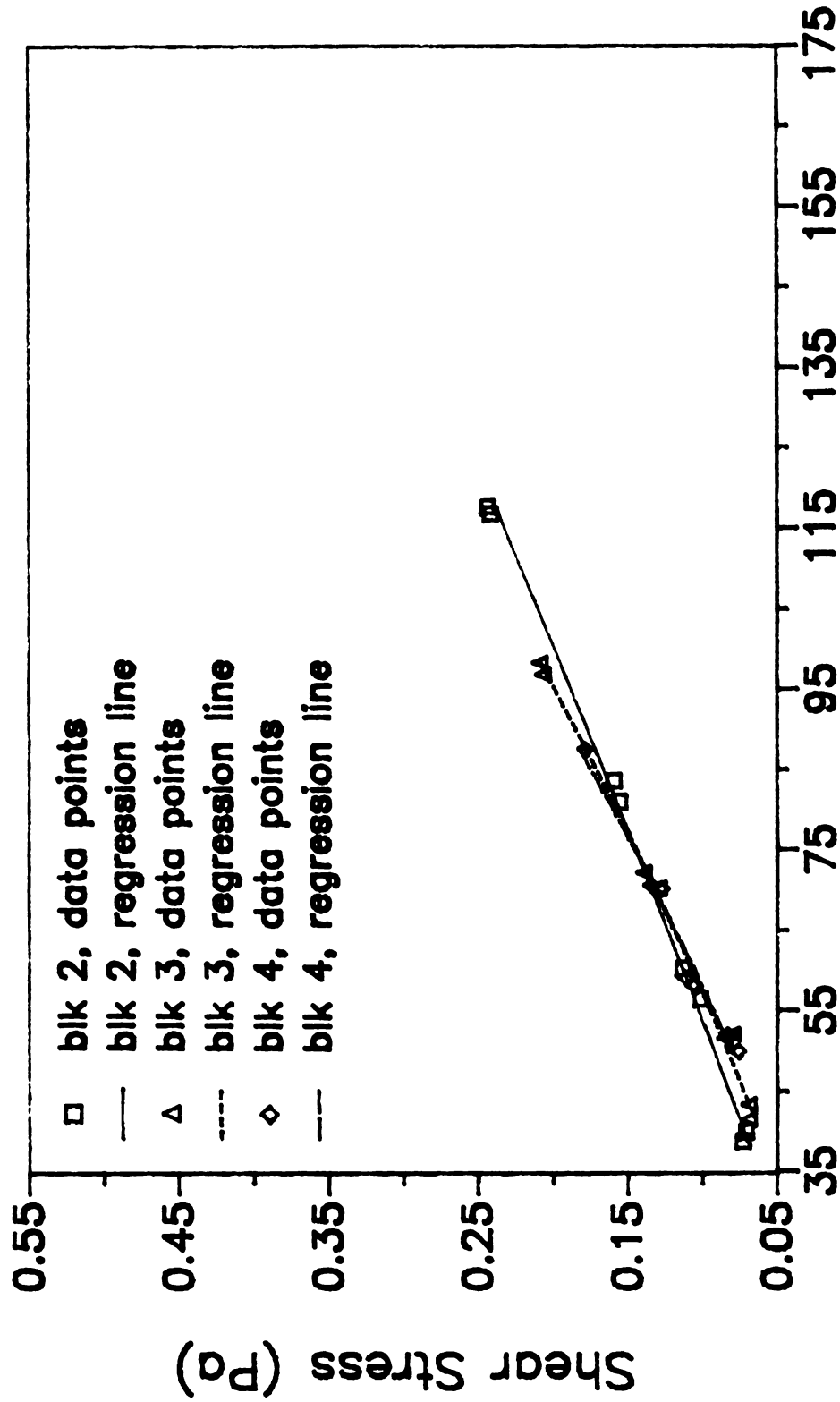

Figure A6 — All Experiments at 143.3°C, 2.72% Starch

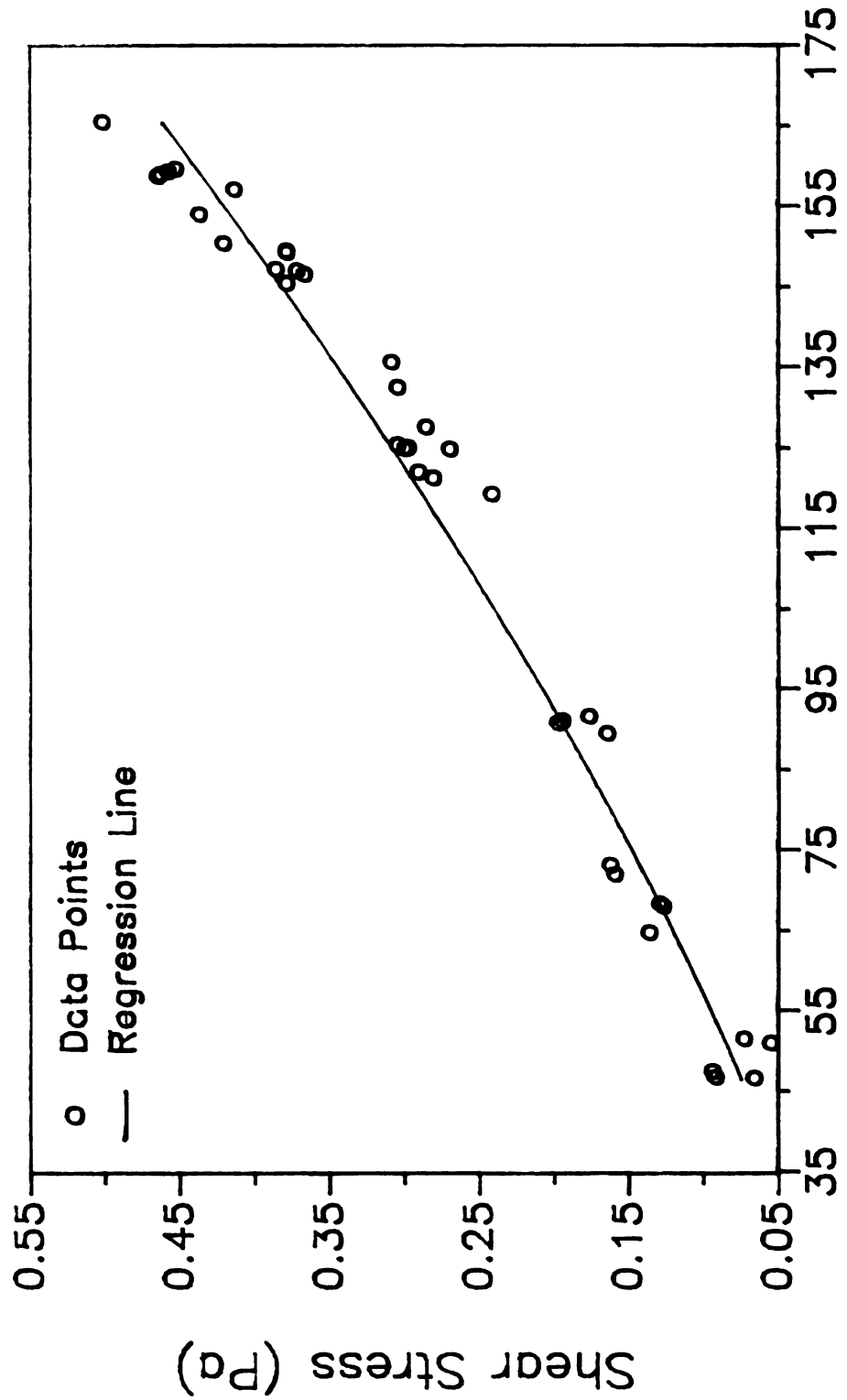

Figure A7 — Pooled Data: 121°C, 1.82% Starch

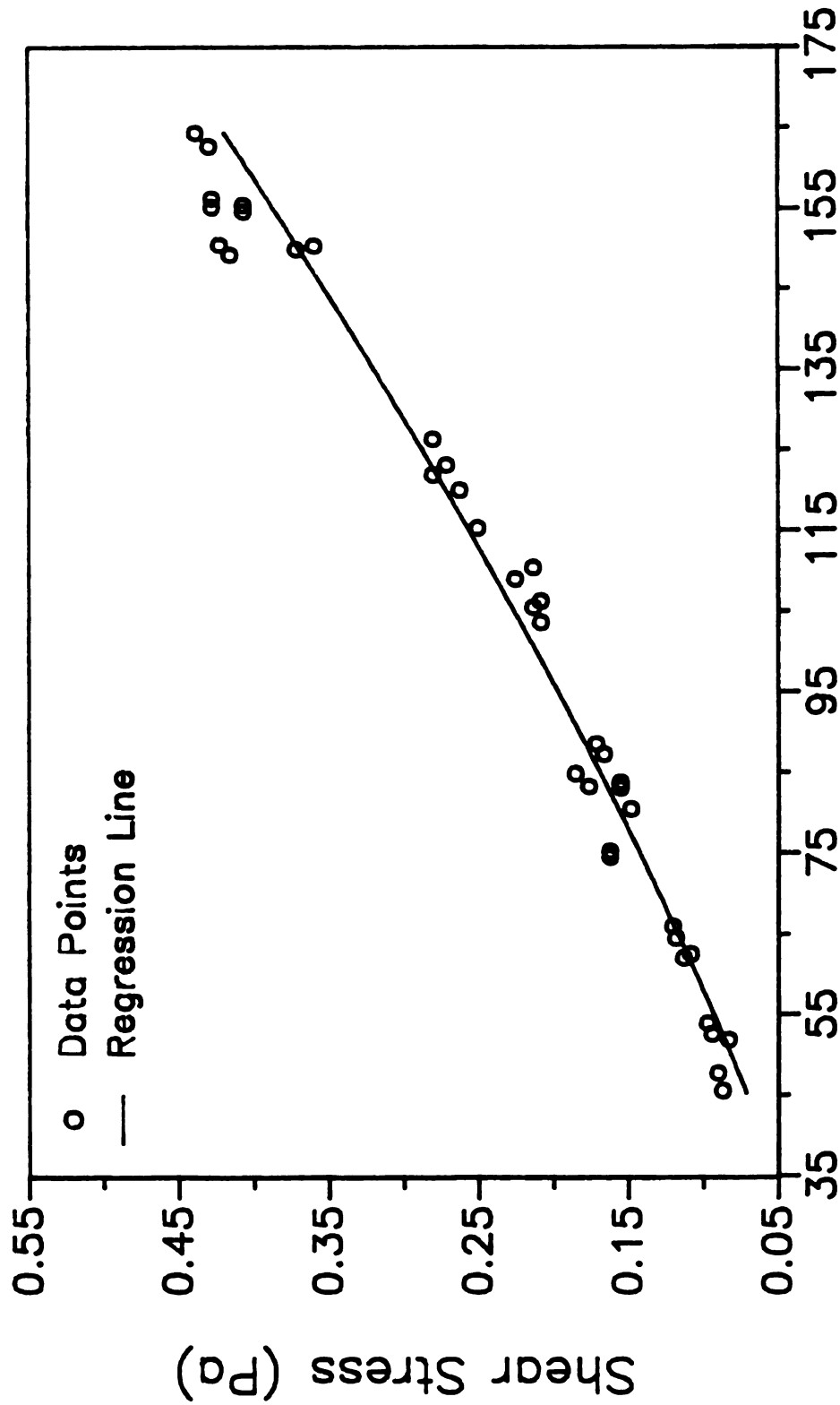

Figure A8 — Pooled Data: 132°C, 1.82% Starch

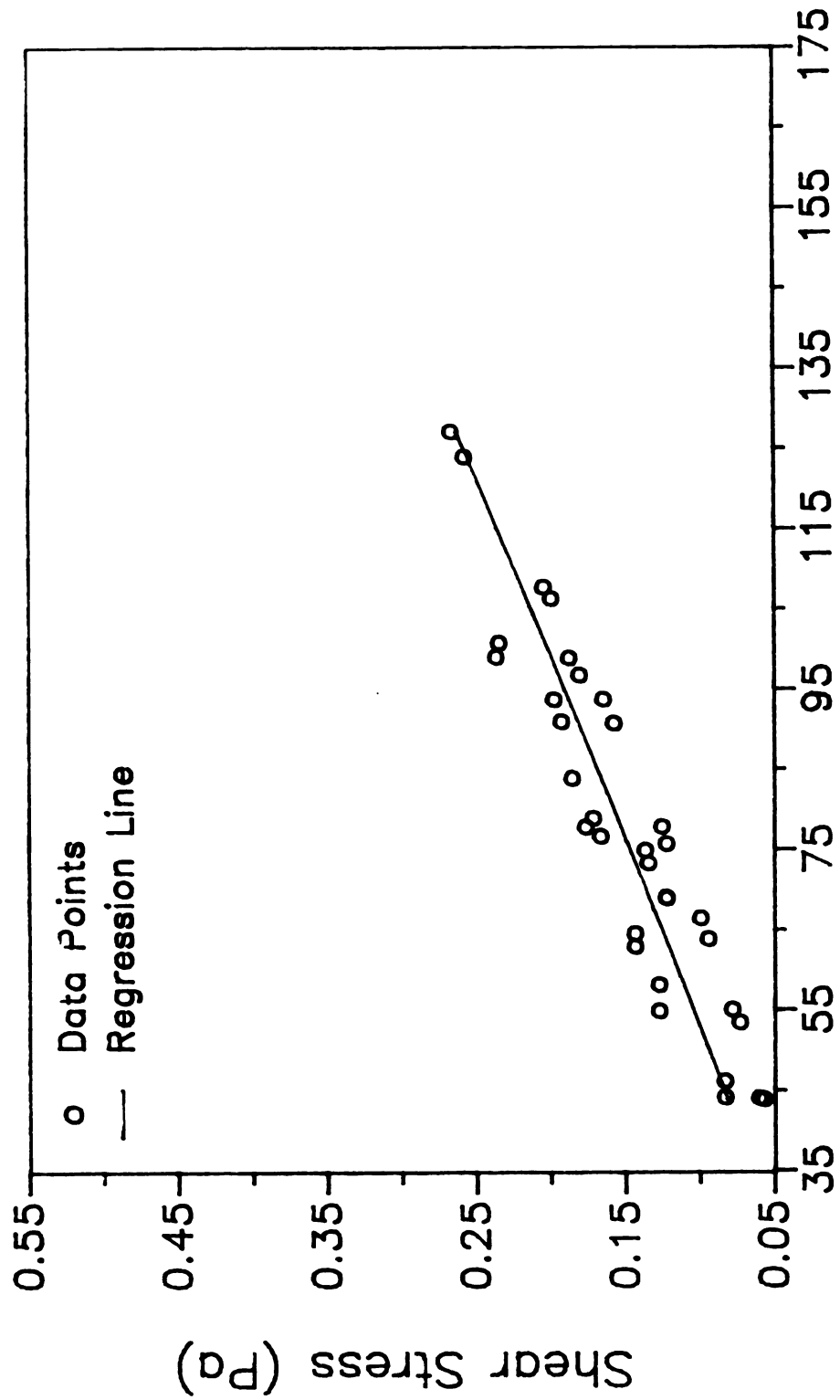

Figure A9 — Pooled Data: 143°C, 1.82% Starch

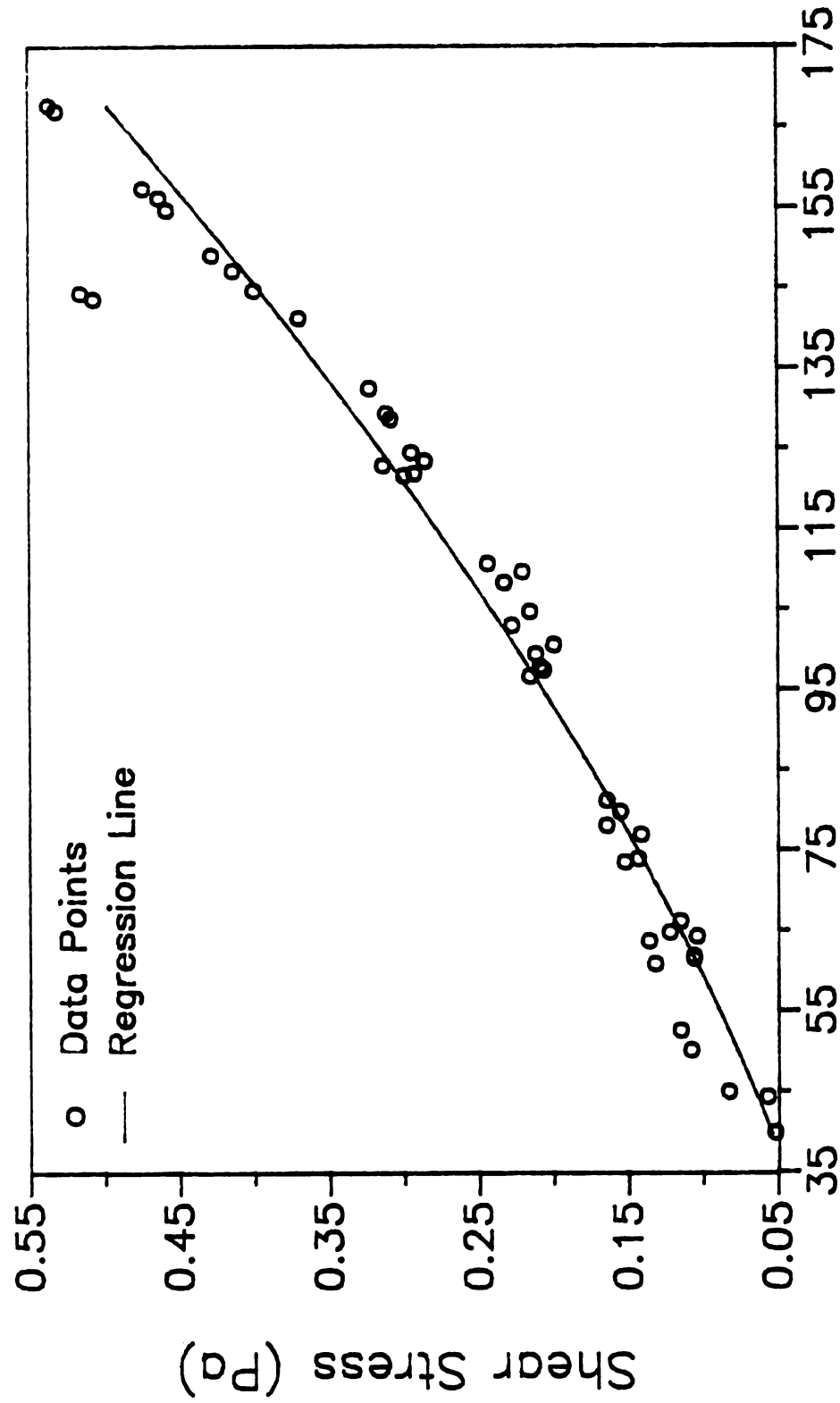

Figure A10 — Pooled Data: 121°C, 2.72% Starch

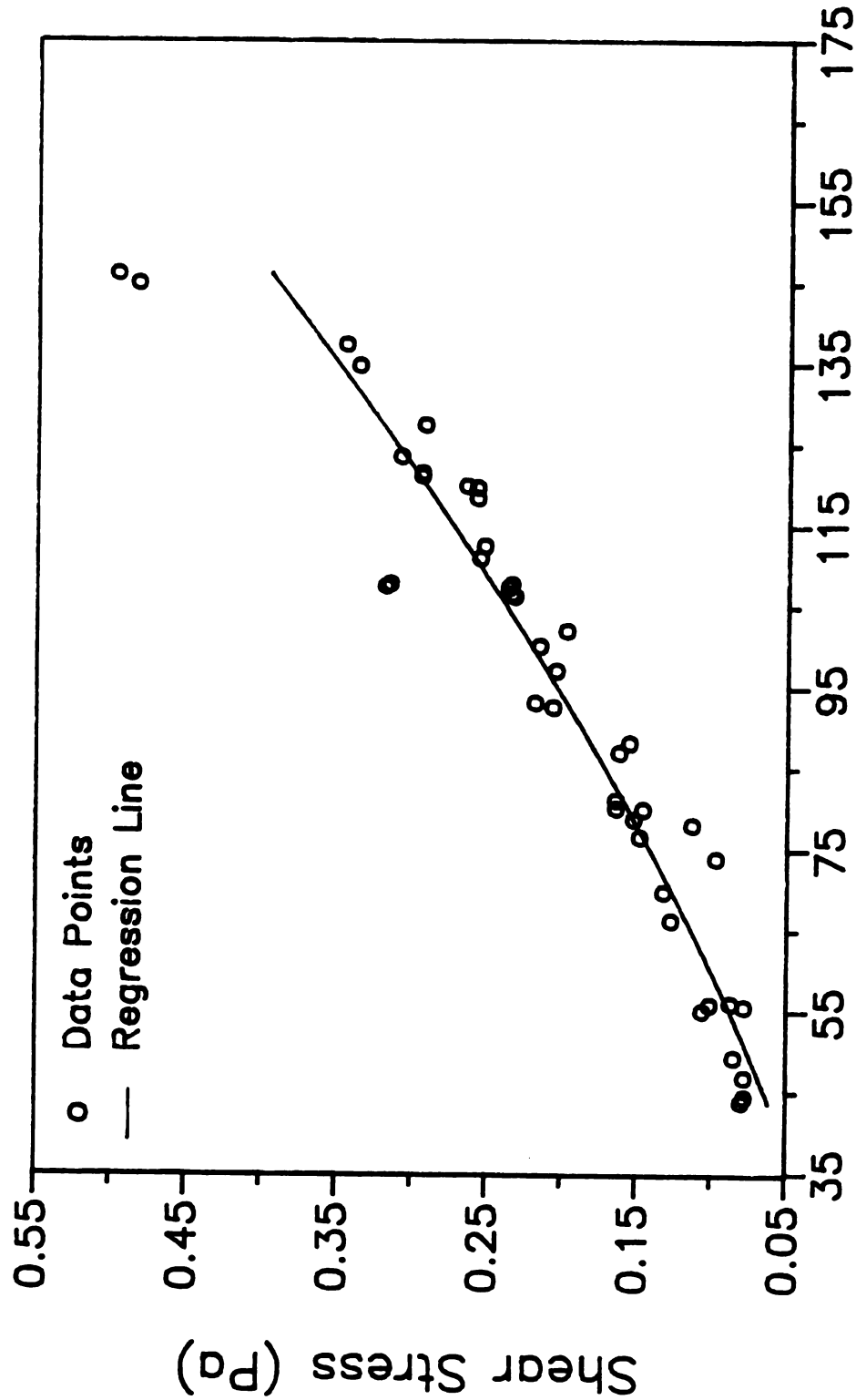

Figure A11 – Pooled Data: 132°C, 2.72% Starch

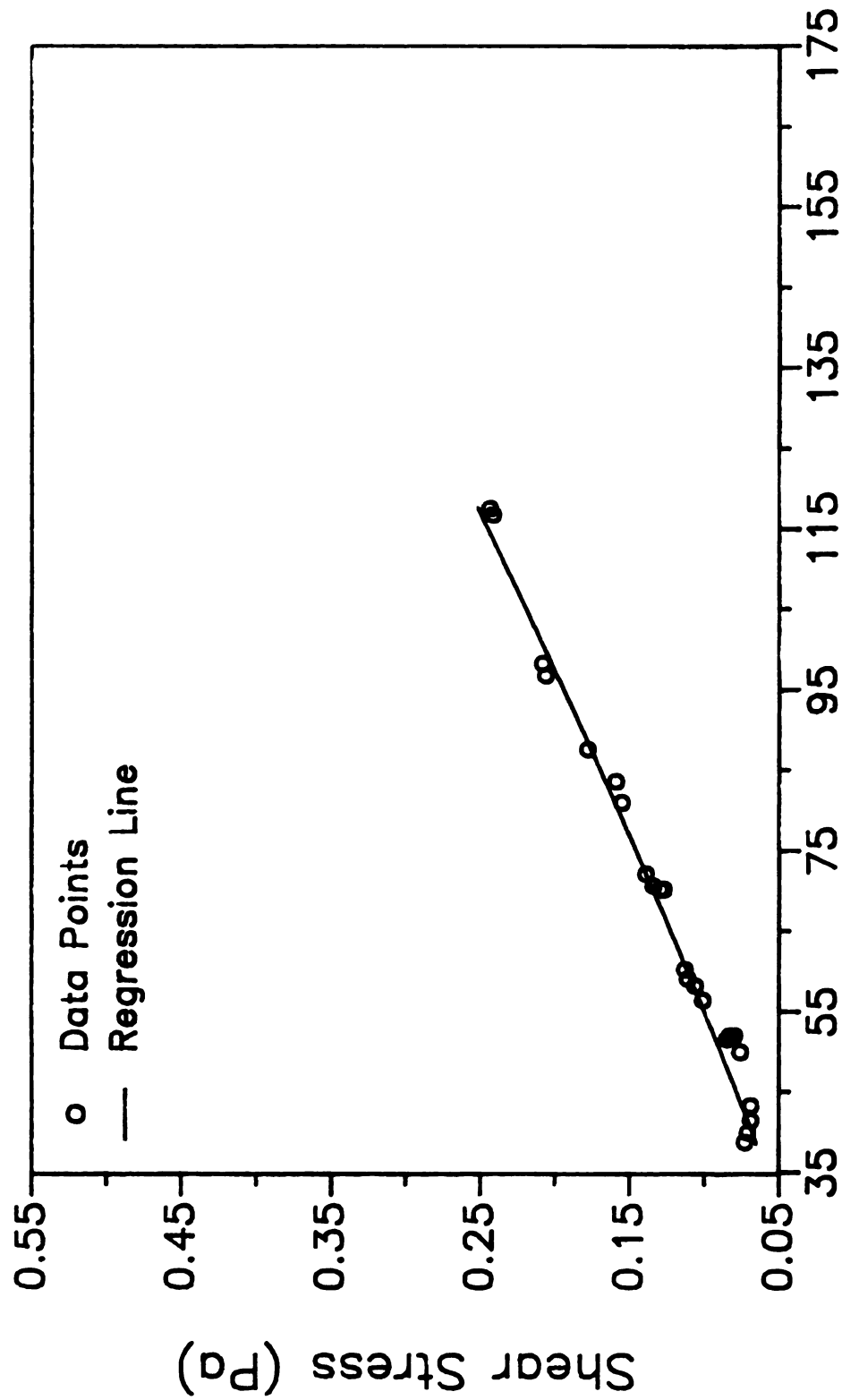

Figure A12 — Pooled Data: 143°C, 2.72% Starch

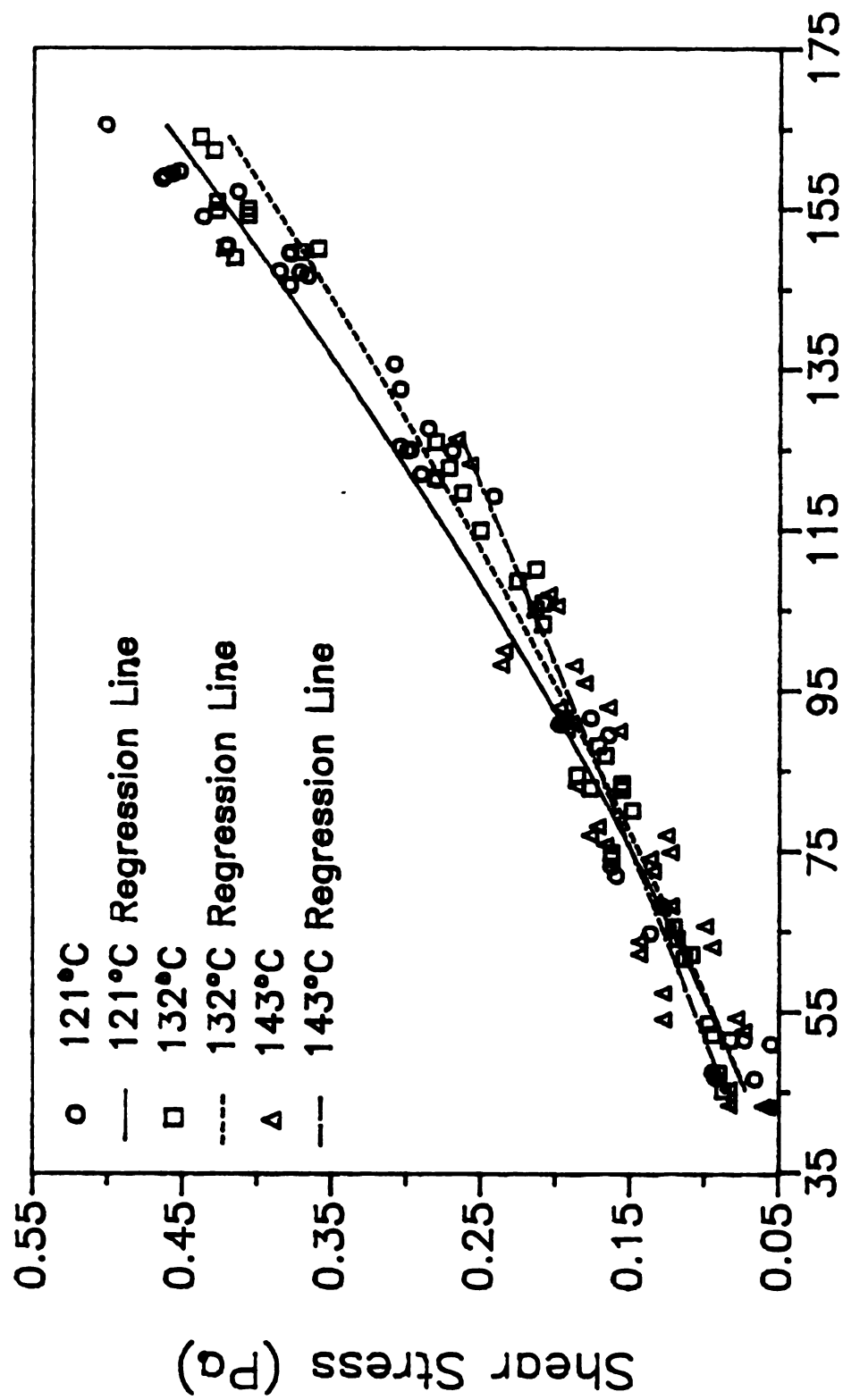

Figure A13 – Temperature Effect, 1.82% Starch

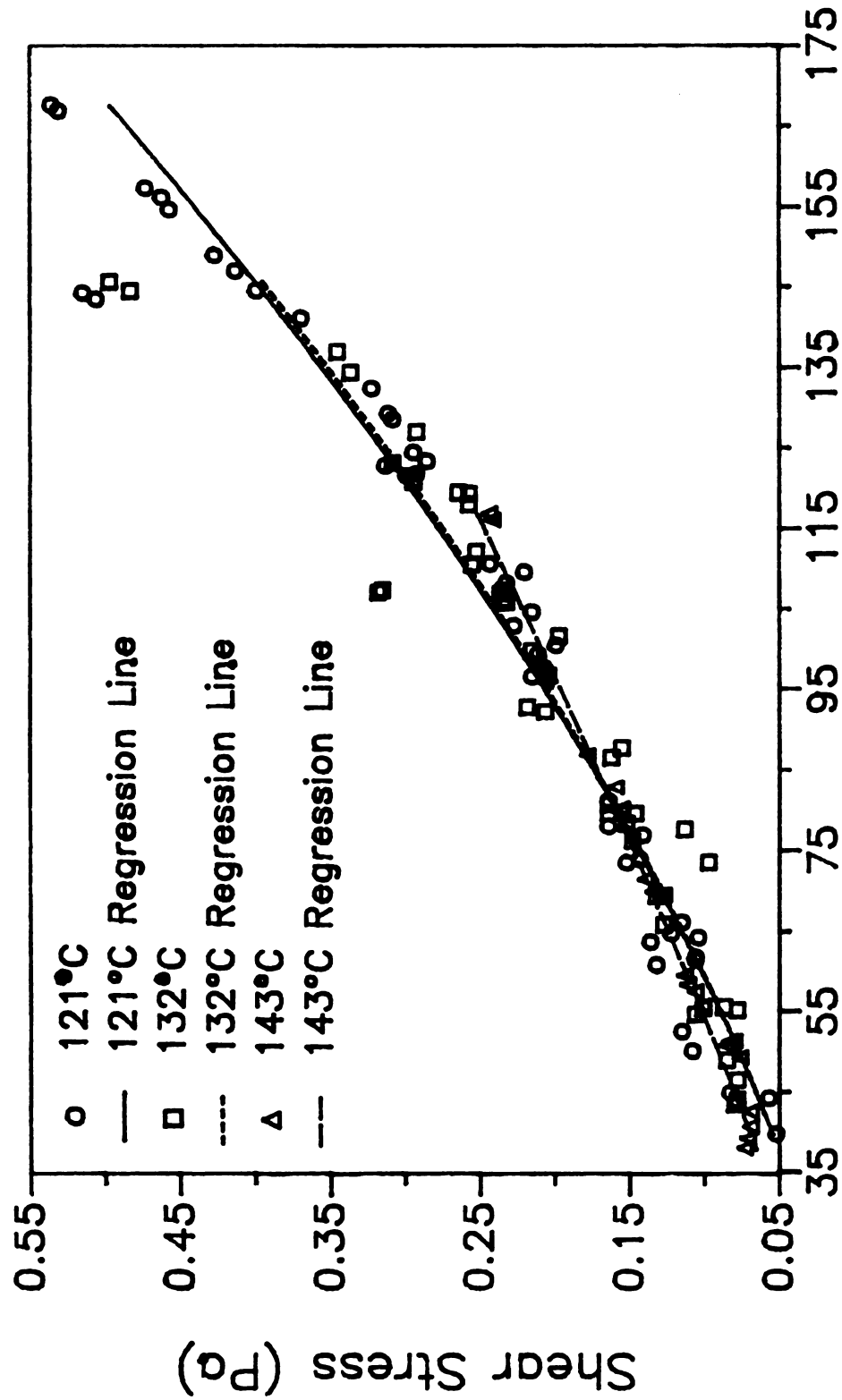

Figure A14 — Temperature Effect, 2.72% Starch

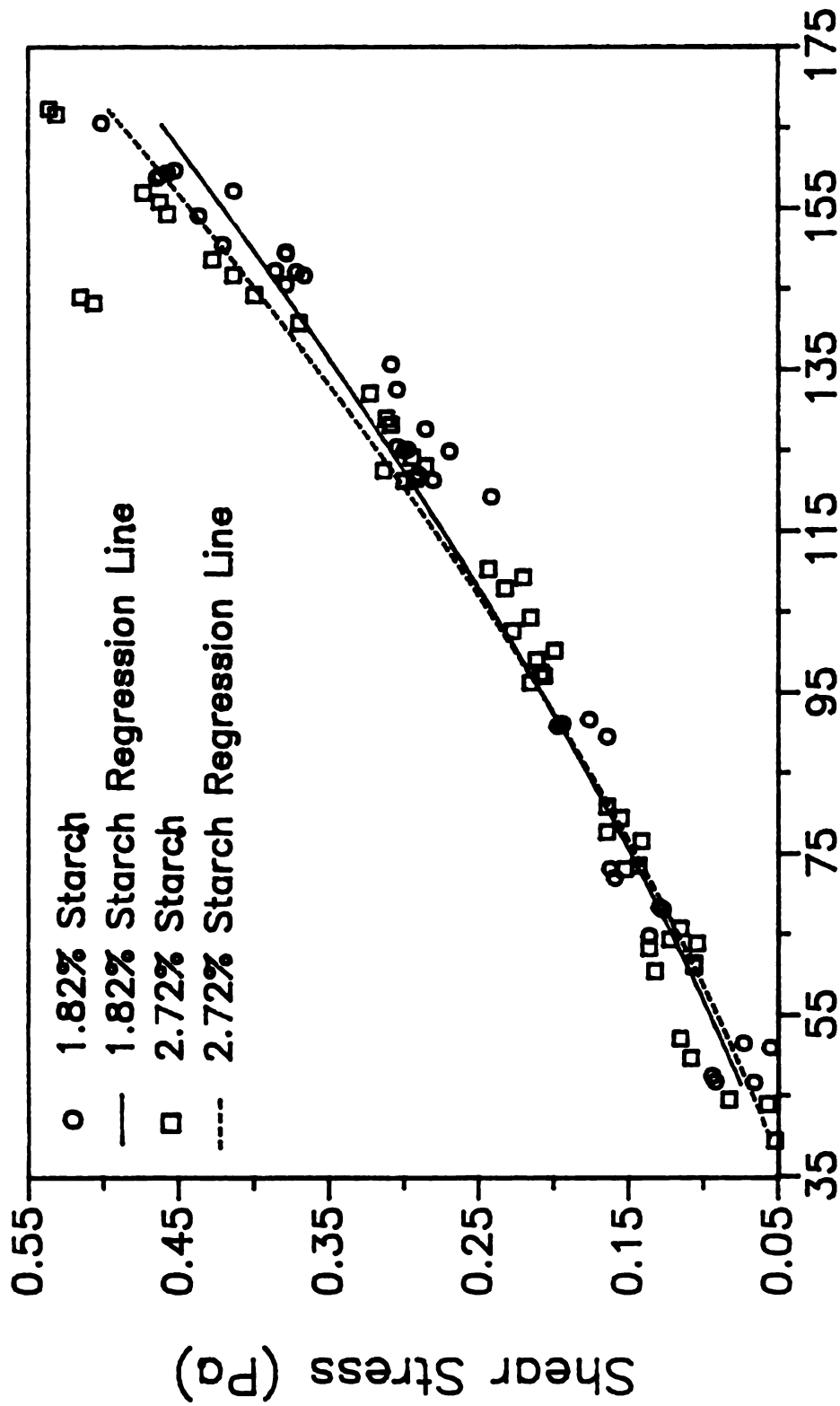

Figure A15 — Concentration Effect, 121°C

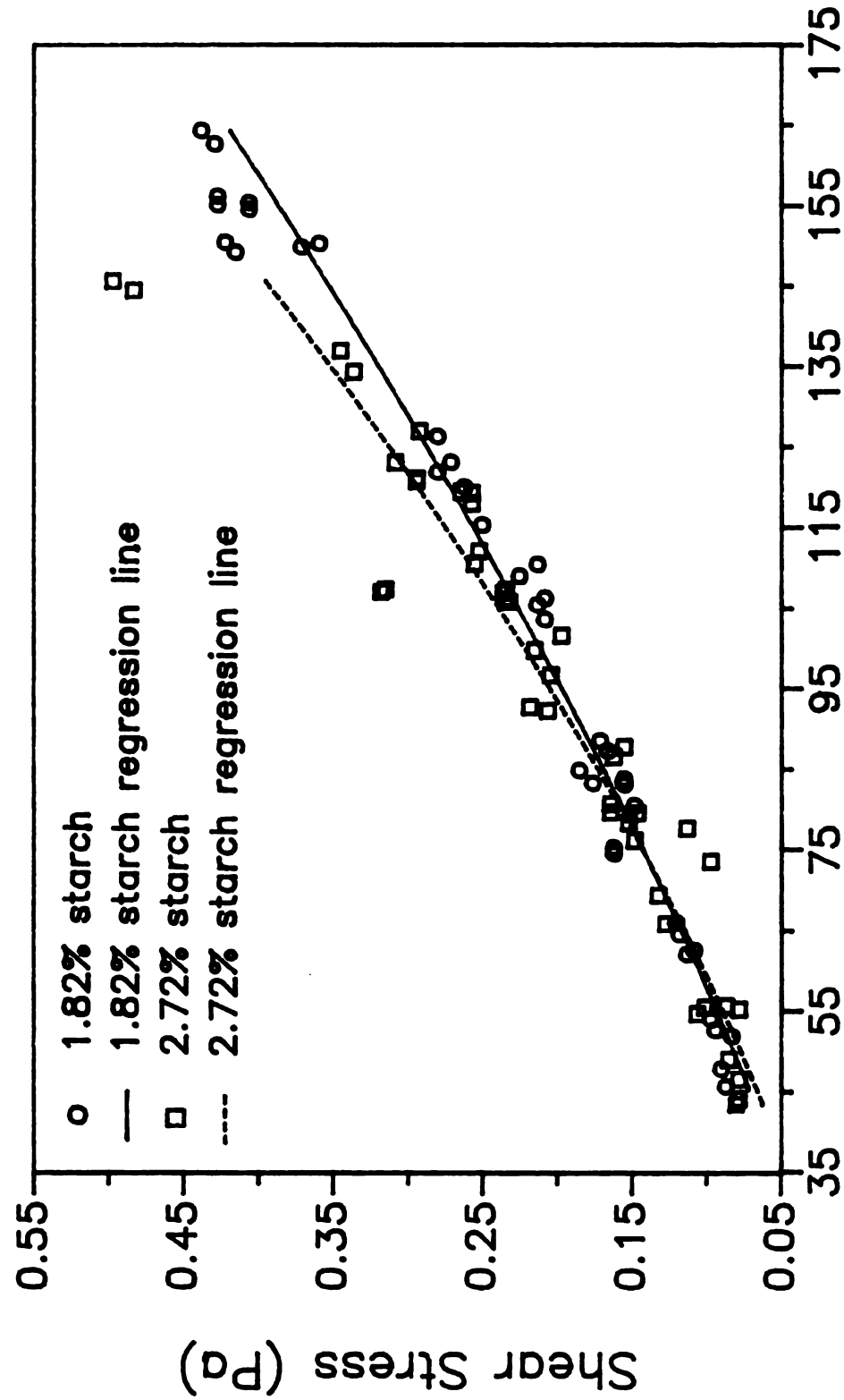

Figure A16 – Concentration Effect, 132°C

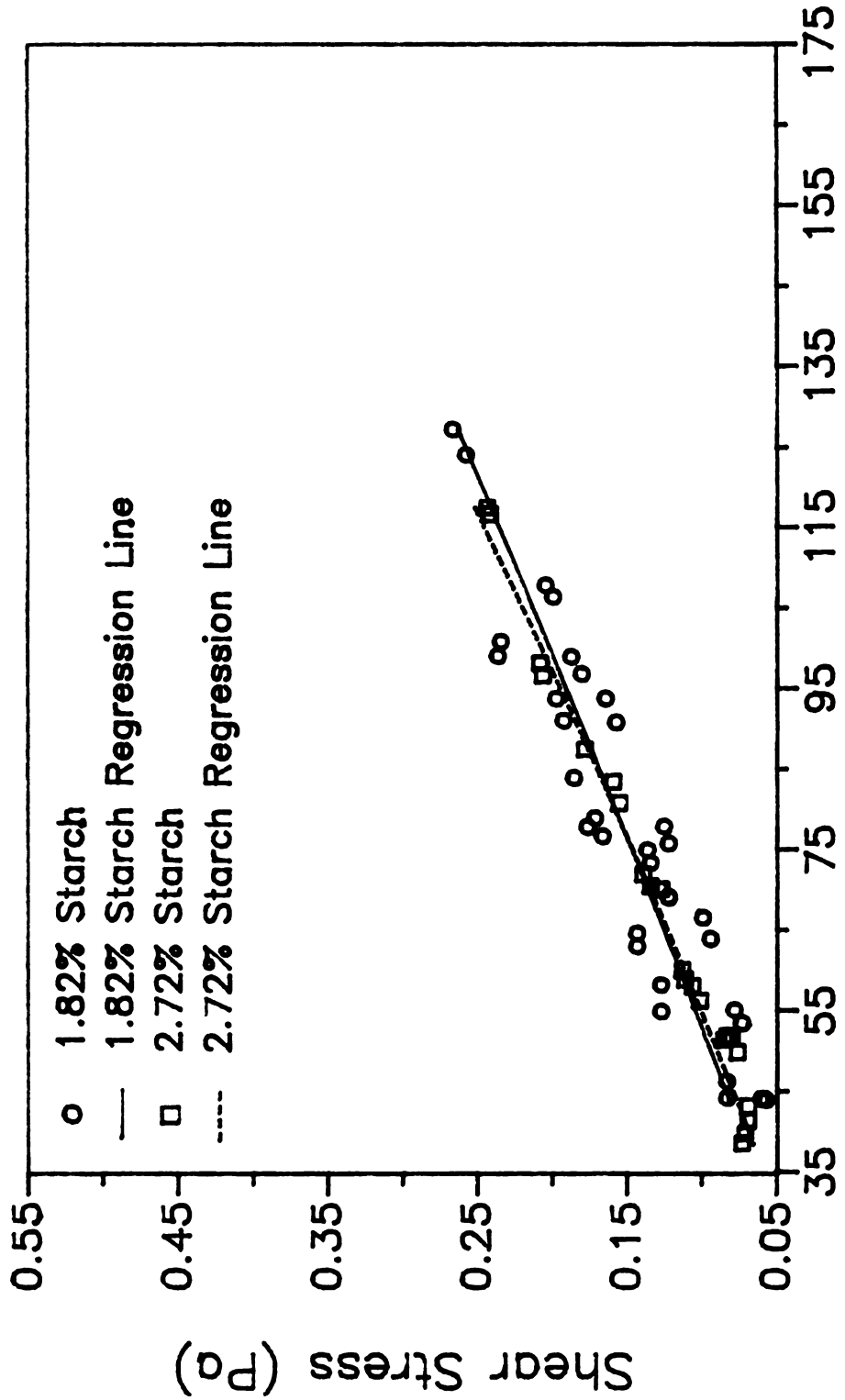

Figure A17 – Concentration Effect, 143°C

APPENDIX B
RAW DATA AS COLLECTED BY THE DATA ACQUISITION SYSTEM: TEMPERATURE GOING IN AND COMING OUT OF THE TUBE VISCOMETER, PRESSURE TRANSDUCER OUTPUT, AND MASS FLOW METER OUTPUT

Table B1. Block 1, 121.1°C, 1.82% starch

T_{in} (°C)	T_{out} (°C)	transducer output (millivolts)	flow meter output (lbs/min)
120.6	118.9	1189	3.952
121.5	118.8	1182	3.800
121.9	119.3	1129	2.857
121.2	119.7	1122	2.739
121.0	120.1	1071	1.340
121.3	119.2	1070	1.309

Table B2. Block 1, 132.2°C, 1.82% starch

T_{in} (°C)	T_{out} (°C)	transducer output (millivolts)	flow meter output (lbs/min)
131.7	129.4	1176	3.861
131.7	129.7	1176	3.833
132.8	130.0	1122	2.688
132.9	130.3	1114	2.643
132.7	129.9	1109	2.500
131.6	130.1	1077	1.587
131.1	129.4	1081	1.615
132.5	128.5	1071	1.361
133.0	129.0	1071	1.337

Table B3. Block 1, 143.3°C, 1.82% starch

T_{in} (°C)	T_{out} (°C)	transducer output (millivolts)	flow meter output (lbs/min)
143.7	140.9	1086	1.791
144.2	140.6	1084	1.728
143.6	139.8	1075	1.444
144.1	139.5	1073	1.394
142.8	140.1	1063	1.114
143.0	139.7	1063	1.062

Table B4. Block 1, 121.1°C, 2.72% starch

T_{in} (°C)	T_{out} (°C)	transducer output (millivolts)	flow meter output (lbs/min)
121.2	118.7	1185	3.841
121.5	119.2	1179	3.767
121.8	119.5	1173	3.678
121.0	118.0	1127	2.938
121.5	118.9	1124	2.997
121.4	119.1	1106	2.619
121.9	119.1	1101	2.557
121.3	119.4	1091	2.245
121.3	119.2	1090	2.236
121.4	118.9	1072	1.780
121.5	118.9	1068	1.755
121.0	119.0	1054	1.339
121.9	118.2	1047	1.287
121.4	118.4	1026	0.863
120.6	118.0	1037	0.796

Table B5. Block 1, 132.2°C, 2.72% starch

T_{in} (°C)	T_{out} (°C)	transducer output (millivolts)	flow meter output (lbs/min)
132.8	129.1	1127	3.181
132.3	130.4	1150	3.510
132.6	130.2	1146	3.422
131.2	130.1	1112	2.945
131.7	129.1	1115	2.947
132.1	129.3	1112	2.903
132.3	129.2	1102	2.571
132.1	129.4	1086	2.431
133.0	128.3	1068	2.049
133.2	129.7	1050	1.813
132.7	129.6	1043	1.722
132.4	129.5	1035	1.169
132.4	129.4	1039	1.154

Table B6. Block 1, 143.3°C, 2.72% starch - experiment failed

Table B7. Block 2, 121.1°C, 1.82% starch

T_{in} (°C)	T_{out} (°C)	transducer output (millivolts)	flow meter output (lbs/min)
120.9	119.3	1217	4.347
120.7	119.7	1200	4.077
120.5	119.1	1201	4.070
120.9	119.5	1167	3.636
121.4	119.3	1164	3.577
120.8	119.4	1130	2.925
121.5	119.0	1126	2.837
121.2	119.3	1086	1.948
121.2	118.9	1085	1.965
121.1	119.0	1060	1.240

Table B8. Block 2, 132.2°C, 1.82% starch

T_{in} (°C)	T_{out} (°C)	transducer output (millivolts)	flow meter output (lbs/min)
132.2	129.3	1183	4.050
132.6	130.0	1180	3.983
132.4	129.8	1093	2.451
132.6	129.6	1091	2.318
132.6	130.0	1068	1.681
132.1	129.8	1068	1.657
132.1	129.4	1052	1.158
132.7	129.1	1050	1.092
132.1	128.4	1040	0.710
132.0	128.3	1039	0.648

Table B9. Block 2, 143.3°C, 1.82% starch

T_{in} (°C)	T_{out} (°C)	transducer output (millivolts)	flow meter output (lbs/min)
143.6	139.2	1102	2.165
144.2	139.8	1103	2.106
144.3	140.4	1081	1.645
143.6	140.3	1077	1.460
143.2	139.5	1056	0.926
143.3	139.2	1056	0.818

Table B10. Block 2, 121.1°C, 2.72% starch

T_{in} (°C)	T_{out} (°C)	transducer output (millivolts)	flow meter output (lbs/min)
121.6	120.2	1223	4.030
120.7	120.3	1219	3.980
121.3	120.8	1136	3.044
122.1	120.8	1130	3.004
120.8	119.9	1087	2.391
121.4	119.5	1092	2.334
121.1	119.6	1062	1.715
121.1	119.1	1063	1.609

Table B11. Block 2, 132.2°C, 2.72% starch

T_{in} (°C)	T_{out} (°C)	transducer output (millivolts)	flow meter output (lbs/min)
131.9	130.2	1138	2.762
131.4	130.1	1137	2.768
133.0	129.8	1095	2.187
132.5	130.3	1090	2.171
132.3	130.4	1072	1.819
132.8	129.9	1072	1.786
132.7	129.5	1058	1.493

Table B12. Block 2, 143.3°C, 2.72% starch

T_{in} (°C)	T_{out} (°C)	transducer output (millivolts)	flow meter output (lbs/min)
143.3	139.7	1106	2.632
143.1	140.1	1105	2.610
143.9	140.1	1070	1.707
143.6	140.0	1068	1.647
143.3	140.0	1050	1.088
143.3	139.8	1045	1.005
144.0	138.2	1032	0.584
144.3	138.1	1033	0.535

Table B13. Block 3, 121.1°C, 1.82% starch

T_{in} (°C)	T_{out} (°C)	transducer output (millivolts)	flow meter output (lbs/min)
121.1	119.2	1164	3.785
121.0	119.3	1164	3.778
121.9	119.2	1132	3.042
121.7	119.8	1105	2.930
121.7	119.6	1077	2.136
122.0	119.3	1072	2.094
121.8	119.1	1025	1.119
120.8	118.5	1033	1.077

Table B14. Block 3, 132.2°C, 1.82% starch

T_{in} (°C)	T_{out} (°C)	transducer output (millivolts)	flow meter output (lbs/min)
132.2	129.4	1185	4.041
132.3	130.0	1185	4.006
131.8	130.2	1122	2.991
131.7	129.7	1118	2.894
132.6	129.5	1098	2.482
133.1	130.0	1075	1.909
132.9	130.0	1073	1.879
132.4	129.6	1053	1.304
132.7	127.3	1048	1.228
131.5	128.2	1043	0.983
131.6	128.2	1042	0.947

Table B15. Block 3, 143.3°C, 1.82% starch

T_{in} (°C)	T_{out} (°C)	transducer output (millivolts)	flow meter output (lbs/min)
143.2	139.5	1082	2.105
143.9	139.4	1079	2.046
143.8	140.2	1060	1.430
143.9	139.9	1059	1.384
143.7	139.7	1054	1.281
142.9	139.7	1054	1.277
143.4	138.8	1037	0.676
143.5	138.5	1037	0.610

Table B16. Block 3, 121.1°C, 2.72% starch

T_{in} (°C)	T_{out} (°C)	transducer output (millivolts)	flow meter output (lbs/min)
121.3	119.0	1232	4.506
121.5	119.5	1230	4.471
120.4	119.6	1134	3.005
121.1	119.4	1128	2.880
121.3	119.3	1099	2.258
121.6	119.5	1094	2.069
121.1	119.2	1072	1.571
121.3	119.0	1067	1.454
121.1	118.3	1060	1.175
121.8	118.0	1058	1.095
120.8	118.1	1051	0.872
121.2	118.0	1048	0.815

Table B17. Block 3, 132.2°C, 2.72% starch

T_{in} (°C)	T_{out} (°C)	transducer output (millivolts)	flow meter output (lbs/min)
133.0	129.8	1128	2.916
132.5	130.4	1111	2.585
132.9	130.4	1110	2.638
132.8	130.4	1094	2.268
131.9	130.5	1089	2.185
132.6	129.8	1067	1.677
133.1	129.6	1065	1.616
132.8	129.7	1056	1.329
132.0	129.4	1047	1.019
132.0	129.1	1045	1.060
132.1	128.3	1038	0.897
132.5	128.1	1035	0.840

Table B18. Block 3, 143.3°C, 2.72% starch

T_{in} (°C)	T_{out} (°C)	transducer output (millivolts)	flow meter output (lbs/min)
142.9	139.6	1091	2.223
142.9	139.6	1090	2.178
144.0	139.9	1061	1.496
143.3	139.8	1057	1.455
143.6	139.7	1038	0.969
143.8	139.4	1036	1.001
143.8	138.8	1031	0.754
143.7	138.7	1031	0.693

Table B19. Block 4, 121.1°C, 1.82% starch

T_{in} (°C)	T_{out} (°C)	transducer output (millivolts)	flow meter output (lbs/min)
121.3	119.4	1198	4.242
121.3	119.6	1196	4.241
121.1	119.4	1161	3.685
121.2	119.4	1159	3.664
121.2	119.4	1134	3.277
121.2	119.3	1132	3.173
121.0	118.8	1117	2.935
120.8	119.0	1124	3.016
121.3	119.2	1057	1.329
120.8	118.7	1056	1.327
121.6	118.5	1042	0.756
122.1	118.1	1041	0.741

Table B20. Block 4, 132.2°C, 1.82% starch

T_{in} (°C)	T_{out} (°C)	transducer output (millivolts)	flow meter output (lbs/min)
132.4	129.9	1190	4.198
132.7	130.4	1186	4.139
131.8	129.8	1156	3.729
131.9	129.8	1161	3.711
132.7	129.5	1093	2.417
132.8	130.0	1091	2.367
133.2	130.0	1068	1.826
132.2	129.5	1065	1.746
131.3	128.7	1037	1.003

Table B21. Block 4, 143.3°C, 1.82% starch

T_{in} (°C)	T_{out} (°C)	transducer output (millivolts)	flow meter output (lbs/min)
143.3	139.8	1116	3.075
143.8	140.3	1112	2.976
142.9	139.6	1089	2.489
143.1	139.9	1087	2.448
144.0	140.2	1072	2.097
143.8	140.5	1069	2.015
143.2	140.1	1055	1.672
143.9	139.8	1054	1.609
143.2	139.7	1044	1.377
143.8	139.1	1042	1.307
143.9	139.2	1035	1.074
143.9	138.9	1033	1.038
143.7	138.7	1030	0.784
143.3	138.2	1029	0.787

Table B22. Block 4, 121.1°C, 2.72% starch

T_{in} (°C)	T_{out} (°C)	transducer output (millivolts)	flow meter output (lbs/min)
121.4	119.0	1205	4.209
121.8	119.5	1200	4.154
121.6	119.8	1198	4.097
122.0	120.0	1160	3.579
121.6	120.0	1140	3.292
121.8	120.2	1135	3.192
120.9	119.4	1096	2.630
120.4	119.2	1094	2.472
121.8	119.1	1046	1.383
121.9	119.0	1047	1.282
120.2	118.7	1023	0.737

Table B23. Block 4, 132.2°C, 2.72% starch

T_{in} (°C)	T_{out} (°C)	transducer output (millivolts)	flow meter output (lbs/min)
131.6	130.4	1215	4.021
131.9	129.7	1209	3.942
132.4	130.4	1134	2.982
132.7	130.2	1128	2.905
132.7	130.0	1102	2.459
131.3	130.1	1101	2.451
132.2	129.3	1103	2.483
131.9	129.8	1071	1.929
132.6	130.0	1064	1.735
132.9	129.1	1036	0.732
132.3	128.8	1035	0.761

Table B24. Block 4, 143.3°C, 2.72% starch

T_{in} (°C)	T_{out} (°C)	transducer output (millivolts)	flow meter output (lbs/min)
143.4	138.4	1078	1.907
143.7	140.7	1059	1.529
143.9	140.3	1056	1.542
143.1	137.7	1049	1.235
143.7	138.3	1047	1.222
143.7	139.4	1037	1.096
143.0	139.4	1034	1.051

APPENDIX C
CALCULATED VALUES OF VOLUMETRIC FLOW RATE, PRESSURE DROP, SHEAR STRESS, SHEAR RATE, AND GENERALIZED AND CRITICAL REYNOLDS NUMBERS FOR EACH EXPERIMENT

Table C1. Block 1, 121.1°C, 1.82% starch

Q $(m^3/s)*10^5$	ΔP (Pa)	σ (Pa)	$\dot{\gamma}$ (1/s)	Re
3.485	630.50	0.436	154.21	1280
3.363	606.97	0.420	150.65	
2.610	428.84	0.297	125.28	
2.516	405.31	0.280	121.50	
1.398	233.90	0.162	73.42	
1.373	230.54	0.159	72.28	

pH=7.28
Critical Re=1948

Table C2. Block 1, 132.2°C, 1.82% starch

Q $(m^3/s)*10^5$	ΔP (Pa)	σ (Pa)	$\dot{\gamma}$ (1/s)	Re
3.444	586.80	0.406	155.56	1344
3.422	586.80	0.406	154.74	
2.498	405.31	0.280	122.11	
2.462	378.42	0.262	120.26	
2.347	361.62	0.250	115.55	
1.610	254.07	0.176	83.53	
1.633	267.51	0.185	85.13	
1.428	233.90	0.162	75.53	
1.409	233.90	0.162	74.82	

pH= not taken
Critical Re=1969

Table C3. Block 1, 143.3°C, 1.82% starch

Q $(m^3/s)*10^5$	ΔP (Pa)	σ (Pa)	$\dot{\gamma}$ (1/s)	Re
1.795	284.31	0.197	93.91	756
1.743	277.59	0.192	91.20	
1.512	247.34	0.171	79.20	
1.471	240.62	0.166	76.94	
1.243	207.01	0.143	64.86	
1.200	207.01	0.143	63.26	

pH=7.31
Critical Re=2203

Table C4. Block 1, 121.1°C, 2.72% starch

Q $(m^3/s)*10^5$	ΔP (Pa)	σ (Pa)	$\dot{\gamma}$ (1/s)	Re
3.396	617.05	0.427	149.16	1283
3.337	596.89	0.413	147.23	
3.266	576.72	0.399	144.79	
2.675	422.12	0.292	122.05	
2.722	412.03	0.285	123.62	
2.420	351.53	0.243	110.90	
2.370	334.73	0.232	108.52	
2.121	301.12	0.208	98.06	
2.114	297.76	0.206	97.67	
1.750	237.26	0.164	81.47	
1.730	223.82	0.155	80.06	
1.397	176.76	0.122	65.07	
1.356	153.24	0.106	62.12	
1.017	82.65	0.057	44.64	
0.963	119.63	0.083	45.28	

pH=7.37
Critical Re=1859

Table C5. Block 1, 132.2°C, 2.72% starch

Q $(m^3/s)*10^5$	ΔP (Pa)	σ (Pa)	$\dot{\gamma}$ (1/s)	Re
2.896	422.12	0.292	127.63	1309
3.161	499.42	0.345	137.55	
3.090	485.97	0.366	134.97	
2.706	371.70	0.257	119.93	
2.707	381.78	0.264	120.13	
2.672	371.70	0.257	118.66	
2.404	338.09	0.234	108.00	
2.291	284.31	0.197	102.28	
1.983	223.82	0.155	88.46	
1.793	163.32	0.133	78.36	
1.719	139.79	0.097	74.25	
1.273	112.90	0.078	55.95	
1.261	126.35	0.087	56.35	

pH=7.82
Critical Re=1787

Table C6. Block 1, 143.3°C, 2.72% starch - experiment failed

Table C7. Block2, 121.1°C, 1.82% starch

Q $(m^3/s)*10^5$	ΔP (Pa)	σ (Pa)	$\dot{\gamma}$ (1/s)	Re
3.800	724.61	0.501	165.74	1340
3.585	667.47	0.462	159.30	
3.579	670.83	0.464	159.00	
3.232	556.56	0.385	147.52	
3.185	546.47	0.378	145.78	
2.664	432.20	0.299	125.21	
2.594	418.75	0.290	122.31	
1.884	284.31	0.197	91.11	
1.897	280.95	0.194	91.43	
1.318	196.93	0.136	65.16	

pH=7.35
Critical Re=1891

Table C8. Block 2, 132.2°C, 1.82% starch

Q $(m^3/s)*10^5$	ΔP (Pa)	σ (Pa)	$\dot{\gamma}$ (1/s)	Re
3.597	610.33	0.422	150.71	1425
3.543	600.25	0.415	149.49	
2.307	307.84	0.213	110.75	
2.200	301.12	0.208	106.57	
1.686	223.82	0.155	84.14	
1.667	223.82	0.155	83.44	
1.264	170.04	0.118	64.90	
1.211	163.32	0.133	62.14	
0.903	129.71	0.090	48.15	
0.853	126.35	0.087	45.99	

pH=7.65
Critical Re=1940

Table C9. Block 2, 143.3°C, 1.82% starch

Q $(m^3/s)*10^5$	ΔP (Pa)	σ (Pa)	$\dot{\gamma}$ (1/s)	Re
2.100	338.09	0.234	101.04	853
2.052	341.45	0.236	99.25	
1.676	267.51	0.185	84.18	
1.525	254.07	0.176	78.13	
1.089	183.48	0.127	58.50	
1.001	183.48	0.127	55.22	

pH=8.44
Critical Re=2061

Table C10. Block 2, 121.1°C, 2.72% starch

Q $(m^3/s)*10^5$	ΔP (Pa)	σ (Pa)	$\dot{\gamma}$ (1/s)	Re
3.547	744.77	0.515	144.58	1129
3.507	731.33	0.506	143.81	
2.759	452.36	0.313	123.12	
2.727	432.20	0.299	121.87	
2.237	287.68	0.199	100.86	
2.192	304.48	0.211	99.71	
1.698	203.65	0.141	77.32	
1.613	207.01	0.143	74.31	
1.461	166.68	0.155	66.54	

pH=8.31
Critical Re=1719

Table C11. Block 2, 132.2°C, 2.72% starch

Q $(m^3/s)*10^5$	ΔP (Pa)	σ (Pa)	$\dot{\gamma}$ (1/s)	Re
2.558	459.09	0.318	107.78	948
2.563	455.73	0.315	108.11	
2.094	314.56	0.218	93.47	
2.081	297.76	0.206	92.92	
1.798	237.26	0.164	81.43	
1.771	237.26	0.164	80.42	
1.535	190.21	0.132	70.13	

pH=7.78
Critical Re=1654

Table C12. Block 2, 143.3°C, 2.72% starch

Q $(m^3/s)*10^5$	ΔP (Pa)	σ (Pa)	$\dot{\gamma}$ (1/s)	Re
2.481	351.53	0.243	117.79	1166
2.463	348.17	0.241	117.00	
1.726	230.54	0.159	83.86	
1.677	223.82	0.155	81.25	
1.222	163.32	0.133	60.53	
1.154	146.51	0.101	56.72	
0.811	102.82	0.071	40.30	
0.771	106.18	0.073	39.10	

pH=8.15
Critical Re=2036

Table C13. Block 3, 121.1°C, 1.82% starch

Q $(m^3/s)*10^5$	ΔP (Pa)	σ (Pa)	$\dot{\gamma}$ (1/s)	Re
3.542	596.89	0.413	157.43	1418
3.351	546.47	0.378	149.87	
3.346	546.47	0.378	149.68	
2.758	438.92	0.304	125.76	
2.668	348.17	0.241	119.62	
2.034	254.07	0.176	92.01	
2.000	237.26	0.164	89.92	
1.222	79.29	0.055	51.47	
1.188	106.18	0.073	52.02	
1.075	96.10	0.066	47.14	

pH=7.57
Critical Re=1807

Table C14. Block 3, 132.2°C, 1.82% starch

Q $(m^3/s)*10^5$	ΔP (Pa)	σ (Pa)	$\dot{\gamma}$ (1/s)	Re
3.589	617.05	0.427	156.51	1399
3.561	617.05	0.427	155.46	
2.743	405.31	0.280	126.70	
2.664	391.87	0.271	123.52	
2.332	324.65	0.225	109.42	
1.870	247.34	0.171	88.96	
1.846	240.62	0.166	87.72	
1.382	173.40	0.120	66.44	
1.321	156.60	0.108	63.01	
1.123	139.79	0.097	54.41	
1.094	136.43	0.094	53.08	

pH=7.75
Critical Re=1903

Table C15. Block 3, 143.3°C, 1.82% starch

Q $(m^3/s)*10^5$	ΔP (Pa)	σ (Pa)	$\dot{\gamma}$ (1/s)	Re
2.051	270.87	0.187	99.18	1038
2.003	260.79	0.180	97.05	
1.500	196.93	0.136	75.25	
1.463	193.57	0.134	73.66	
1.379	176.76	0.122	69.45	
1.376	176.76	0.122	69.33	
0.886	119.63	0.083	46.56	
0.832	119.63	0.083	44.53	

pH=7.44
Critical Re=2081

Table C16. Block 3, 121.1°C, 2.72% starch

Q $(m^3/s)*10^5$	ΔP (Pa)	σ (Pa)	$\dot{\gamma}$ (1/s)	Re
3.927	775.02	0.536	168.00	1366
3.899	768.30	0.531	167.29	
2.728	445.64	0.308	128.93	
2.628	425.58	0.294	124.83	
2.131	328.01	0.227	103.37	
1.980	311.20	0.215	97.05	
1.583	237.26	0.164	78.50	
1.489	220.46	0.152	73.98	
1.266	196.93	0.136	64.17	
1.202	190.21	0.132	61.33	
1.024	166.68	0.115	53.05	
0.979	156.60	0.108	50.61	

pH=7.57
Critical Re=1944

Table C17. Block 3, 132.2°C, 2.72% starch

Q $(m^3/s)*10^5$	ΔP (Pa)	σ (Pa)	$\dot{\gamma}$ (1/s)	Re
2.682	425.48	0.294	121.83	1147
2.415	368.34	0.255	111.30	
2.458	364.98	0.252	112.85	
2.160	311.20	0.215	100.49	
2.093	294.40	0.204	97.47	
1.683	220.46	0.152	79.13	
1.634	213.73	0.148	76.96	
1.402	183.48	0.127	66.66	
1.152	153.24	0.106	55.49	
1.185	146.51	0.101	56.28	
1.054	122.99	0.085	49.78	
1.008	112.90	0.078	47.33	

pH=7.54
Critical Re=1926

Table C18. Block 3, 143.3°C, 2.72% starch

Q $(m^3/s)*10^5$	ΔP (Pa)	σ (Pa)	$\dot{\gamma}$ (1/s)	Re
2.147	301.12	0.208	98.54	1006
2.110	297.76	0.206	97.06	
1.554	200.29	0.139	72.46	
1.521	186.85	0.129	70.53	
1.125	122.99	0.085	51.91	
1.151	116.26	0.080	52.42	
0.949	99.46	0.069	43.70	
0.899	99.46	0.069	41.85	

pH=8.17
Critical Re=1912

Table C19. Block 4, 121.1°C, 1.82% starch

Q $(m^3/s)*10^5$	ΔP (Pa)	σ (Pa)	$\dot{\gamma}$ (1/s)	Re
3.716	660.75	0.457	159.77	1435
3.716	654.02	0.452	160.10	
3.271	536.39	0.371	147.51	
3.255	529.67	0.366	147.04	
2.945	445.64	0.308	136.09	
2.862	438.92	0.304	132.97	
2.672	388.51	0.269	125.31	
2.737	412.03	0.285	128.08	
1.389	186.85	0.129	68.85	
1.388	183.48	0.127	68.58	
0.932	136.43	0.094	48.05	
0.920	133.07	0.092	47.33	

pH=7.79
Critical Re=1956

Table C20. Block 4, 132.2°C, 1.82% starch

Q $(m^3/s)*10^5$	ΔP (Pa)	σ (Pa)	$\dot{\gamma}$ (1/s)	Re
3.716	633.86	0.438	164.74	1455
3.668	620.41	0.429	163.08	
3.338	519.58	0.359	150.79	
3.323	536.39	0.371	150.35	
2.280	307.84	0.213	105.96	
2.239	301.12	0.208	104.14	
1.803	223.82	0.155	84.00	
1.739	213.73	0.148	81.03	
1.139	119.63	0.083	52.46	

pH=8.19
Critical Re=1869

Table C21. Block4, 143.3°C, 1.82% starch

Q $(m^3/s)*10^5$	ΔP (Pa)	σ (Pa)	$\dot{\gamma}$ (1/s)	Re
2.842	385.14	0.266	127.42	1388
2.761	371.70	0.257	124.31	
2.364	294.40	0.204	108.10	
2.331	287.68	0.199	106.68	
2.044	237.26	0.164	94.11	
1.977	227.18	0.157	91.16	
1.698	180.12	0.125	78.27	
1.646	176.76	0.122	76.13	
1.457	143.15	0.099	66.92	
1.400	136.43	0.094	64.33	
1.210	112.90	0.078	55.51	
1.181	106.18	0.073	52.90	
0.974	86.02	0.060	44.53	
0.976	82.65	0.057	44.37	

pH=7.63
Critical Re=1877

Table C22. Block 4, 121.1°C, 2.72% starch

Q $(m^3/s)*10^5$	ΔP (Pa)	σ (Pa)	$\dot{\gamma}$ (1/s)	Re
3.690	684.27	0.473	157.75	1337
3.646	667.47	0.462	156.60	
3.601	660.75	0.457	155.10	
3.187	533.03	0.369	141.60	
2.957	465.81	0.322	132.90	
2.878	449.00	0.311	129.80	
2.429	317.92	0.220	110.15	
2.302	311.20	0.215	105.18	
1.432	149.87	0.104	64.83	
1.352	153.24	0.106	62.06	
0.916	75.57	0.052	40.43	

pH=7.41
Critical Re=1815

Table C23. Block 4, 132.2°C, 2.72% starch

Q $(m^3/s)*10^5$	ΔP (Pa)	σ (Pa)	$\dot{\gamma}$ (1/s)	Re
3.573	717.88	0.497	146.41	1254
3.509	697.72	0.483	145.25	
2.735	445.64	0.308	123.91	
2.673	425.48	0.294	121.58	
2.314	338.09	0.234	107.04	
2.307	334.73	0.232	106.70	
2.333	341.45	0.236	107.83	
1.886	233.90	0.162	87.45	
1.730	210.37	0.146	80.47	
0.921	116.26	0.080	44.40	
0.944	112.90	0.078	45.03	

pH=8.22
Critical Re=1869

Table C24. Block 4, 143.3°C, 2.72% starch

Q $(m^3/s)*10^5$	ΔP (Pa)	σ (Pa)	$\dot{\gamma}$ (1/s)	Re
1.889	257.43	0.178	87.92	923
1.581	193.57	0.134	70.98	
1.592	183.48	0.127	70.60	
1.341	159.96	0.111	59.46	
1.331	153.24	0.106	58.60	
1.228	119.63	0.083	52.43	
1.191	109.54	0.076	50.39	

pH=7.57
Critical Re=1867

LIST OF REFERENCES

LIST OF REFERENCES

Bagley, E.B. 1957. End corrections in the capillary flow of polyethylene. J. Appl Phys. 28: 624-7

Bagley, E.B. and Christianson, D.D. 1982. Swelling capacity of starch and its relationship to suspension viscosity - effect of cooking time, temperature, and concentration. J. Texture Studies. 13: 115-26

Beck, J.V. 1989. Personal communication. Michigan State University, East Lansing, MI.

Beck, J.V. and Arnold, K.J. 1977. "Parameter Estimation in Engineering and Science," John Wiley and Sons, New York, NY.

Bertsch, A.J. and Cerf, O. 1983. Dynamic viscosities of milk and cream from 70 to 135°C. J. Dairy Research 50: 193-200

Bird, R.B., Stewart, W.E. and Lightfoot, E.N. 1960. "Transport Phenomena," John Wiley and Sons, New York, NY.

Christianson, D.D. and Bagley, E.B. 1983. Apparent viscosities of dispersions of swollen cornstarch granules. Cereal Chem. 60(2): 116-21

Christianson, D.D., Baker, F.L., Loffredo, A.R. and Bagley, E.B. 1982. Correlation of microscopic structure of corn starch granules with rheological properties of cooked pastes. Food Microstruc. 1: 13-24

Colas, B. 1986. Flow behavior of crosslinked corn starches. Lebensmittal-Wissenschaff Technologie 19(4): 308-11

Darby, R. 1976. "Viscoelastic Fluids: An Introduction to Their Properties and Behavior," Marcel Dekker, Inc., New York, NY.

Dignan,D. 1988. Personal communication. FDA, Washington, D.C.

Doebelin, E.O. 1983. "Measurement Systems," 3rd ed. McGraw-Hill Book Co., New York, NY.

Doublier, J.L. 1981. Flow behavior of wheat starch pastes. Starch 33(12): 415-20

Doublier, J.L. 1987. A rheological comparison of wheat, maize, faba bean and smooth pea starches. J. Cereal Sci. 5: 247-62

Eisensmith, S. 1987. "Plotit," Scientific Programming Enterprises, Haslett, MI.

Evans, I.D. and Haisman, D.R. 1979. Rheology of gelatinized starch suspensions. J. Texture Studies 10: 347-70

FDA 1981. Indirect food additives: adjuvants, production aids and sanitizers, Fed. Reg. 46(6): 2341

FDA 1984a. Indirect food additives: adjuvants, production aids and sanitizers, Fed. Reg. 49(50): 9415

FDA 1984b. Aseptic packaging system supplement to instructions for establishment registration and process filing for acidified and low acid canned foods, FDA, Washington, D.C.

Fennema, O.R. (Ed.) 1976. "Principles of Food Science: Part I Food Chemistry," Marcel Dekker, Inc., New York, NY.

Ford, E.W. 1984. Rheological analysis of starch thickened strained apricots using mixer viscometry techniques. M.S. thesis, Michigan State University, East Lansing, MI.

Garcia, E.J. and Steffe, J.F. 1987. Comparison of friction factor equations for non-Newtonian fluids in pipe flow. J. Food Process Engr. 9: 93-120

Hanks, R.W. and Ricks, B.L. 1974. Laminar-turbulent transition in flow of pseudoplastic fluids with yield stresses. J. Hydronautics. 8(4): 163-8

Hoseney, R.C. 1986. "Principles of Cereal Science and Technology," American Association of Cereal Chemists, Inc., St Paul, MN.

Incropera, F.P. and Dwitt, D.P. 1985. "Introduction to Heat Transfer," John Wiley and Sons, New York, NY.

Katz, J.R. 1928. Gelatinization and retrogradation of starch in relation to the problem of bread staling. In "A Comprehensive Survey of Starch Chemistry, Vol. 1," Walton, R.P. (ed.). The Chemical Catalog Co., New York, NY.

Larkin, J. 1988. Personal communication. FDA, Food Engineering Division, Cincinatti, OH.

Lehninger, A.L. 1973. "A Short Course in Biochemistry," Worth Publishers, Inc., New York, NY.

Lineback, D.R. 1984. The starch granule organization and properties. Bakers Dig. 58(2): 16-21

Mooney, M. 1931. Explicit formulas for slip and fluidity. J. of Rheology 2(2): 210-22

Neter, J., Wasserman, W. and Kutner, M.H. 1985. "Applied Linear Statistical Models," 2nd ed. Richard D. Irwin, Inc., Homewood, IL.

Potter, M.C. and Foss, J.F. 1982. "Fluid Mechanics," Great Lakes Press, Okemos, MI.

Rabinowitsch, B. 1929. Uber die viskositat und elasticitat von solen. Zeitschrift fur Physikalische Chemie 145A: 1-26

Reynolds, W.C. and Perkins, H.C. 1977. "Engineering Thermodynamics," McGraw-Hill Book Co., New York, NY.

Salas-Valerio, W.F. 1988. Flow distribution of non-Newtonian fluids from a manifold system. M.S. thesis, Michigan State University, East Lansing, M.I.

Skelland, A.H.P. 1967. "Non-Newtonian Flow and Heat Transfer," John Wiley and Sons, New York, NY.

Stefanovic, S. 1988. Personal communication. Pure-Pak, Inc., Walled Lake, MI.

Steffe, J.F. and Morgan, R.G. 1986. Pipeline design and pump selection for non-Newtonian fluid foods. Food Technol. 40(12): 78-85

Tung, T.T., Ng, K.S. and Hartnett, J.P. 1978. Pipe friction factors for concentrated aqueous solution of polyacrylamide. Lett. Heat Mass Transfer 5: 59. [In Advances in Heat Transfer, Vol. 15, Academic Press, New York, NY.]

USDA 1984. Guidelines for aseptic processing and packaging systems in meat and poultry plants, USDA, Washington, D.C.

Vercruysse, M.C.M. 1987. Design criteria for an on-line viscometer for baby food puree. M.S. thesis, Michigan State University, East Lansing, MI.

Whistler, R.L., BeMiller, J.N. and Paschall, E.F. (Eds.). 1984. "Starch Chemistry and Technology," 2nd ed. Academic Press, Inc., Orlando, FL.

Whorlow, R.W. 1980. "Rheological Techniques," Halsted Press, John Wiley and Sons, New York, NY.

Wong, R.B.K. and Lelievre, J. 1982. Rheological characteristics of wheat starch pastes under steady shear conditions. J. Applied Polymer Sci. 27: 1433-40

Yoo. S.S. 1974. Heat transfer and friction factors for non-Newtonian fluids in turbulent pipe flow. Ph.D. Thesis, University of Illinois at Chicago Circle. [In Advances in Heat Transfer, Vol. 15, Academic Press, New York, NY.]

Zobel, H.F. 1984. Gelatinization of starch and mechanical properties of starch pastes. Ch. 9. In "Starch Chemistry and Technology," Whistler, R.L. BeMiller, J.N. and Paschall, E.F. (Eds.). p. 285. Academic Press, Inc., Orlando, FL.